

ELECTRON BEAM TECHNOLOGY FOR THE REMOVAL OF THE  
CYANOTOXIN, MICROCYSTIN-LR, AND THE CYANOBACTERIA,  
*MICROCYSTIS AERUGINOSA*, IN CONTAMINATED WATERS

A Dissertation

by

ALEXANDRA MICHELLE FOLCIK

Submitted to the Graduate and Professional School of  
Texas A&M University  
in partial fulfillment of the requirements for the degree of

DOCTOR OF PHILOSOPHY

Chair of Committee,	Suresh D. Pillai
Committee Members,	Natalie Johnson
	Robert Burghardt
	Virender Sharma

Intercollegiate Faculty Chair,	Ivan Rusyn
-----------------------------------	------------

December 2021

Major Subject: Toxicology

Copyright 2021 Alexandra M. Folcik

## ABSTRACT

Increasing global water scarcity is underscoring the need for efficient and reliable treatment technologies within the water treatment process. Ionizing radiation technologies present promising strategies for the remediation of many emerging contaminants. In particular, high energy electron beam (eBeam) technology is a chemical-free advanced oxidation reduction process (AORP) that is generated from commercial electricity and has been proven effective for the breakdown of various organic and inorganic pollutants. Similar variables effecting water availability, such as rising temperatures and nutrient pollution, are also feeding the rising occurrence of harmful cyanobacterial blooms (cyanoHABs). CyanoHABs are responsible for producing an array of hepato- and neuro-toxins that pose threats to human and animal health. Drinking water sources that are affected by a cyanoHAB provide a critical human exposure scenario. The cyanobacterium *Microcystis aeruginosa* is commonly associated with freshwater cyanoHABs and is responsible for producing a class of hepatotoxins termed microcystins. Of the over 100 variants of microcystin, microcystin-LR (MC-LR) is the most prevalent and most toxic.

This project aimed to investigate the effects of eBeam treatment on the cyanotoxin, MC-LR, and the cyanobacteria, *Microcystis aeruginosa*. The results demonstrated that low doses of eBeam treatment (<400 Gy) are sufficient to degrade MC-LR at environmentally relevant concentrations. The degradation mechanism of MC-LR appears to be primarily oxidative and degradation products fail to exhibit

cytotoxicity *in vivo*. eBeam doses >2 kGy were sufficient to prevent *M. aeruginosa* cell growth and induced cell lysis. Cell lysis occurred on a time delay of approximately 2 hours following irradiation. However, cell lysis was seen to be coupled to light damage during incubation following eBeam treatment and not the eBeam treatment itself. Finally, eBeam treatment was able to degrade MC-LR in surface water samples by >99% regardless of water quality. The results of these studies suggest eBeam technology is a promising addition into the drinking water treatment scheme for the remediation of cyanoHABs in drinking water.

## DEDICATION

I could dedicate this dissertation to many people that have impacted me along the road to here, but I will only highlight a few. First, I would like to dedicate this work to myself. Despite the sleepless nights, the self-doubt, and the fluctuating motivation, I have proven to myself that I could do it. I hope this 200 something page document serves as a reminder to anyone facing adversity that the grind does pay off. I also dedicate this dissertation to my friends and my family (both in blood and chosen) for their encouragement and willingness to always lend an ear – even if they did not know what I was talking about. But most importantly, I dedicate this dissertation to Dilan and Indy. To Dilan who continued to love and support me through this rollercoaster journey and to Indy whose empathy comforted me many times through stress and anxiety. It hasn't always been easy, but there are no shortcuts to anywhere worth going.

## ACKNOWLEDGEMENTS

I would first like to thank my committee chair, Dr. Suresh Pillai, for his mentorship, encouragement of me to develop my skills as a scientist, and his willingness to allow me to travel the world in the name of science. His insistence on me believing in “the secret” seems to have paid off. Next, I would like to acknowledge the support and guidance of the other members of my committee, Dr. Natalie Johnson, Dr. Robert Burghardt, and Dr. Virender Sharma. Thirdly, thank you to my lab mates for their continuous help on experiments and acting as a sounding board to talk through ideas and problems. I would like to acknowledge the Interdisciplinary Toxicology Program, their faculty, and Kim Daniel for their support and help in preparing me for my future career in toxicology. A big thank you to both Cory and Smriti at IMAC for their support in both chemical analysis and navigating a PhD. And thank you to Sara and Mickey at NCEBR for their help with irradiating my many samples.

## CONTRIBUTORS AND FUNDING SOURCES

### **Contributors**

This work was supervised by a dissertation committee consisting of Professor Suresh Pillai of the Department of Food Science and Technology, Professor Natalie Johnson and Professor Virender Sharma of the Department of Environmental and Occupational Health, and Professor Robert Burghardt of the Department of Veterinary Integrative Biosciences.

The analytical data collection in Chapters 3-6 was performed by Dr. Cory Klemashevich at the Integrated Metabolomics Analysis Center (IMAC) at Texas A&M University. And analytical data collection in Chapter 4 was also performed by the West Coast Metabolomics Center at the University of California Davis. eBeam irradiation in all chapters were performed by Ms. Sara Parsons at the National Center for Electron Beam Research (NCEBR) at Texas A&M University. Finally, bioinformatic analysis in chapter 5 was completed by the team at Zymo Research. Some of the laboratory analyses performed in Chapter VII were completed by Ms. Shelby Ruggles and Ms. Abbey Pollok. All other work conducted for the dissertation was completed by the student independently.

### **Funding Sources**

Graduate study was supported by the University/Association of Former Students Graduate Merit Fellowship from Texas A&M University, an institutional training grant from the National Institutes of Health (T32 ES026568), Texas A&M AgriLife Research H8708, and USDA-ARS funding.

This work was also performed as part of the activities of the International Atomic Energy Agency (IAEA) Collaborating Centre at Texas A&M University.

## NOMENCLATURE

ADDA	N-methyldehydroalanine and 3-amino-9-methoxy-2,6,8-trimethyl-10-phenyldeca-4,6-dienoic acid
AOP	Advanced Oxidation Process
AORP	Advanced Oxidation Reduction Process
CaMKII	Calcium-calmodulin-dependent Multifunctional Protein Kinase II
CB	Cyanobacteria
CCL	Candidate Contaminant List
CYN	Cylindrospermopsins
cyanoHAB	Cyanobacterial Harmful Algal Bloom
DIC	Dark Incubated Cultures
DNA-PK	DNA-dependent Protein Kinase
eBeam	Electron Beam
ELISA	Enzyme-Linked Immunosorbent Assay
EPS	Extracellular Polysaccharides
FDR	False Discovery Rate
GSH	Glutathione
GST	Glutathione S-transferase
HAB	Harmful Algal Bloom
HILIC QE HF MS/MS	Hydrophobic Interaction Liquid Chromatography Q Extractive HF Mass Spectrometry



IARC	International Agency for Research on Cancer
IMAC	Integrated Metabolomics Analysis Core
kGy	Kilogray
LC-HRAMS	Untargeted Liquid Chromatography High Resolution Accurate Mass Spectrometry
LD <sub>50</sub>	Lethal Dose
LIC	Light Incubated Cultures
LPS	Lipopolysaccharide
LOD	Limit of Detection
LOQ	Limit of Quantification
MALDI TOF/TOF MS	Matrix-Assisted Laser Desorption/Ionization Coupled to Time of Flight Mass Spectrometry
MAPK	Mitogen-activated Protein Kinase
MAyNC	Metabolically Active yet Non-Culturable
MC	Microcystin
<i>mcy</i>	Microcystin Biosynthesis Gene Cluster
MC-LA	Microcystin-LA
MC-LF	Microcystin-LF
MC-LR	Microcystin-LR
MC-LW	Microcystin-LW
MC-RR	Microcystin-RR
MC-YR	Microcystin-YR

MDha	N-methyl Dehydroalanine
MDS	Multidimensional Scaling
MeAsp	b-linked D-erythro-b-methylaspartic Acid
MeV	Million Electron Volts
NCEBR	National Center for Electron Beam Research
NER	Nucleotide Excision Repair
NHEJ	Nonhomologous End Joining
NOAEL	No Observed Adverse Effect Level
NOM	Natural Organic Matter
NRPS	Non-Ribosomal Peptide Synthetases
OATP	Organic Anion Transporting Polypeptide
OD	Optical Density
PP	Protein Phosphatase
PKS	Polyketide Synthase
POD	Peroxidase
PS	Photosystem
PSP	Paralytic Shellfish Poison
RfD	Reference Dose
ROS	Reactive Oxygen Species
SOD	Superoxide Dismutase
TEM	Transmission Electron Microscopy
TDI	Tolerable Daily Intake

TDS	Total Dissolved Solids
TOC	Total Organic Carbon
UF	Uncertainty Factor
USEPA	United States Environmental Protection Agency
WHO	World Health Organization

## TABLE OF CONTENTS

	Page
ABSTRACT .....	ii
DEDICATION.....	iv
ACKNOWLEDGEMENTS .....	v
CONTRIBUTORS AND FUNDING SOURCES.....	vi
NOMENCLATURE .....	viii
TABLE OF CONTENTS.....	xii
LIST OF FIGURES .....	xvii
LIST OF TABLES.....	xxii
CHAPTER I INTRODUCTION .....	1
Motivation .....	1
Potential Impact on the Field.....	2
Research Objectives.....	4
Specific Objectives.....	4
CHAPTER II LITERATURE REVIEW.....	6
Introduction .....	6
Microcystins.....	7
History of Microcystins .....	7
Microcystin Producing Genera .....	7
Microcystin Structure .....	8
Mechanism of Toxicity.....	9
Metabolism and Biotransformation.....	12
Organ Toxicity .....	13
Regulations Governing Microcystins .....	15
Other Cyanotoxins .....	31
Nodularins.....	31
Cylindrospermopsins.....	34
Saxitoxins .....	34

Anatoxins .....	35
Lipopolysaccharides .....	35
Remediation Strategies .....	36
Ionizing Radiation .....	36
Gamma Irradiation .....	37
X-Ray .....	37
Electron Beam Technology .....	39
Effects of Ionizing Radiation .....	39
Methods .....	42
Current Research Using Ionizing Radiation Technologies .....	43
Gamma Irradiation .....	43
Electron Beam Irradiation .....	50
Research Approach .....	54
CHAPTER III RESPONSE OF <i>M. AERUGINOSA</i> AND MICROCYSTIN-LR TO ELECTRON BEAM IRRADIATION .....	59
Abstract .....	59
Introduction .....	60
Materials and Methods .....	60
Laboratory Propagation of <i>M. aeruginosa</i> .....	60
Quantification of Microcystin-LR .....	60
Electron Beam Treatment .....	62
Response of <i>M. aeruginosa</i> Cells to Varying eBeam Doses .....	62
Microscopic Examination of Structural Integrity .....	63
Stability and Residual Toxicity of Microcystin-LR Exposed to Varying eBeam Doses .....	63
Potential of Microcystin-LR Release from eBeam Exposed <i>M. aeruginosa</i> Cells..	64
Data Analysis .....	65
Results and Discussion .....	65
Cyanobacterial Inactivation .....	65
Stability and Residual Toxicity of Microcystin-LR .....	69
Potential of Microcystin-LR Release from eBeam-exposed <i>M. aeruginosa</i> Cells..	74
Conclusion .....	78
CHAPTER IV TOXICITY AND POSSIBLE ELECTRON BEAM MEDIATED DEGRADATION MECHANISMS OF MICROCYSTIN-LR .....	80
Abstract .....	80
Introduction .....	80
Materials and Methods .....	81
Quantification of Microcystin-LR .....	81
In Vitro Toxicity Assay .....	81
Electron Beam Treatment .....	82

Scavenger Study.....	82
MC-LR Degradation Product Analysis .....	83
Data Analysis .....	83
Results and Discussion.....	84
Radiolytic Species Responsible for eBeam MC-LR Degradation .....	84
MC-LR Degradation Products .....	91
Effect of eBeam Treated MC-LR on Target Cell Viability.....	102
Conclusion.....	104
CHAPTER V MOLECULAR RESPONSES OF <i>MICROCYSTIS AERUGINOSA</i> TO VARYING ELECTRON BEAM DOSES .....	106
Abstract .....	106
Introduction .....	106
Materials and Methods.....	107
Laboratory Propagation of <i>M. aeruginosa</i> .....	107
Electron Beam Treatment.....	107
Experimental Design.....	108
Quantification of Microcystin-LR .....	108
DNA Extraction and Fragmentation Analysis .....	108
Transcriptomic Analysis.....	110
RNA Extraction.....	110
Library Preparation and RNAseq.....	110
Bioinformatic Analysis.....	110
Results .....	112
<i>M. aeruginosa</i> Cell Growth .....	112
<i>M. aeruginosa</i> Toxin Production .....	113
eBeam Induced DNA Fragmentation.....	113
eBeam Induced Changes in <i>M. aeruginosa</i> Global Gene Expression .....	116
Influence of Incubation Period Post eBeam Exposure on Gene Expression.....	119
eBeam Induced Changes in <i>M. aeruginosa</i> Photosystem Gene Expression .....	123
eBeam Induced Changes in <i>M. aeruginosa</i> mcyA-J Gene Expression.....	127
Discussion .....	127
<i>M. aeruginosa</i> Cell Growth and Toxin Production.....	128
eBeam Induced DNA Fragmentation.....	129
eBeam Induced Changes in <i>M. aeruginosa</i> Global Gene Expression .....	130
eBeam Induced Changes in <i>M. aeruginosa</i> Photosystem Gene Expression .....	131
eBeam Induced Changes in <i>M. aeruginosa</i> mcyA-J Gene Expression.....	132
Conclusion.....	134
CHAPTER VI THE INFLUENCE OF LIGHT ON ELECTRON BEAM INDUCED DAMAGE IN <i>M. AERUGINOSA</i> .....	136
Abstract .....	136

Introduction .....	136
Materials and Methods .....	137
Laboratory Propagation of <i>M. aeruginosa</i> .....	137
Electron Beam Treatment.....	137
Quantification of Microcystin-LR .....	138
DNA Extraction and Fragmentation Analysis .....	138
Results and Discussion.....	138
<i>M. aeruginosa</i> Cell Growth in Dark Incubation Conditions .....	139
<i>M. aeruginosa</i> Toxin Production in Dark Incubation Cultures (DIC).....	141
eBeam Induced DNA Fragmentation.....	144
Conclusion.....	146
CHAPTER VII APPLICABILITY OF ELECTRON BEAM TECHNOLOGY FOR THE REMEDIATION OF MICROCYSTIN-LR IN SURFACE WATERS FROM MULTIPLE GEOGRAPHIC LOCATIONS.....	147
Abstract .....	147
Introduction .....	147
Materials and Methods.....	148
Sampling .....	148
Water Chemistry .....	148
Electron Beam Treatment.....	149
Water Samples Treatment and Quantification.....	149
Effect of Fulvic Acid.....	150
Data Analysis .....	150
Results and Discussion.....	150
Chemistry of Surface Water Samples .....	151
Effect of Water Quality on MC-LR Degradation .....	155
Fulvic Acid Effects on MC-LR Degradation.....	158
Conclusion.....	159
CHAPTER VIII CONCLUSION .....	161
Summary .....	161
Novelty of Research.....	163
CHAPTER IX FUTURE RESEARCH.....	164
Future Directions for <i>M. aeruginosa</i> .....	164
Future Directions for MC-LR.....	165
Future Directions for Implementation.....	166
REFERENCES .....	168
APPENDIX A CRITICAL REVIEW SEARCH TERMS .....	187

APPENDIX B WATER QUALITY PARAMETER DATA ..... 188



## LIST OF FIGURES

	Page
Figure 1. The chemical structure of Microcystin-LR. Created with ChemDraw.....	8
Figure 2. Microcystin-LR mechanism of action. Adapted from Valerio et al. (2010). <sup>34</sup> Was published open access in Toxins and is covered under a Creative Commons Attribution License ( <a href="https://creativecommons.org/licenses/by-nc-sa/3.0/">https://creativecommons.org/licenses/by-nc-sa/3.0/</a> ). Organic anion transporting polypeptide (OATP), protein phosphatase 1 and 2A (PP1/PP2A), calcium-calmodulin-dependent multifunctional protein kinase II (CaMKII), mitogen-activated protein kinases (MAPKs). .....	10
Figure 3. Chemical structures of common cyanotoxins. Created with ChemSketch. ....	33
Figure 4. Schematic and photographs of the electron beam linear accelerator at the National Center for Electron Beam Research (NCEBR) at Texas A&M University. A) Schematic of an electron beam linear accelerator utilized for water treatment; B) The accelerating structure of the electron beam at NCEBR; C) The magnetic scan horn and conveyor belt of the electron beam at NCEBR.....	38
Figure 5. Reaction products for hydroxyl radical reaction with the A) benzene group and B) diene group of ADDA moiety of MC-LR. Reprinted (adapted) with permission from Song, Weihua, et al. "Radiolysis studies on the destruction of microcystin-LR in aqueous solution by hydroxyl radicals." <i>Environmental Science &amp; Technology</i> 43.5 (2009): 1487–1492. <sup>104</sup> Copyright (2009) American Chemical Society. ....	48
Figure 6. Response of <i>M. aeruginosa</i> cells to 0, 0.6, 2.1, and 4.9 kGy eBeam irradiation doses over 14 days. (Error bars represented as standard deviation, Limit of detection (LOD) = $2.5 \times 10^5$ cells/ml). .....	66
Figure 7. Irradiated cultures exhibited a visibly detectable color change over time following irradiation. From left to right: 0, 0.6, 2.1, and 4.9 kGy.....	67
Figure 8. Brightfield and auto-chlorophyll fluorescence microscopy images of <i>M. aeruginosa</i> cells. A) Unirradiated cells. Cells appear normal and intact; B) Cells immediately after irradiation at 4.9 kGy. Cells are still structurally intact but have slight discoloring in the center of the cells indicating possible internal or membrane damage; C) Cells 24 h after irradiation at 4.9 kGy. Cells have completely lysed and free chlorophyll is fluorescing on the slide. ....	68

Figure 9. Degradation of MC-LR after 0, 0.29, 0.39, 0.64, 2.1, and 5.1 kGy eBeam irradiation treatment. A) Analytical determination of remaining MC-LR using LC-HRAM after eBeam treatment. B) MC-LR remaining after eBeam irradiation as determined by EPA method 546 ADDA-specific ELISA. Increasing absorbance corresponds to a decrease in binding of MC-LR to the detection antibody. (* = $p \leq 0.05$ ; error bars represent standard deviation).....	70
Figure 10. Protein phosphatase 2A inhibition assay toxicity of MC-LR after 0, 0.29, 0.39, 0.64, 2.1, and 5.1 kGy eBeam irradiation treatment as determined using a protein phosphatase 2A inhibition assay. (* = $p \leq 0.05$ ; error bars represent standard deviation).....	71
Figure 11. Time course study of intracellular MC-LR (pellet) and extracellular MC-LR (supernatant) at 0 and 5.4 kGy eBeam treatment .....	75
Figure 12. Products identified as significant (in red) in 0.18 kGy t-butanol amended samples vs. 0 kGy t-butanol amended samples (>2 fold change; $p \leq 0.05$ ).....	86
Figure 13. Products identified as significant (in red) in 1.15 kGy t-butanol amended samples vs. 0 kGy t-butanol amended samples (>2 fold change; $p \leq 0.05$ ).....	87
Figure 14. Products identified as significantly upregulated (in red) in 0.18 kGy N <sub>2</sub> sparged samples vs. 0 kGy N <sub>2</sub> sparged samples (>2 fold change; $p \leq 0.05$ ). ..	92
Figure 15. Products identified as significant (in red) in 0.18 kGy pH 13 adjusted samples vs. 0 kGy pH 13 adjusted samples (>2 fold change; $p \leq 0.05$ ). .....	93
Figure 16. Products identified as significant (in red) in 1.15 kGy pH 13 adjusted samples vs. 0 kGy pH 13 adjusted samples (>2 fold change; $p \leq 0.05$ ). .....	94
Figure 17. MALDI TOF/TOF spectra. A) Spectra of 0.5 $\mu$ M MC-LR irradiated at 0.29 kGy. Peak identified at 789.110 m/z and possible chemical structure. B) Spectra of 0.5 $\mu$ M MC-LR irradiated at 5.1 kGy. Peak identified at 699.057 m/z and possible chemical structure.....	98
Figure 19. Change in cell viability in HEPG2 cells dosed with 5.48 kGy irradiated or 0 kGy non-irradiated MC-LR over 96 hours using the CCK-8 assay. (Error bars represented at standard deviation; * = $p \leq 0.05$ determined via Tukey's multiple comparisons test) .....	103
Figure 18. Initial dose response of MC-LR on HEPG2 cells over 120 hours using the CCK-8 assay. (No error bars are shown as this was a preliminary study with technical replicates only.).....	103

Figure 20. Experimental design for timed experiment. <i>M. aeruginosa</i> cultures were irradiated in 30 ml screw cap vials at 0, 2.02, or 5.03 kGy. Following irradiation, cultures were transferred to flasks and incubated in lighted conditions on an orbital shaker. Sampling aliquots were taken at 0, 2, 4, 6, and 24 hours post eBeam exposure for further analysis. Schematic created with BioRender.....	109
Figure 21. Response of <i>M. aeruginosa</i> cells to 0, 2.02, and 5.03 kGy eBeam irradiation doses. (Error bars are represented as standard deviation; * = $p \leq 0.05$ determined via Tukey's multiple comparisons test).....	112
Figure 22. Intracellular and extracellular MC-LR concentrations following eBeam treatment at 0, 2.02 and 5.03 kGy over time. A) Intracellular MC-LR concentration. B) Extracellular MC-LR concentration. (Error bars represented as standard deviation; Intracellular limit of quantification (LOQ) = 1 $\mu\text{g/L}$ ; Extracellular LOQ = 2.5 $\mu\text{g/L}$ ; * = $p \leq 0.05$ ; ** = $p \leq 0.01$ ; *** = $p \leq 0.001$ ) .....	114
Figure 23. DNA fragmentation as a percent of total DNA fragments in 0 kGy, 2.02 kGy, and 5.03 kGy eBeam exposed <i>M. aeruginosa</i> cultures over time. A) 50 – 10,000 bp length fragments; B) 10,000 – 20,000 bp length fragments; C) 10,000 – 30,000 bp length fragments.....	115
Figure 24. Multidimensional scaling (MDS) plot of all <i>M. aeruginosa</i> samples. Samples appear clustered by eBeam treatment dose. Shapes indicate doses of 0, 2.02, and 5.03 kGy. Colors indicate time following eBeam treatment at 0, 2, 4, 6, and 24 hours. Untreated cultures also showed clustering across sample timepoints (circle shape). .....	117
Figure 25. Heatmap of expression patterns of top 100 differentially expressed genes with greatest variance in eBeam treated and untreated <i>M. aeruginosa</i> cultures. ....	118
Figure 26. Heatmap showing expression patterns of top 100 genes with the smallest false discovery rate (FDR) in untreated <i>M. aeruginosa</i> cultures. Each three-column group represents incubation time as indicated by color. ....	120
Figure 27. Heatmap showing expression patterns of top 100 genes with the smallest false discovery rate (FDR) in 2.02 kGy eBeam treated <i>M. aeruginosa</i> cultures. Each three-column group represents incubation time as indicated by color.....	121
Figure 28. Heatmap showing expression patterns of top 100 genes with the smallest false discovery rate (FDR) in 5.03 kGy eBeam treated <i>M. aeruginosa</i>	

cultures. Each three-column group represents incubation time as indicated by color.....	122
Figure 29. Heatmap showing expression patterns of photosystem I (PSI) genes in <i>M. aeruginosa</i> exposed to 0, 2.02, and 5.03 kGy eBeam doses over time following irradiation. Values plotted are log2 fold changes against mean values. ....	124
Figure 30. Heatmap showing expression patterns of photosystem II (PSII) genes in <i>M. aeruginosa</i> exposed to 0, 2.02, and 5.03 kGy eBeam doses over time following irradiation. Values plotted are log2 fold changes against mean values. ....	125
Figure 31. Heatmap showing expression patterns of the <i>mcy</i> gene cluster in <i>M. aeruginosa</i> exposed to 0, 2.02, and 5.03 kGy eBeam doses over time following irradiation. Values plotted are log2 fold changes against mean values. ....	126
Figure 32. Response of <i>M. aeruginosa</i> cells to 0, 2.19, and 5.37 kGy ebeam irradiation doses. A) Cell concentrations in eBeam treated cultures incubated in the dark over 96 hours. B) Cell concentrations in eBeam treated cultures incubated in the light (12:12 day:night) over 48 hours. C) Zoomed in view on dark incubated cultures from 0 – 6 hours. D) Zoomed in view on light incubated cultures from 0 – 6 hours. (Error bars represented as standard deviation; * = $p \leq 0.05$ determined via Tukey's multiple comparisons test) .....	140
Figure 33. Intracellular and extracellular MC-LR concentrations following eBeam treatment at 0, 2.19, and 5.37 kGy over time. A) Intracellular MC-LR concentration in eBeam treated cultures incubated in the dark over 96 hours. B) Extracellular MC-LR concentration in eBeam treated cultures incubated in the dark over 96 hours. C) Intracellular MC-LR concentration in eBeam treated cultures incubated in the light over 48 hours. D) Extracellular MC-LR concentration in eBeam treated cultures incubated in the light over 48 hours. (Error bars represented as standard deviation; * = $p \leq 0.05$ ; ** = $p \leq 0.01$ ; *** = $p \leq 0.001$ ; **** = $p \leq 0.0001$ ) .....	142
Figure 34. DNA fragmentation as a percent of total DNA fragments in eBeam treated <i>M. aeruginosa</i> cultures over time. A) 50 – 10,000 bp length fragments in dark incubated cultures over 96 hours; B) 10,000 – 20,000 bp length fragments in dark incubated cultures over 96 hours; C) 10,000 – 30,000 bp length fragments in dark incubated cultures over 96 hours; D) 50 – 10,000 bp length fragments in light incubated cultures over 48 hours; E) 10,000 – 20,000 bp length fragments in light incubated cultures over 48 hours; F) 10,000 – 30,000 bp length fragments in light incubated cultures over 48	

hours. (Error bars represented as standard deviation; \* =  $p \leq 0.05$ ; \*\* =  $p \leq 0.01$ ; \*\*\* =  $p \leq 0.001$ ; \*\*\*\* =  $p \leq 0.0001$ ) ..... 145

Figure 35. Sampling locations of water samples used in this study. An interactive version of this map can be accessed here: <https://bit.ly/2UeZhAO>..... 152

Figure 36. Water quality parameters measured in surface water samples. A) pH; B) Alkalinity; C) TDS; D) Dissolved oxygen. (Error bars represent standard deviation.)..... 154

Figure 37. MC-LR degradation in surface water samples following eBeam treatment at  $5.11 \pm 0.079$  kGy. ( $p \leq 0.0001$ ; error bars represent standard deviation). . 157

Figure 38. MC-LR degradation in deionized water supplemented with 0, 50, or 100  $\mu\text{g/L}$  FA following eBeam treatment at  $5.11 \pm 0.079$  kGy. ( $p \leq 0.0001$ ; error bars represent standard deviation). ..... 159

## LIST OF TABLES

	Page
Table 1. Examples of international regulations and guidance values for cyanotoxins in drinking water. Adapted from Ibelings et al. (2015). <sup>60</sup> .....	16
Table 2. State regulations and guidance values for cyanotoxins in drinking water and recreational water.....	21
Table 3. Common cyanotoxins, main producing genera, and primary mechanism of action.....	32
Table 4. Significant products in 0.18 kGy t-butanol amended samples vs. 0 kGy t-butanol amended samples (>2 fold change; $p \leq 0.05$ ) identified by LC-HRAM. Suggested compound names identified by mzCloud or ChemSpider Databases.....	88
Table 5. Significant products in 1.15 kGy t-butanol amended samples vs. 0 kGy t-butanol amended samples (>2 fold change; $p \leq 0.05$ ) identified by LC-HRAM. Suggested compound names identified by mzCloud or ChemSpider Databases.....	89
Table 6. Significant products in 0.18 kGy N <sub>2</sub> sparged samples vs. 0 kGy N <sub>2</sub> sparged samples (>2 fold change; $p \leq 0.05$ ) identified by LC-HRAM. Suggested compound names identified by mzCloud or ChemSpider Databases.....	95
Table 7. Significant products in 0.18 kGy pH 13 adjusted samples vs. 0 kGy pH 13 adjusted samples (>2 fold change; $p \leq 0.05$ ) identified by LC-HRAM. Suggested compound names identified by mzCloud or ChemSpider Databases.....	95
Table 8. Significant products in 1.15 kGy pH 13 adjusted samples vs. 0 kGy pH 13 adjusted samples (>2 fold change; $p \leq 0.05$ ) identified by LC-HRAM. Suggested compound names identified by mzCloud or ChemSpider Databases.....	95
Table 9. Significant products in 2.14 kGy treated samples vs. 0 kGy untreated samples (>2 fold change; $p \leq 0.05$ ) identified by LC-HRAM. Suggested compound names identified by mzCloud or ChemSpider Databases.....	97
Table 10. Significant products in 5.03 kGy treated samples vs. 0 kGy untreated samples (>2 fold change; $p \leq 0.05$ ) identified by LC-HRAM. Suggested compound names identified by mzCloud or ChemSpider Databases.....	97

Table 11. Degradation products in 41 Gy, 126 Gy, and 343 Gy treated samples vs. 0 Gy untreated samples identified by HILIC QE HF MS. Shaded ions exhibit a dose response with increasing treatment dose. ....	100
Table 12. MC-LR identified by HILIC QE HF MS as [M+2H] <sup>2+</sup> ion at different sample doses. ....	100
Table 13. Water samples with the highest remaining MC-LR following 5.11 ± 0.079 kGy eBeam treatment. ....	156
Table 14. Water samples with the lowest remaining MC-LR following 5.11 ± 0.079 kGy eBeam treatment. ....	156
Table 16. Defined search terms used for critical literature review and the number of papers identified with each database. ....	187
Table 17. MC-LR concentrations (µg/L) and degradation efficiency in 5.11 ± 0.079 kGy eBeam treated source water samples and untreated samples. (Error expressed as standard deviation.) ....	188
Table 18. Measured water quality parameters in source water samples. (Error expressed as standard deviation). ....	189

# CHAPTER I

## INTRODUCTION

### **Motivation**

Over the past decade, up to 63 million people in the United States have been exposed to potentially unsafe drinking water.<sup>1</sup> This contaminated water has resulted from years of industrial discharge, agricultural runoff, and treatment plant pipe deterioration.<sup>1</sup> In 2018, the United States Environmental Protection Agency (USEPA) estimated that local water systems would need to invest nearly \$472.6 billion in the coming twenty years to prevent contaminated water.<sup>2</sup> Reliably supplying clean water requires an understanding of potential contaminants and the necessary treatment procedures for their effective removal.

Harmful algal blooms (HABs) occur when there is exponential overgrowth of photosynthetic microorganisms (algae and/or cyanobacteria) in a waterbody.<sup>3</sup> Such blooms may exist in freshwater, brackish water, or in marine environments. However, blooms occurring in freshwaters are typically caused by cyanobacteria and termed cyanoHABs. In recent years, cyanoHABs have been observed to increase in frequency and severity as a result of several factors including rising water temperatures and anthropogenic nutrient pollution.<sup>4</sup> Seasonal trends have been observed with highest concentrations of being observed in late summer and early fall.<sup>5</sup> These blooms can cause damage to the aquatic environment by inhibiting sunlight penetration and depleting oxygen content in the source water.<sup>6</sup> Further, cyanoHABs pose threats to an already



dwindling water supply worldwide due to their production of various cyanotoxins that can be harmful to both wildlife and humans.

Of particular concern are a class of cyanotoxins called microcystins (MCs). MCs are hepatotoxic heptapeptides with over 200+ identified variants with various degrees of toxicity.<sup>7</sup> Of these variants, microcystin-LR (MC-LR) is the most common and most toxic.<sup>8</sup> All cyanotoxins, including MC-LR, represent an increasing global water-quality issue when source waters supplying drinking water contain these blooms. In this case, effective treatment strategies are needed to address both the toxins and the producing cyanobacterial cells.

Conventional water treatment strategies including coagulation, flocculation, sedimentation, and filtration are generally effective for MC treatment, provided that levels of cells and toxin remain at low levels.<sup>9,10</sup> However, during extensive blooms, conventional treatments may not be sufficient to prevent intrusion of these toxins into drinking water. Further, treatment plant residuals such as sediments and sludges that contain these cyanobacteria and cyanotoxins become classified as hazardous wastes requiring further treatment prior to disposal.<sup>11,12</sup> Therefore, there is a need for reliable treatment strategies for cyanotoxins that prevent contaminated drinking water even when source waters experience severe blooms.

### **Potential Impact on the Field**

Thirty-four of the fifty U.S. states have HAB monitoring programs with over 25 of these states reporting reoccurring HABs every year.<sup>13,14</sup> The state of Ohio has had multiple outbreaks of microcystin in finished drinking water in the past decade resulting

in “Do not drink” advisories being issued.<sup>15</sup> Outside of the U.S., toxic blooms are a global concern with examples in: the Baltic Sea in Europe, Lake Victoria in Africa, Lake Taihu in Asia, Murray River in Australia, various reservoirs in South America, and even occurrences in Antarctica.<sup>16,17</sup> In Brazil, 76 hemodialysis patients died after exposure to water contaminated with microcystins and other cyanotoxins during treatment.<sup>18,19</sup> In China, low-level chronic exposure to microcystin is thought to be related to higher rates of hepatocellular carcinoma than anywhere in the world (>60/100,000 people).<sup>3</sup> These incidents highlight the global public health risk associated with HABs and the ingestion of MCs.

Chemical oxidation strategies have been investigated for MC-LR removal at drinking water treatment plants including chlorine, potassium permanganate, copper sulfate, and hydrogen peroxide.<sup>20</sup> Unfortunately, these treatments have been found largely ineffective and additionally may introduce disinfection byproducts into the water supply during treatment. Other studies have investigated several advanced oxidation processes (AOPs) such as UV/H<sub>2</sub>O<sub>2</sub>, Fenton reagent, modified natural magnetite, and ozone.<sup>7,21–23</sup> And while some of these AOPs have been successful at degrading MC-LR, these processes require ideal conditions for full breakdown of MC-LR. Presently, many drinking water plants utilize ozonation to treat MC-LR. However, besides the optimal conditions needed for full degradation, studies have shown that ozone may be ineffective against intracellular MC-LR as well as it is causing the lysing of cyanobacterial cells causing further MC-LR release.<sup>24,25</sup> In response, the USEPA has advised against pre-treatment of drinking water with ozonation to prevent further MC-LR release.<sup>26</sup>

There is an urgent need for a reliable technology that not only has the capacity to degrade MC-LR into non-toxic constituents, but also to inactivate the cyanobacterial cells. The significance of this research is that it addresses a contaminant of emerging concern in drinking water. The USEPA has listed cyanotoxins as one of the contaminants of concern in both the Candidate Contaminant List 3 and 4 (CCL-3 and 4).<sup>27</sup> Furthermore, this research advances the understanding of high energy electron beam (eBeam) technology being utilized for environmental applications.

### **Research Objectives**

The overall objective of this research was to determine the effects of high energy electron beam (eBeam) doses on both the degradation of microcystin-LR (MC-LR) and the survival of *Microcystis aeruginosa*. The central hypothesis was that high energy electron beam technology is able to inactivate *M. aeruginosa*, as well as break down MC-LR into non-toxic constituents in drinking water. The long-term goal of this project is to establish the scientific foundation for implementing eBeam technology into drinking water treatment for MC-LR and *M. aeruginosa*.

### *Specific Objectives*

The central hypothesis was investigated by pursuing the following specific aims:

1. To determine the mechanisms of inactivation of *M. aeruginosa* cells at various eBeam doses. Working hypothesis: Low doses of electron beam will result in inactivation of *M. aeruginosa* cells preventing further synthesis of MC-LR.
2. To identify degradation products of MC-LR and their associated toxicity.

Working hypothesis: Exposure of MC-LR to electron beam doses will result in

increasing amounts of structural variants of MC-LR with decreased toxicity proportional to increasing doses.

3. To demonstrate that eBeam technology can degrade MC-LR in surface water samples from multiple geographic locations. Working hypothesis: MC-LR is susceptible to eBeam doses irrespective of water chemistry.

## CHAPTER II

### LITERATURE REVIEW\*

#### **Introduction**

The increasing occurrence of harmful algal blooms (HABs) is contributing to the decrease of an already dwindling water supply worldwide. HABs occur due to ecosystem imbalances where large colonies of algae and/or cyanobacteria grow out of control and release odor and taste compounds, as well as harmful toxins, into the surrounding waterbody.<sup>20</sup> Increased occurrence of HABs can be attributed to rising temperatures and escalating anthropogenic nutrient pollution (namely nitrogen [N] and phosphorus [P]) in affected waterbodies.<sup>4</sup> However, no one factor has been identified as the cause of these blooms.<sup>28</sup> The resulting eutrophication prompts accelerated algal and cyanobacterial growth developing into thick mats of green biomass.

The main culprits of freshwater blooms are not eukaryotic algae, but cyanobacteria (previously classified as blue green algae). Therefore, they will be referred herein as cyanoHABs. Cyanobacteria differ from heterotrophic bacteria in that they are the only phylum of bacteria that use oxygenic photosynthesis as their main form of energy. Certain cyanobacteria are also able to reduce nitrogen and carbon in aerobic conditions which has aided in their evolution and their ability to exist in marine, freshwater, and dry habitats.<sup>29</sup> Many species also produce various toxic secondary metabolites (cyanotoxins). It is estimated that approximately 75% of cyanobacterial

\*Adapted with permission from: "A critical review of ionizing irradiation technologies for the remediation of waters containing Microcystin-LR and *M. aeruginosa*" by Folcik, A. M., & Pillai, S. D., 2020. *Radiation Physics and Chemistry*, 109128, Copyright 2020 by Elsevier.

blooms exhibit toxicity.<sup>28</sup> The following sections examine the most common classes of cyanotoxins and their associated toxicities.

## *Microcystins*

### *History of Microcystins*

Toxic algal blooms have been noted in literature as far back as 1878 when George Francis published “Poisonous Australian Lake.”<sup>30</sup> Francis described the presence of thick algae as looking like green oil paint inches deep on Lake Murray, as well as the death of livestock following ingestion of the green muck. Animal lethalties due to MC-LR have since been reported in a variety of species, including: flamingos, cattle, dogs, ducks, laboratory rats and mice, turtles, etc.<sup>31-38</sup>

The largest human intoxication event occurred in 1996 when a hemodialysis center in Caruaru, Brazil experienced the largest modern day human microcystin poisoning due to contaminated water used in treatment. 100 patients developed acute liver failure after being exposed to 19.5 µg/L of MC intravenously during treatment. Of these patients, 76 died of the resulting liver failure.<sup>18,19</sup> A study that followed soon after correlated chronic sublethal ingestion of microcystins in drinking water with an increased incidence of liver cancer in China.<sup>39</sup> Recently in 2011, the Kansas Department of Health and Environment received 25 reports of human illness due to cyanotoxins. Seven of the reports were confirmed by follow up and symptoms were consistent with MC exposure. Fortunately, there were no fatalities.<sup>40</sup>

### *Microcystin Producing Genera*

Of particular importance to human health are microcystins. Microcystins (MCs)

are a group of hepatotoxic cyanotoxins produced by a variety of cyanobacteria including: *Microcystis spp.*, *Anabaena spp.*, and *Plankthotrix spp.*, and to a lesser extent *Dolichospermum spp.*, *Geitlerinema spp.*, *Leptolyngbya spp.*, *Pseudanabaena spp.*, *Synechococcus spp.*, *Spirulina spp.*, *Phormidium spp.*, *Nostoc spp.*, *Oscillatoria spp.*, and *Radiocystis spp.*<sup>8</sup> *Microcystis aeruginosa* is the most common cyanobacterial species found in freshwaters worldwide and has been associated with a number of human, livestock, and wildlife poisonings.<sup>41</sup> *M. aeruginosa* commonly produces Microcystin-LR (MC-LR) which is the most toxic and most prevalent of the over 200 identified variants of MCs.<sup>7,8</sup>

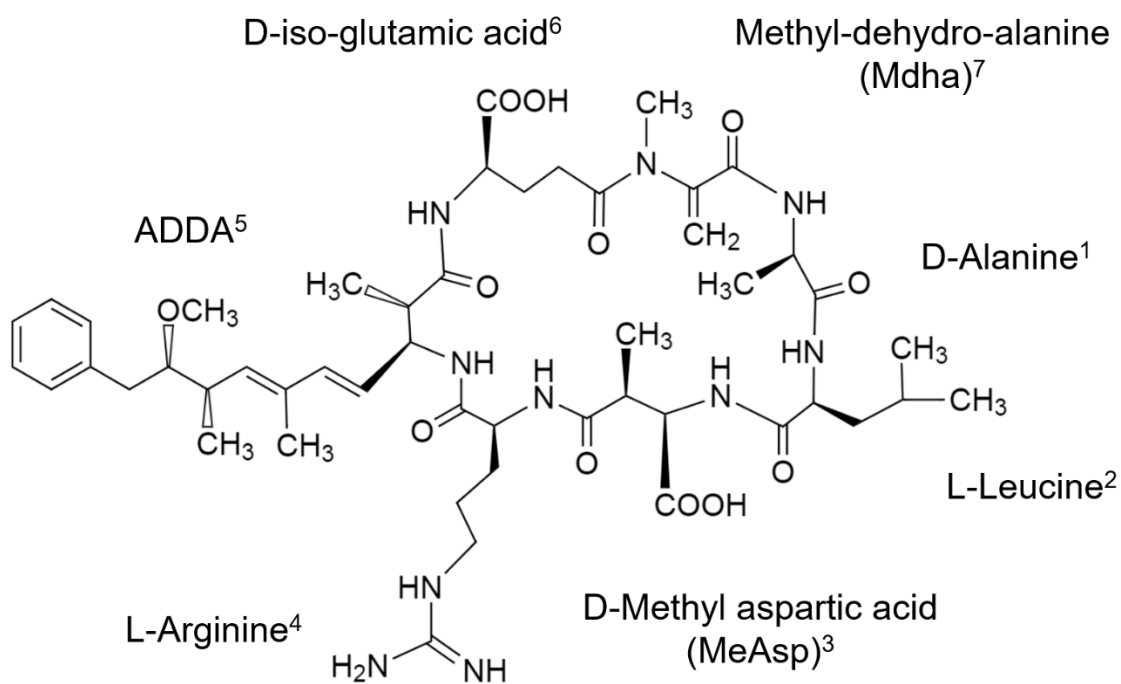


Figure 1. The chemical structure of Microcystin-LR. Created with ChemDraw.

Microcystin Structure

All MCs share a common structure including a cyclic heptapeptide ring containing 3 D-amino acids (alanine, glutamic acid, and methylaspartic acid), two ‘unusual’ amino acids (N-methyldehydroalanine and 3-amino-9-methoxy-2,6,8-trimethyl-10-phenyldeca-4,6-dienoic acid (ADDA)), and two variable L-amino acids (X and Z).<sup>20</sup> MC-LR (995.2 g/mol) contains leucine and arginine in the X and Z positions, respectively, and accounts for 46–99.8% of total HAB microcystin concentrations (Fig. 1).<sup>42</sup> Other less common variants include MC-LA, MC-YR, MC-RR, MC-LF, and MC-LW, however, these variants have varying levels of toxicity that are less than that of MC-LR.

#### *Mechanism of Toxicity*

MC-LR's biologic activity is attributed to the ADDA moiety and simple stereochemical changes to this group have been shown to drastically reduce the molecule's toxicity.<sup>43,44</sup> Once ingested, MC-LR cannot diffuse through the cells' plasma membranes due to its large size and therefore requires an active uptake mechanism to enter cells. A study by Eriksson et al. (1990) determined through the use of radiolabeled MC-LR that up-take seems to be explicit to hepatocytes within the liver.<sup>45</sup> Specifically, MC-LR was seen to enter hepatocytes through active transport via transporters in the organic anion transporting polypeptide (OATP) superfamily (Fig. 2).<sup>46,47</sup>

To further understand OATP roles in uptake, a study by Fisher et al. (2003) identified that MC-LR may have specificity for rat OAT1b2 as other cells expressing OATP transporters did not allow crossing of MC-LR.<sup>46</sup> Further, OATp1b2-null mice demonstrated complete resistance to hepatotoxicity due to MC-LR exposure.<sup>48</sup> These



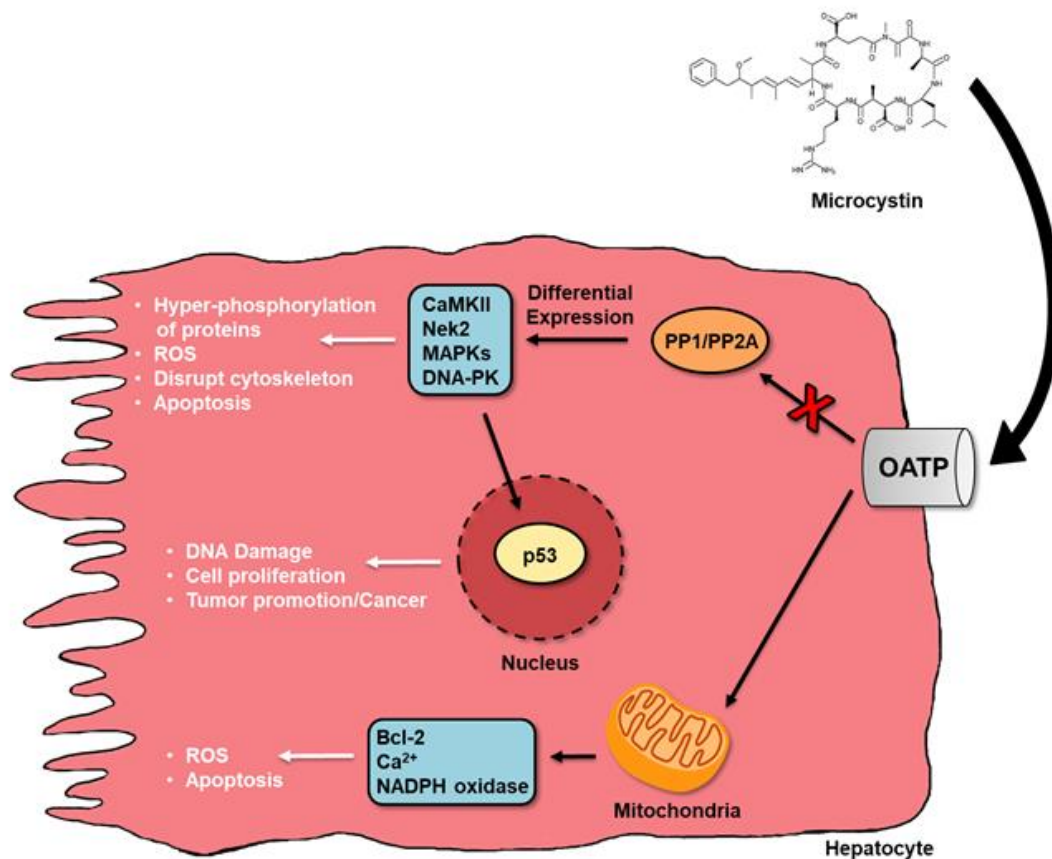


Figure 2. Microcystin-LR mechanism of action. Adapted from Valerio et al. (2010).<sup>34</sup> Was published open access in *Toxins* and is covered under a Creative Commons Attribution License (<https://creativecommons.org/licenses/by-nc-sa/3.0/>). Organic anion transporting polypeptide (OATP), protein phosphatase 1 and 2A (PP1/PP2A), calcium-calmodulin-dependent multifunctional protein kinase II (CaMKII), mitogen-activated protein kinases (MAPKs).

studies suggest that only particular OATPs are capable of transporting MC-LR across cell membranes. Other cells, such as oocytes expressing other OATP members, were not found to transport MC-LR further suggesting a specificity for certain OATP transporters. Using this same oocyte expression system in *Xenopus laevis*, Fischer et. al (2004) identified human OATP1B1, OATP1B3, and OATP1A2 as favored transport family members.<sup>46</sup>

After entering the cell, the most thoroughly studied pathways for MC-LR activity is through the inhibition of serine/threonine protein phosphatases.<sup>49</sup> MC-LR has strong affinity for protein phosphatases 1 and 2A (PP1 & PP2A), binding irreversibly to the catalytic subunits of the enzymes, rendering them inactive. Research has suggested the mechanism of binding is that of two steps: first, with binding of the ADDA moiety of MC-LR to the enzyme, and second, with the creation of covalent adducts preventing disassociation.<sup>49</sup> The toxin binding occurs at three places within the phosphatase enzyme including the D-glutamic acid on MC-LR with the catalytic metal atoms of the phosphatase, the carboxyl group of the MeAsp on MC-LR with the arginine and tyrosine on the phosphatase blocking the active site, and finally the ADDA moiety on MC-LR with the hydrophobic groove region on the phosphatase also adjacent to the active site.<sup>50</sup>

Given their importance in cell function and cell cycle regulation, pathways involved with MC-LR toxicity are primarily mediated by the normal functions of PP1 and PP2A. Normally, phosphatases are responsible for reversible phosphorylation of regulatory enzymes within the cell. After inhibition, loss of dephosphorylation ability has been shown to activate calcium-calmodulin-dependent multifunctional protein kinase II (CaMKII) which could regulate downstream ROS formation. Inhibition of phosphatases also activates Nek2 kinase through binding with the Nek2/PP1 holoenzyme complex potentially resulting in the deregulation of mitotic progression and chromosome segregation. This pathway could be responsible for tissue injury and/or tumor development. Finally, PP2A mediates the expression of mitogen-activated protein kinases (MAPKs) which are responsible for moderating proto-oncogene expression,

mitosis, differentiation, proliferation, and cell survival and apoptosis. Disruption of MAPK mediation can lead to downstream effects in all areas, respectively.<sup>47</sup>

MC-LR has also been associated with genotoxic effects in addition to its cytotoxic effects. A study completed by Douglas et al. (2001) identified that MC-LR phosphorylase inhibition further led to the phosphorylation-induced loss of the activity of DNA-dependent protein kinase (DNA-PK). This in turn is linked to the inhibition of two DNA repair pathways, nucleotide excision repair (NER) and double strand break repair by nonhomologous end joining (NHEJ).<sup>51</sup> Additionally, the activity of the nuclear phosphoprotein P53 is likely deregulated in part by MC-LR toxicity. P53 is a substrate of PP2A and plays important roles as a transcriptional trans-activator in DNA repair, apoptosis, and tumor suppression pathways.<sup>50</sup> Genotoxic effects may induce mitochondrial apoptosis through deregulation of P53. P53 also regulates the expression of Bcl-2 gene family members responsible for anti- and proapoptotic- signaling. These genes also play important roles in the mitochondrial-dependent apoptosis pathway.<sup>47</sup>

A final, less understood, pathway that may be involved in MC-LR toxicity includes the cell's mitochondria and two potential pathways have been suggested.<sup>47</sup> The first involves a large  $\text{Ca}^{2+}$  influx induced by MC-LR which permeabilizes the outer-membrane of the mitochondria leading to mitochondrial apoptosis. Second, reactive oxygen species generation may increase the NADPH oxidase activity within the mitochondria.<sup>47</sup> Mitochondrial damage from MCs has been linked to effects in the liver, kidney, heart, and reproductive organs.<sup>52</sup>

### Metabolism and Biotransformation

MC metabolism and biotransformation are still relatively unknown for many species. Kondo et al. (1990) determined synthetically, and then in both mice and rats, that MCs can be conjugated to glutathione (GSH) and cysteine conjugates. They also identified a third product resulting from epoxidation followed by hydrolysis and sulfate conjugation of the ADDA group coupled with GSH conjugation at the Mdha group on MC.<sup>53</sup> These conjugation steps with GSH and MC are suggested to play a role in the detoxification metabolism of MCs. A second study by the Kondo group dosed rats with MC-LR and identified the same biotransformed MCs as phase 2 metabolism products being a glutathione conjugate, a cysteine conjugate, and an oxidized ADDA diene conjugate.<sup>54</sup> It is thought that MC metabolism, as with many other xenobiotics, is catalyzed by cytochrome p450 oxidases and glutathione S-transferases (GSTs). The biotransformed products may then be excreted from the cells and eliminated via the bile. However, this pathway has not yet been confirmed for MC-LR or other MCs.<sup>50</sup>

### Organ Toxicity

In general, MCs are liver toxins targeting hepatocytes as discussed in the ‘ Mechanism of ’ section. At the organ level, MC-LR’s mode of action exhibits as liver inflammation, hemorrhage, acute pneumonia, and the potential promotion of tumors in the liver and testes.<sup>26,55</sup> Acute recreational exposure to MC-LR has been linked to skin irritations, allergic reactions, abdominal pain, headache, sore throat, vomiting, nausea, diarrhea, and blistering of the mouth.<sup>56,57</sup> The EPA’s Cyanotoxin Public Fact-sheet also lists liver inflammation and hemorrhage, acute pneumonia, acute dermatitis, kidney damage, and potential tumor growth promotion as MC-LR’s potential health

effects.<sup>26</sup> However, liver failure due to hemorrhaging and hepatocyte death are the most direct MC-LR health effects.

In November 2006, the EPA released its Toxicological Review of microcystins LR, RR, YR, and LA to investigate the potential hazard of microcystins as they are currently an unregulated class of water contaminants.<sup>58</sup> In the assessment, the reviewers were able to derive short-term, subchronic, and chronic oral RfDs for MC-LR. The short-term and subchronic exposure RfD was derived to be 0.006  $\mu\text{g}/\text{kg}\text{-day}$ . However, an uncertainty factor (UF) of 1000 was used to account for interspecies extrapolation, interindividual variability, and database deficiencies, which suggests that there is a large deficiency in knowledge regarding these molecules. The chronic RfD was derived to be 0.003  $\mu\text{g}/\text{kg}\text{-day}$  with the same 1000 UF using a free-standing no observed adverse effect level (NOAEL) from a female mouse study. The review further failed to report RfDs for the other assessed congeners as well as inhalation RfCs for any microcystin due to inadequate quality of evidence in the literature.<sup>58</sup> In 2010, the International Agency for Research on Cancer (IARC) investigated the potential carcinogenic effects of nitrates and cyanotoxins. They concluded to list MC-LR as possibly carcinogenic to humans (group 2B), however, they note that there is strong evidence that supports a plausible tumor promoter mechanism.<sup>55</sup> Most recently in 2015, the EPA released a second report titled, “Health Effects Support Document for the Cyanobacterial Toxin Microcystins.” In this document, the reviewers concluded to raise the RfD for MCLR to 0.05  $\mu\text{g}/\text{kg}\text{-day}$  based upon a subchronic rat study completed in 1999. As mentioned previously, there is no current enforced regulation for the presence of MCs in water. The

EPA has published a 10-day drinking water health advisory of 0.3 µg/L for bottle-fed infants and pre-school children and 1.6 µg/L for school-age children and adults.<sup>59</sup>

### Regulations Governing Microcystins

Human exposure to MCs primarily occurs through ingestion of contaminated water during recreational activities or via insufficiently treated drinking water. The first provisional drinking water guideline for MC-LR was released in 1998 by the World Health Organization (WHO). Using a 13-week mouse study, the WHO suggested a guideline value of 1 µg/L based upon a NOAEL of 40 µg kg<sup>-1</sup> bodyweight d<sup>-1</sup>.<sup>33</sup> In the majority of countries that regulate MC-LR in drinking water and recreational sources, this original WHO guideline value (or the underlying TDI of 0.04 µg kg<sup>-1</sup> bodyweight) is used.<sup>60</sup> Table 1 shows guideline values used by various countries for regulation of cyanotoxins in drinking water.

Within the United States, MCs and other cyanotoxins are not regulated via the Safe Water Drinking Act.<sup>5</sup> Cyanotoxins were listed on the EPA's third drinking water Candidate Contaminate List (CCL-3), as well as the following CCL-4. The purpose of the CCL is to identify drinking water contaminants that are known to occur in public water systems, but that are not currently subject to any drinking water regulations. However, their inclusion on the previous CCL's has not resulted in regulation.

The US EPA published a 10-day drinking water health advisory (HA) for microcystins at 0.3 µg/L for bottle fed infants and pre-school children and 1.6 µg/L for school-age children and adults.<sup>61</sup> However, due to HAs not being true federal regulations, many states have been hesitant to enforce it. As of 2016, Minnesota, Ohio,

Table 1. Examples of international regulations and guidance values for cyanotoxins in drinking water. Adapted from Ibelings et al. (2015).<sup>60</sup>

Country or Source Document	Specific Cyanotoxins and/or Cyanobacteria Regulated	Regulation Values*	Comments
WHO	Microcystin-LR	(P)GV: 1 µg/L	Considered provisional due to database limitations.
Argentina	Does not have country requirements for RMF or cyanotoxin surveillance; some water utilities have implemented RMF and/or cyanotoxin surveillance and refer to WHO (P)GV of 1 µg/L		
Australia	Microcystin (toxicity equivalents of Microcystin-LR): equivalent to 6500 cells/ml or a biovolume of 0.6 mm <sup>3</sup> /L of a highly toxic strain of <i>Microcystis aeruginosa</i>	GV: 1.3 µg/L	The Australian Drinking Water Guidelines (2011) are a set of national guidelines which include fact sheets with information on key cyanotoxins.  Health Alert can be triggered by the toxin concentrations or the equivalent cell or biovolume concentrations. Trigger levels for each of the four key toxin-producing species are also provided for immediate notification to the health authority.  Individual states/territories use the national framework as the basis for their specific regulatory requirements.
	Nodularin: HAL at 40,000 cells/ml or a biovolume of 9.1 mm <sup>3</sup> /L of a highly toxic strain of <i>Nodularia spumigena</i>	--	
	Cylindrospermopsin: equivalent to 15,000 – 20,000 cells/ml or a biovolume of 0.6 – 0.8 mm <sup>3</sup> /L of <i>Cylindrospermopsis raciborskii</i>	HAL: 1 µg/L	
	Saxitoxins (toxicity equivalents to saxitoxin): equivalent to 20,000 cells/ml or a biovolume of 5 mm <sup>3</sup> /L of a highly toxic strain of <i>A. circinalis</i>	HAL: 3 µg/L	
Brazil	Cyanobacteria	GV: 10,000 – 20,000 cells/ml or 1 mm <sup>3</sup> /L biovolume	> 10,000 cells/ml weekly monitoring is required; > 20,000 cells/ml toxicity testing and/or quantitative cyanotoxin analysis in drinking-water are required
	Microcystins	S: 1 µg/L	
	Cylindrospermopsin	GV: 15 µg/L	
	Saxitoxin	GV: 3 µg/L	

Table 1. Continued

Country or Source Document	Specific Cyanotoxins and/or Cyanobacteria Regulated	Regulation Values*	Comments
Canada	Microcystin-LR	MC: 1.5 µg/L	MC is considered protective against exposure to other microcystins; monitoring frequencies driven by bloom occurrence – more frequent where there is a history of bloom formation
	Anatoxin-a	(P)MC: 3.7 µg/L	Only regulated in Quebec
Czech Republic	Cyanobacteria in raw water (determined via cell counts, biomass, or chlorophyll-a concentration)	≥ 1 colony/ml or ≥ 5 filaments/ml	Vigilance Level: quantification of cyanobacteria in the raw water at least once per week; visual observations of the abstraction point (water blooms at the surface of water level)
		≥ 2,000 cells/mL or ≥ 0.2 mm <sup>3</sup> /L biovolume or ≥ 1 µg/L chlorophyll-a	Alert Level 1: attempt reduction by changing abstraction depth. If that is not possible, ascertain that treatment sufficiently reduces cyanobacteria and toxins (data from operational parameters, if necessary also toxin analyses)
		≥ 100,000 cells/mL or ≥ 10 mm <sup>3</sup> /L biovolume or ≥10 µg/L chlorophyll-a	Alert Level 2: Same as Alert Level 1, but with stronger emphasis on treatment efficacy and microcystin monitoring
	Microcystin-LR in treated water	S: 1 µg/L	Monitored once per week in treated water
Cuba	Phytoplankton	< 20,000 cells/ml	Monthly visual inspection and sampling at least four months a year
	Cyanobacteria	≤ 1500 cells/ml	
	Phytoplankton and Cyanobacteria	20,000 – 100,000 cells/ml with >50% cyanobacteria	Alert: increased sampling (weekly and more sites); daily inspection; notification to public health unit and local managers; report to local government; warning of the public
	Cyanobacteria (known to be toxic)	At least one known toxic species	
	Reported toxic effects (human or animal)		Action: Same as for “Alert”, but with increased actions for public communication and water use restrictions
	Scum: consistently present or confirmed bloom persistence		



Table 1. Continued

Country or Source Document	Specific Cyanotoxins and/or Cyanobacteria Regulated	Regulation Values*	Comments
Denmark	No cyanotoxin drinking water regulation but use WHO (P)GV of 1 µg/L when needed		
France	Microcystins (total)	S: 1 µg/L	Analysis required in raw water at the point of distribution only when cyanobacteria proliferate (determined by visual observation and/or analytical analysis)
Finland	Cyanobacteria (potentially toxic) in raw water: as cell counts or biomass; biomass is equal to biovolume assuming a 1:1 ratio of volume to mass	> 5000 cells/ml or > 1 mg/L biomass	Microcystin monitoring; enhanced treatment
		> 100,000 cells/ml or > 20 mg/L biomass	Change of abstraction site and/or restrictions of water use; information to the water users, particularly if microcystins are found in finished drinking water
	Microcystins (total) in raw water	> 1 µg/L	
	Microcystins (total) in finished drinking water	GV: > 1 µg/L	Restrictions for water use
		GV: > 10 µg/L	Ban on water use
Germany	No specific cyanotoxin regulations as only ~20% of water supply is from surface water and from well protected reservoirs. However, for nonregulated chemicals, the Drinking-water Ordinance requires that they do not occur in hazardous concentrations. On this basis, where cyanobacteria do occur, the WHO (P)GV can be applied for microcystins. National guidance for substances with incomplete toxicological evidence proposes <0.1 µg/L if carcinogenesis cannot be excluded (until data are generated that allow higher levels), and this can be applied to Cylindrospermopsin.		
Hungary	Drinking-water legislation includes “biological parameters” to be monitored by microscopy, e.g cyanobacteria		The frequency of examination is based on amount of water supplied and source of drinking water (cyanobacteria if source is surface water); at least once a year for every network for all biological parameters
Italy	National decree includes “algae” as accessory parameter to monitor if local authorities presume a risk. For this assessment, it uses the provisional WHO (P)GV of 1 µg/L for Microcystin-LR.		

Table 1. Continued

Country or Source Document	Specific Cyanotoxins and/or Cyanobacteria Regulated	Regulation Values*	Comments
Netherlands	No specific regulations for cyanotoxins in drinking water, although about 40% of water supply is from surface water, mainly from well protected reservoirs and infiltration basins. However, concentrations of micro-organisms may not exceed levels which may have adverse consequences for public health. For the production of drinking water, there are barriers in the treatment process to prevent cyanobacterial cells and microcystins from reaching finished drinking water. In case contamination should happen, the Netherlands would apply WHO guidance.		
New Zealand	Microcystins (as MC-LR equivalents)	(P)MV: 1.3 µg/L	Effective implementation of the protocols required by Public Health Risk Management Plans (PHRMPs) has prevented concentrations > (P)MV from reaching the consumers
	Cylindrospermopsin	(P)MV: 1 µg/L	
	Saxitoxin	(P)MV: 1 µg/L	
	Anatoxin-a	(P)MV: 6 µg/L	
	Anatoxin-a(s)	(P)MV: 1 µg/L	
	Homoanatoxin-a	(P)MV: 2 µg/L	
	Nodularin	(P)MV: 1 µg/L	
Singapore	Microcystin-LR	(P)MV: 1 µg/L	Every supplier of piped drinking water is legally required to prepare and implement a water safety plan to ensure that the piped drinking water supplied complies with the piped drinking water standards (stated as 1 µg/L for total microcystin-LR, in free and cell-bound forms).
Poland	GV for Microcystin-LR is excluded from Polish legislation because EU Drinking Water Directive does not include cyanotoxins		
Spain	Microcystins	S: 1 µg/L	To be analyzed when eutrophication is evident in the water sources.

Table 1. Continued

Country or Source Document	Specific Cyanotoxins and/or Cyanobacteria Regulated	Regulation Values*	Comments
Turkey	Cyanobacteria	> 5000 cells/ml or > 1 µg/L chlorophyll-a	Monthly analysis if in raw water; if exceeded, weekly sampling (of water column) and toxin analysis
	Microcystins (total)	1 µg/L MC-LR equivalents	If > 1 µg/l, toxin analysis in treated water and advanced treatment (ozonation or active carbon) or alternative water supply
United States	Cyanotoxins	--	Not regulated under the safe drinking water act. However, cyanotoxins have been listed on CCL 1 and 2. CCL 3 and 4, as well as UCMR 4 have included specifically microcystin-LR, cylindrospermopsin, anatoxin-a, etc.
	Microcystin-LR	HA: 0.3 µg/L for bottle fed infants/children HA: 1.6 µg/L for school age children and adults	10-day drinking water health advisory
	Cylindrospermopsin	HA: 0.7 µg/L for bottle fed infants/children HA: 3 µg/L for school age children and adults	
Uruguay	Microcystin-LR	S: 1 µg/L	Decree: "Drinking water should not contain amounts of cyanobacteria that could affect water characteristics or human health"
South Africa	Microcystin-LR	GV: 1 µg/L	Supported by guidelines for chlorophyll-a and cyanobacterial cell counts

\*S = Standard Value; GV = Guideline Value; MC = Maximum Concentration; MV = Maximum Value; HAL = Health Alert Level; HA = Health Advisory; (P) = Provisional

Table 2. State regulations and guidance values for cyanotoxins in drinking water and recreational water.

State	State Government HAB Resources	Monitoring Data Published	Drinking Water Guidance/Action Level <sup>62</sup>	Recreational Water Guidance/Action Level <sup>62</sup>
Alabama	<a href="#">General information</a>	N		
Alaska	<a href="#">Alaska Harmful Algal Bloom Network</a>	N		
Arizona	<a href="#">General information</a> ; <a href="#">Arizona Water Watch</a>	Y – reporting app available		
Arkansas	<a href="#">HAB Management Plan</a> ; <a href="#">HAB Complaint Form</a>	N		
California	<a href="#">California HABs Portal</a>	Y		<u>Advisory:</u> Microcystin-LR: 0.8 µg/L Anatoxin-a: 90 µg/L Cylindrospermopsin: 4 µg/L
Colorado	<a href="#">General information</a>	N		
Connecticut	<a href="#">General information</a>	N		<u>Visual Rank Category 1:</u> Visible material not likely, cyanobacteria/water is gen. clear.  <u>Visual Rank Category 2:</u> Cyanobacteria present in low numbers. There are visible small accumulations but water is generally clear.  <u>Visual Rank Category 3:</u> Cyanobacteria present in high numbers. Scums may/not be present. Water is discolored. Large areas affected. Color assists to rule out sediment and other algae. Resulting posted beach closure

Table 2. Continued

State	State Government HAB Resources	Monitoring Data Published	Drinking Water Guidance/Action Level <sup>62</sup>	Recreational Water Guidance/Action Level <sup>62</sup>
Delaware	<a href="#">General information (red tide)</a> ; <a href="#">Citizen Monitoring Program</a>	Y		
Florida	<a href="#">Algal Bloom Dashboard</a>	Y		
Georgia	<a href="#">General information</a>	N		
Hawaii	None	N		
Idaho	<a href="#">General information</a>	N		<u>'Recommended' Posting:</u> - Surface scum visible and associated with toxigenic taxa - Sum of all potentially toxigenic taxa $\geq 100,000$ clls/ml - The density of Microcystis of Planktothrix $>40,000$ cells/ml
Illinois	<a href="#">General information</a> ; <a href="#">Monitoring data</a>	Y		<u>Local Lake Management Informed</u> Microcystin-LR: approach or exceed $10 \mu\text{g/L}$

Table 2. Continued

State	State Government HAB Resources	Monitoring Data Published	Drinking Water Guidance/Action Level <sup>62</sup>	Recreational Water Guidance/Action Level <sup>62</sup>
Indiana	<a href="#">General health information</a> ; <a href="#">Blue-green algae information</a>	Y		<p><u>Level 1: Use common sense practices</u> Very low/no risk &lt; 4 µg/L microcystin-LR</p> <p><u>Level 2: Reduce contact with water</u> Low to moderate risk 4 to 20 µg/L microcystin-LR</p> <p><u>Level 3: Consider avoiding water contact</u> Serious risk &gt; 20 µg/L microcystin-LR</p> <p><u>Warning Level:</u> Cylindrospermopsin: 5 µg/L</p>
Iowa	<a href="#">General information</a> ; <a href="#">Water Monitoring</a>	Y		<p><u>Caution:</u> Bloom present but no toxin data available</p> <p><u>Warning:</u> Microcystin-LR: ≥20 µg/L</p>

Table 2. Continued

State	State Government HAB Resources	Monitoring Data Published	Drinking Water Guidance/Action Level <sup>62</sup>	Recreational Water Guidance/Action Level <sup>62</sup>
Kansas	<a href="#">General information</a>	Y		<p><u>Public Health Advisory: Avoid contact</u>  Microcystin: &gt;4 µg/L to &lt;20 µg/L  Cyanobacterial cells: &gt;20,000 cells/ml to &lt;100,000 cells/ml</p> <p><u>Public Health Warning: All water contact restricted:</u>  Microcystin: &gt;20 µg/L  Cyanobacterial cells: &gt;100,000 cells/ml</p>
Kentucky	<a href="#">Harmful Algal Bloom Viewer</a> ; <a href="#">General information</a>	N		<p><u>Advisory: Contact Discouraged</u>  Cyanobacterial cells: &gt;20,000 cells/ml</p> <p><u>Caution: Closure/Contact Prohibited</u>  Cyanobacterial cells: &gt;100,000 cells/ml</p>
Louisiana	None	N		
Maine	<a href="#">General information</a>	N		
Maryland	<a href="#">General information</a> ; <a href="#">Interactive Bloom Map</a>	Y		
Massachusetts	<a href="#">General information</a>	N		<p><u>Advisory: Avoid Contact with Water</u>  Microcystin-LR: 14 µg/L  Cyanobacterial cells: ≥70,000 cells/ml</p>
Michigan	<a href="#">General information</a>	Y		

Table 2. Continued

State	State Government HAB Resources	Monitoring Data Published	Drinking Water Guidance/Action Level <sup>62</sup>	Recreational Water Guidance/Action Level <sup>62</sup>
Minnesota	<a href="#">General information</a>	Y	Microcystin-LR: 0.1 µg/L Anatoxin-a: 0.1 µg/L	
Mississippi	<a href="#">General information</a> ; <a href="#">Mississippi Beach Monitoring Program</a>	N		
Missouri	<a href="#">General information</a>	N		
Montana	<a href="#">General information</a>	N		
Nebraska	<a href="#">General information</a> ; <a href="#">Beach Watch</a>	Y		<u>Health Alert:</u> Microcystin-LR: ≥20 µg/L
Nevada	<a href="#">General information</a>	N		
New Hampshire	<a href="#">General information</a> ; <a href="#">Beach Tracker</a>	N		<u>Public Health Advisory:</u> >50% of cell counts from toxigenic cyanobacteria
New Jersey	<a href="#">HAB Events System</a> ; <a href="#">General information</a>	N		
New Mexico	<a href="#">General Fact Sheet</a>	N		
New York	<a href="#">General information</a> ; <a href="#">NYHABs Reporting System</a>	Y		
North Carolina	<a href="#">General information</a> ; <a href="#">Algal Bloom Report Dashboard</a>	Y		<u>Advisory/Closure:</u> Visible discoloration of the water or a surface scum may be considered for microcystin testing
North Dakota	<a href="#">General information</a> ; <a href="#">HAB Map</a>	N		



Table 2. Continued

State	State Government HAB Resources	Monitoring Data Published	Drinking Water Guidance/Action Level <sup>62</sup>	Recreational Water Guidance/Action Level <sup>62</sup>
Ohio	<a href="#">Information for Recreational Waters;</a> <a href="#">Information for Public Water Systems</a>	Y	<u>Do Not Drink (children &lt;6 and sensitive populations)</u> Microcystin: 0.3 µg/L Anatoxin-a: 20 µg/L Cylindrospermopsin: 0.7 µg/L Saxitoxin: 0.2 µg/L  <u>Do Not Drink (children &gt;6 and adults)</u> Microcystin: 1.6 µg/L Anatoxin-a: 20 µg/L Cylindrospermopsin: 3.0 µg/L Saxitoxin: 0.2 µg/L	<u>Public Health Advisory: swimming/wading not recommended</u> Microcystin-LR: 6 µg/L Anatoxin-a: 80 µg/L Cylindrospermopsin: 5 µg/L Saxitoxin: 0.8 µg/L  <u>No Contact Advisory: avoid all contact</u> Microcystin-LR: 20 µg/L Anatoxin-a: 300 µg/L Cylindrospermopsin: 20 µg/L Saxitoxin: 3 µg/L
Oklahoma	<a href="#">General information</a>	N		<u>Blue-Green Algae Awareness Level Advisory:</u> Microcystin: >20 µg/L Cyanobacterial cells: ≥100,000 cells/ml

Table 2. Continued

State	State Government HAB Resources	Monitoring Data Published	Drinking Water Guidance/Action Level <sup>62</sup>	Recreational Water Guidance/Action Level <sup>62</sup>
Oregon	<a href="#">General information</a> ; <a href="#">Current Cyanobacteria Advisories</a> ; <a href="#">Cyanotoxin Resources for Drinking Water</a>	Y	<u>&lt;5 years</u> Microcystin: 0.3 µg/L Anatoxin-a: 0.7 µg/L Cylindrospermopsin: 0.7 µg/L Saxitoxin: 0.3 µg/L  <u>Adults</u> Microcystin: 1.6 µg/L Anatoxin-a: 3 µg/L Cylindrospermopsin: 3 µg/L Saxitoxin: 1.6 µg/L	<u>Public Health Advisory:</u> - Option 1: Visible scum and cell count or toxicity - Option 2: Toxigenic species >100,000 cells/ml - Option 3: Microcystis or Planktothrix >40,000 cells/ml - Option 4: Microcystin: 10 µg/L Anatoxin-a: 20 µg/L Cylindrospermopsin: 6 µg/L Saxitoxin: 100 µg/L
Pennsylvania	<a href="#">General information</a> ; <a href="#">Erie County HABs information</a>	N		
Rhode Island	<a href="#">General information</a>	N		<u>Health Advisories:</u> Visible cyanobacterial scum or mat and/or Microcystin-LR: ≥14 µg/L and/or Cyanobacterial cells: ≥70,000 cells/ml
South Carolina	<a href="#">General information</a> ; <a href="#">S.C. Beach Guide</a>	N		
South Dakota	<a href="#">General information</a>	N		
Tennessee	<a href="#">General information</a>	N		

Table 2. Continued

State	State Government HAB Resources	Monitoring Data Published	Drinking Water Guidance/Action Level <sup>62</sup>	Recreational Water Guidance/Action Level <sup>62</sup>
Texas	<a href="#">General information</a>	N		<u>Blue-Green Algae Awareness Level Advisory:</u> Microcystin: $\geq 20$ $\mu\text{g/L}$ Cyanobacterial cells: $\geq 100,000$ cells/ml
Utah	<a href="#">General information</a>	Y		
Vermont	<a href="#">General information</a> ; <a href="#">Cyanobacteria Tracker</a>	Y	Microcystin-LR: $\geq 0.16$ $\mu\text{g/L}$ Anatoxin-a: $\geq 0.5$ $\mu\text{g/L}$ Cylindrospermopsin: $\geq 0.5$ $\mu\text{g/L}$	<u>Beach Closure:</u> Visible presence of cyanobacterial scum and Microcystin-LR: $\geq 6$ $\mu\text{g/L}$ or Cyanobacterial cells: 4,000 cells/ml Anatoxin-a: $\geq 10$ $\mu\text{g/L}$

Table 2. Continued

State	State Government HAB Resources	Monitoring Data Published	Drinking Water Guidance/Action Level <sup>62</sup>	Recreational Water Guidance/Action Level <sup>62</sup>
Virginia	<a href="#">General information</a>	Y		<p><u>Local Agency Notification: bi-weekly sampling</u> Microcystis: 5,000 to &lt;20,000 cells/ml</p> <p><u>Public Notification: weekly sampling</u> Microcystis: 20,000 to 100,000 cells/ml</p> <p><u>Immediate Notification to Avoid All Recreational Activity: weekly sampling</u> Microcystis: &gt;100,000 cells/ml or Microcystin: &gt;6 µg/L or Blue-green algal scum or mats on water surface</p>
Washington	<a href="#">Washington State Toxic Algae</a>	Y		<p><u>Caution: When bloom is forming or a bloom scum is visible</u> <u>Warning: Toxic Algae Present</u> <u>Danger: Lake Closed</u></p> <p>Microcystin-LR: 6 µg/L Anatoxin-a: 1 µg/L Cylindrospermopsin: 4.5 µg/L Saxitoxin: 75 µg/L</p>
West Virginia	<a href="#">General information; HAB Response Plan for Recreational Waters</a>	N		

Table 2. Continued

<b>State</b>	<b>State Government HAB Resources</b>	<b>Monitoring Data Published</b>	<b>Drinking Water Guidance/Action Level<sup>62</sup></b>	<b>Recreational Water Guidance/Action Level<sup>62</sup></b>
Wisconsin	<a href="#">General information</a>	N		<u>Advisory/Closure:</u> >100,000 cells/ml or scum layer
Wyoming	<a href="#">Harmful Cyanobacterial Blooms</a> ; <a href="#">HCB Advisories Map</a>	N		

Oregon, and Vermont have issued state specific drinking water guidance or action levels for MCs (see Table 2).

### *Other Cyanotoxins*

There are a variety of other cyanotoxins that are produced in cyanoHABs in addition to MCs, such as: nodularins, saxitoxins, anatoxins, etc. These toxins are generally classified by their mode of action (ie. hepatotoxins, neurotoxins, and dermatotoxins) but may also be classified according to their chemical structures (ie. peptides, alkaloids, or lipidic compounds).<sup>63</sup> Table 3 displays the common cyanotoxins, producing genera, and primary mechanism of action in order of commonality.<sup>64,65</sup> Figure 3 displays chemical structures of these common cyanotoxins.

### *Nodularins*

Nodularins are another class of hepatotoxic cyanotoxins produced by *Nodularia spp.* Unlike MC producing genera, *Nodularia spp.* are generally responsible for blooms in brackish waters and estuarine environments. Nodularin's structure is closely related to that of MCs and is composed of a cyclic pentapeptide including the biologically active ADDA moiety. The remaining amino acids are D-erythro-β-methyl-aspartic acid (d-MAsp), L-arginine, D-glutamate, and N-methyldehydrobutyryne (Mdhb) (Figure 3).<sup>66</sup> Less structural variation is seen in nodularins than MCs and the mechanism of action is also similar to that of MCs. However, unlike MC, nodularins do not bind covalently, but instead non-covalently, to protein phosphatases 1 or 2A.<sup>64</sup> This may contribute to nodularins additional carcinogenic properties.<sup>67</sup> Effected tissues are primarily hepatocytes due to active transport of nodularins to the liver through bile, however,

Table 3. Common cyanotoxins, main producing genera, and primary mechanism of action.

<b>Toxin</b>	<b>Producing Genera</b>	<b>Associated Toxicity</b>	<b>Primary Mechanism of Action</b>
Microcystins	<i>Anabaena, Microcystis, Plankthotrix</i>	Hepato-	Inhibition of protein phosphatases (PP1 and PP2A)
Nodularins	<i>Nodularia</i>	Hepato-	Inhibition of protein phosphatases (PP1 and PP2A)
Saxitoxins	<i>Aphanizomenon, Anabaena, Cyndrospermopsis, Lyngbya</i>	Neuro-	Binding and blocking the sodium channels in neural cells
Anatoxins	<i>Anabaena, Aphanizomenon, Cyndrospermopsis, Microcystis, Oscillatoria, Planktothrix</i>	Neuro-	Binding irreversibly to the nicotinic acetylcholine receptors
Anatoxin – a	<i>Anabaena</i>	Neuro-	Inhibition of Ach-esterase activity
Cyndrospermopsin	<i>Anabaena, Aphanizomenon, Cyndrospermopsis, Raphidiopsis, Umezakia</i>	Hepato-	Inhibitor of protein biosynthesis cytogenetic damage on DNA
Lipopolysaccharide	Various	Various	Potential irritant; affects any exposed tissue

Adapted from Wiegand and Pflugmacher (2005) and Ferrão-Filho and Kozlowsky-Suzuki (2011).<sup>64,65</sup>

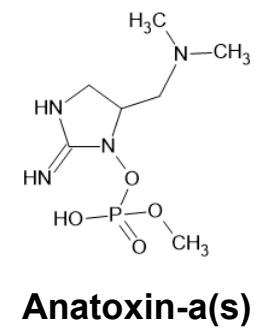
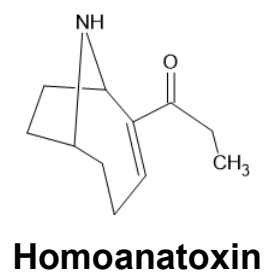
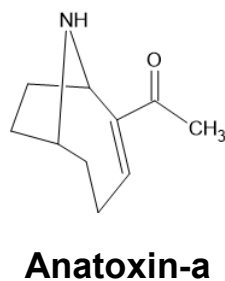
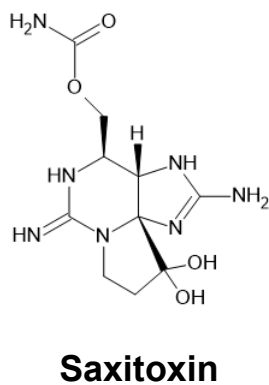
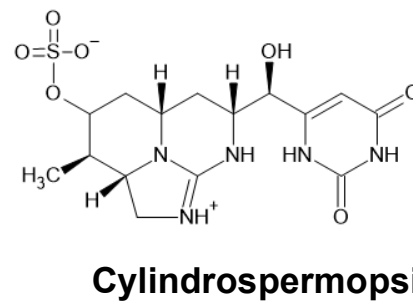
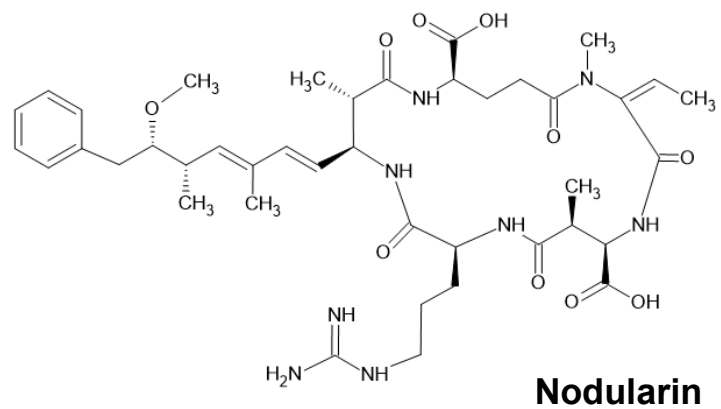


Figure 3. Chemical structures of common cyanotoxins. Created with ChemSketch.



specific methods of transport are still being investigated.

### Cylindrospermopsins

Cylindrospermopsin (CYN) is the third common hepatotoxic cyanotoxin. CYN is an alkaloid toxin with the primary producer being *Cylindrospermopsis raciborskii*.<sup>67</sup> Its chemical structure contains a central functional guanidino moiety and a hydroxymethyluracil group attached to a tricyclic carbon backbone (Figure 3).<sup>64</sup> CYN has been shown to cause liver, kidney, thymus, and heart toxicity in rodents, with irreversible inhibition of protein biosynthesis being the primary mode of action. Presence of an intact pyrimidine ring is necessary for toxic effects. Further, CYN has been shown to be mutagenic and possibly carcinogenic through the induction of DNA strand breakage and disruption of kinetochore spindles resulting in chromosome loss. Unlike MC and nodularin, CYNs small size allows for diffusion into cells instead of facilitation by active transport.<sup>64</sup>

### Saxitoxins

Cyano-neurotoxins, while not as common as the cyano-hepatotoxins, are very strong and fast acting toxins. In mouse bioassays, death occurs between two to 30 minutes due to respiratory arrest.<sup>68</sup> Saxitoxin, the most potent neurotoxin, is an alkaloid composed of a trialkyl tetrahydropurine with four variable positions resulting in more than 30 congeners (Figure 3).<sup>64,67</sup> Saxitoxins are produced by both dinoflagellates and cyanobacteria, with no one genus being mainly responsible. Saxitoxin produced by dinoflagellates is commonly known as paralytic shellfish poison (PSP) due to its accumulation in shellfish. Saxitoxin's main mechanism of action is the blocking of

neuronal transmission through binding to voltage-gated Na<sup>+</sup> channels in nerve cells. This in turn stops the influx of sodium resulting in muscle paralysis and respiratory arrest, leading to death.<sup>64</sup> The most common exposure to saxitoxins occur due to ingestion of shellfish and other organisms where saxitoxins can bioaccumulate. Human death has occurred following as little as 1 mg of the toxin.<sup>67</sup>

### Anatoxins

Anatoxins and their derivatives are a class of neurotoxic cyanotoxins produced by some cyanoHABs. Cyano-neurotoxins, while not nearly as common as the cyano-hepatotoxins, are very strong and fast acting toxins. In mouse bioassays, death has been seen to occur between two to 30 minutes due to respiratory arrest.<sup>68</sup> The three most common anatoxins include anatoxin-a, homoanatoxin, and anatoxin-a(s). Anatoxin-a and homoanatoxin are secondary amine alkaloids whereas anatoxin-a(s) is a unique phosphate ester of a cyclic N-hydroxyguanidine structure (Figure 3).<sup>64</sup> Anatoxin-a and homoanatoxin have similar LD<sub>50</sub> values (200-250 µg/kg) and both act by mimicking acetylcholine causing death by respiratory arrest.<sup>68</sup> Both toxins also bind irreversibly to nicotinic acetylcholine receptors leading to overstimulation of muscle cells from the influx of sodium ions. Anatoxin-a(s) is currently known to be exclusively produced by *Anabaena spp.* and exhibits toxicity through anticholinesterase activity. Anatoxin-a(s) is roughly 10 times more toxic to mice than anatoxin-a as seen by Carmichael et al. (1990).<sup>69</sup> However, the toxin has only been seen to occur rarely.<sup>68</sup>

### Lipopolysaccharides

A final class of cyanotoxins, the endotoxic lipopolysaccharides (LPS), are toxins

that are a part of the outer cell layer of the cyanobacteria wall and other gram-negative bacteria. These toxins consist of lipid A, core polysaccharides, and an outer polysaccharide chain. In cyanobacteria, the presence of a greater variety of long chain unsaturated fatty acids, hydroxy fatty acids, and the lack of a phosphate group distinguish this group of LPS from bacterial LPS.<sup>64</sup> Cyano-LPS are usually far less potent than those from enteric-bacteria but have been shown to be involved with fever induction, septic shock syndrome, and aggravation of toxicant-induced liver injury. Overall, cyano-LPS have shown much lower potency than those from bacteria.<sup>64</sup>

### *Remediation Strategies*

The increasing health concerns of MCs represents a critical need for further research into more effective removal and/or remediation strategies.<sup>70</sup> Current treatment relies on conventional oxidants (mainly ozone) to remove MCs in water. However, these conventional oxidants have varying levels of efficiency, are reliant on specific operational parameters for breakdown of pollutants and are often chemical additives which may create secondary harmful disinfection byproducts.<sup>20,24,25,71</sup> Other advanced oxidation processes (AOPs) or advanced oxidation reduction processes (AORPs) could present more efficient and chemical-free approaches for degrading MCs and other pollutants. In particular, ionizing radiation technologies have been proven effective at removing a variety of chemicals and biologics in water systems.<sup>72-76</sup>

### *Ionizing Radiation*

Ionizing radiation encompasses radiation that has sufficient energy to remove an electron from an atom. Gamma irradiation, electron beam (eBeam) irradiation, and X-

rays are three forms of ionizing radiation that are in commercial use today for food pasteurization, phytosanitary treatment of fresh produce, and for medical device sterilization.<sup>77</sup> All three technologies require adequate shielding to contain their energy within a treatment vessel/area.

### Gamma Irradiation

Gamma irradiation is a form of ionizing radiation produced during radioactive decay of radionuclides such as  $\text{Co}^{60}$  or  $\text{Cs}^{137}$ . Gamma irradiation is composed of photons that have no mass or charge. Photons from  $\text{Co}^{60}$  have energies of 1.17 and 1.33 MeV while photons from  $\text{Cs}^{137}$  have 0.662 MeV energy.<sup>78</sup> Since these photons have no mass or charge, they are highly penetrating. However, because of their source, gamma irradiation cannot be “switched off.” Moreover, accidental worker exposure to radioactive sources or security issues (ie. theft or terrorism), and reduced availability is now limiting the use of these technologies commercially.

### X-Ray

X-rays are another form of ionizing radiation. Commercially, X-rays are created using highly energetic electrons (usually 5 MeV or 7.5 MeV) striking a high atomic number material such as tantalum or using X-ray tubes. This creates X-ray photons as a result of energy changes of electrons orbiting around the nucleus of an atom. Like gamma photons, X-ray photons are also highly penetrating. However, generation of X-rays via this process (namely Bremsstrahlung radiation) has a very low conversion efficiency thereby implying that the cost of X-ray treatment will be orders of magnitude higher than eBeam treatment.<sup>79</sup> X-rays also have a low dose rate but, like unlike gamma

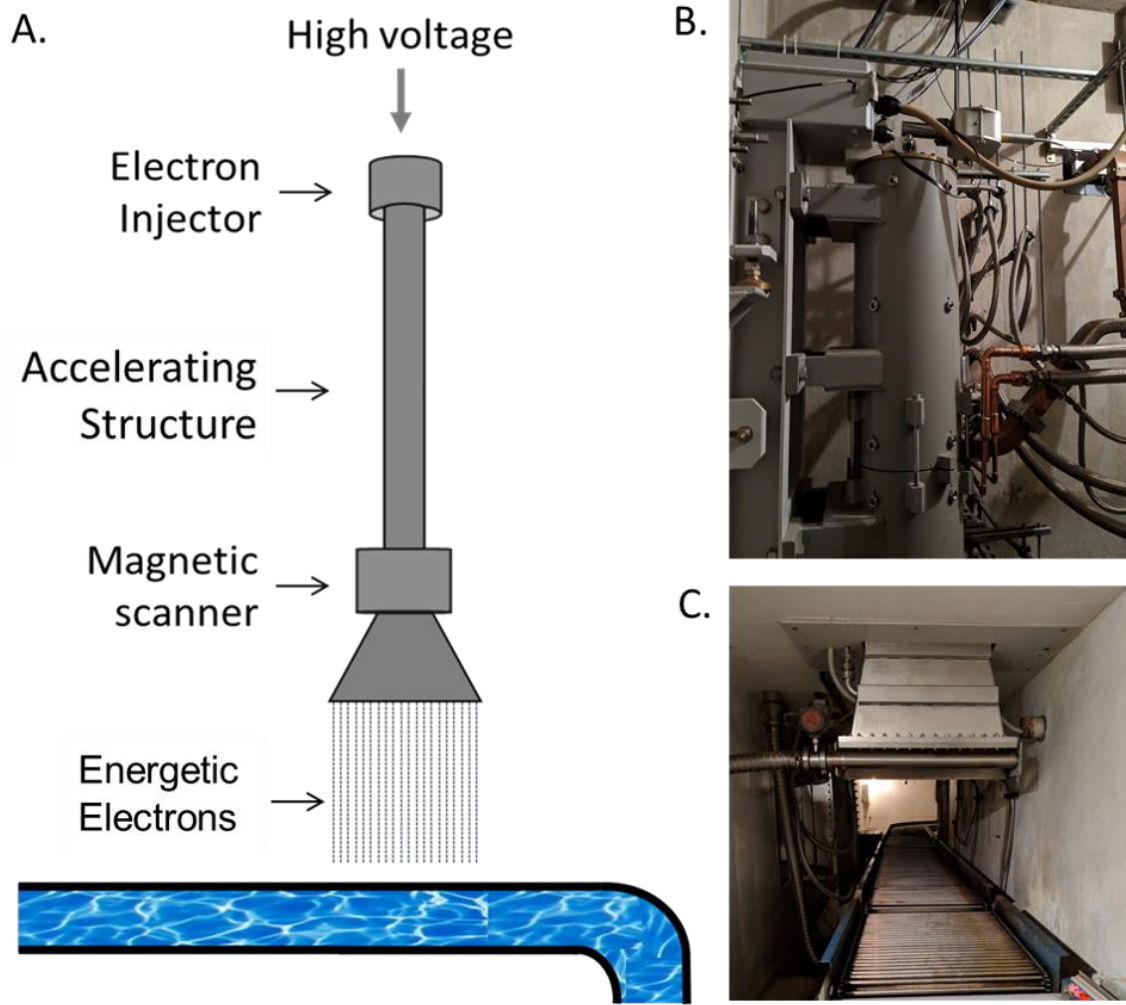


Figure 4. Schematic and photographs of the electron beam linear accelerator at the National Center for Electron Beam Research (NCEBR) at Texas A&M University. A) Schematic of an electron beam linear accelerator utilized for water treatment; B) The accelerating structure of the electron beam at NCEBR; C) The magnetic scan horn and conveyor belt of the electron beam at NCEBR.

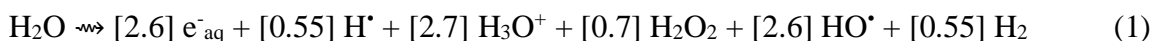
sources, X-ray generation can be switched on or off.

### Electron Beam Technology

Electron beam is a form of ionizing technology. However, eBeam and X-rays are produced from commercial electricity and, therefore, issues facing Co<sup>60</sup> and Cs<sup>137</sup> are non-existent with this technology. Highly energetic electrons (usually 10 MeV) are generated using an electron gun and compact linear accelerators (Figure 4). These electrons are then allowed to interact with the target material to effect the change that is desired. Although significantly less penetrating than gamma irradiation, eBeam technology has a higher dose rate (allowing for faster processing), facilitates greater dose flexibility, is currently cheaper to install, and most importantly, the beam can be switched off when not in use.<sup>80</sup> Recent improvements in eBeam technology, in terms of reliability and compactness, have resulted in greater commercial adoption of these systems in the medical device sterilization and food processing industries.

### Effects of Ionizing Radiation

The effects of ionizing radiation are determined by the amount of energy absorbed per unit mass of the target material. This is defined as absorbed dose measured in grays (Gy) or kilograys (kGy) (1 Gy = 1 Joule/kilogram). There is only minimal temperature increase with dose resulting in only around 2.5°C at 10 kGy. During ionizing radiation treatment, the radiolysis of water creates both reactive oxidative and reductive species (eq. (1)). The values in brackets represent ‘G-values’ or quantities of each species produced per 100 eV of absorbed energy.<sup>79</sup>



The mechanism of action of ionizing radiation is mediated either by direct damage to the chemical bonds of molecules and/or indirectly through the radiolysis of water molecules. Direct damage occurs when the charged particles directly transfer their energy to the product. Because photons have no mass or charge, photons may pass directly through matter without interacting or may interact via multiple reactions as they lose energy. In the case of electrons in eBeam irradiation, the primary energetic electrons always interact with electrons or the nucleus of other atoms. This interaction results in the ejection of secondary electrons from other atoms, which then interact to produce tertiary electrons, etc.<sup>79</sup> This process is known as nuclear elastic scattering.

Charged particles can interact with matter in three ways. First, “soft” collisions occur when the charged particle passes another atom at a distance. This distanced interaction is enough to influence the atom by distorting it which can cause it to excite to a higher energy level or may even ionize the atom causing it to eject a valence electron. Soft collisions result in the smallest amount of energy lost from the original charged particle.<sup>81</sup> The second interaction is known as “hard” collisions. Hard collisions occur when the charged particle interacts with a single electron on another atom. This results in the ejection of this electron from the atom. The ejected electron retains a considerable amount of energy to further interact with other matter. Hard collisions result in a much greater energy loss from the original charged particle. The third interaction of charged particles are known as Coulomb-force or electrostatic interactions. These interactions take place mainly in the nucleus of the affected atom.<sup>82</sup> During coulomb-force

interactions, there is little to no transfer of energy to the affected atom. However, these interactions are responsible for deflecting electrons for further interactions.<sup>81</sup>

As mentioned above, indirect damage resulting from ionizing radiation is caused by the reactive oxygen species (ROS) produced during the radiolysis of water. Free radicals are atoms that contain unpaired electrons. These chemical species are therefore very reactive due to the lack of a stable number of electrons in their outer shell. Due to their reactivity, these species are very short lived.

Damage to both chemical pollutants and microorganisms are caused by a sum of these direct and indirect interactions. In living organisms, DNA is the largest biomolecule present in the cell and therefore is the primary target of these interactions.<sup>83</sup> DNA damage occurs due to cleavage of phosphodiester bonds in the DNA structure which induce single stranded and double stranded DNA strand breaks.<sup>84</sup> While mechanisms exist in microorganisms to facilitate DNA repair of single stranded breaks, double stranded breaks are much more difficult to repair.<sup>85</sup> During this damage response, the cell may also mis-repair the DNA inducing more stress and may become irreparable.

Aside from DNA, damage to proteins has also been seen to occur in microorganisms. Indirect creation of ROS species during irradiation is further increased within the cell by endogenous stress induced, ROS-producing systems. In particular, the creation of hydroxyl radicals, hydrogen peroxide, and superoxide anions have been linked to protein damage in irradiated cells.<sup>86</sup> Irradiation induced redox imbalances have been linked to damage of sulfur residues, for example in methionine and cysteine.<sup>87</sup> Protein aggregation has also been observed following ultraviolet C radiation.<sup>88</sup> Further,



DNA repair processes in microorganisms depend on proteins for proper functioning, so damage to proteins further complicates post-irradiation cell survival.<sup>86</sup> Therefore, a cell's ability to survive irradiation is dependent upon 'detoxifying enzymes' and ROS scavenging mechanisms.

Although extensive intracellular damage has been observed following ionizing radiation, numerous studies have demonstrated a lack in membrane damage following such irradiation.<sup>89-92</sup> Evidence has also been presented suggesting that cells maintain metabolic activity following ionizing radiation treatment.<sup>90,91,93,94</sup> Because of this, irradiated microbes have been described as entering a metabolically active, yet non-culturable (MAyNC) state. In this state, the cells are considered inactivated and not "dead."

Given the growing applications of ionizing technology in environmental remediation there is a need to explore the utility of ionizing radiation technology for emerging contaminants such as cyanotoxins and toxin-producing cyanobacterial cells.<sup>95</sup> The primary objective of this review is to describe the current state of the science surrounding the use of ionizing irradiation technologies for the degradation of MC-LR and the inactivation of the cyanobacteria, *M. aeruginosa*.

## **Methods**

Qualitative systematic review techniques were employed in this overview. Existing studies were obtained using a defined set of search terms (see Appendix A). The databases utilized included Google Scholar, Science Direct, and PubMed. Studies published since the initial publishing of this review were identified and included in this

adapted version. Articles were excluded if: microcystins were not the target chemical or *M. aeruginosa* was not the target organism, ionizing radiation was not utilized, or the article was not available in English translation. No studies utilizing x-ray radiation techniques were identified. Qualifying articles were reviewed, and results are summarized. Articles were included regardless of study quality. However, strengths and/or limitations, use of statistics, and bias were discussed for each study.

### **Current Research Using Ionizing Radiation Technologies**

#### *Gamma Irradiation*

In the 1990s, Wayne W. Carmichael published a series of articles on cyanotoxins and cyanobacterial blooms which emphasized the importance of monitoring cyanotoxins in water.<sup>69,96,97</sup> However, preliminary research started as early as the 1960s on irradiation techniques for the removal of these toxins.

Chronologically speaking, the first paper that investigated the controlling of cyanobacterial populations with ionizing irradiation was Morton and Derse in 1968.<sup>98</sup> The authors aimed to investigate the use of gamma irradiation to control algal/cyanobacterial culture growth. They investigated five HAB related organisms including: *Anabaena circinalis*, *Aphanizomenon flos aquae*, *Microcystis aeruginosa*, *Chlorella pyrenoidosa* (green algae), and *Gomphonema sp.* (diatom). Radiation was performed using a 500 Ci Co<sup>60</sup> gamma source and samples were dosed based upon exposure times. Concentration of cells in cultures were determined using absorbance at 600 nm on a spectrophotometer. The authors reported that 1–1.5 kGy was necessary to ‘control growth substantially’ for *Chlorella*, *Anabaena*, and *Microcystis*, whereas

*Gomphonema* and *Aphanizomenon* were more resistant. In particular, *M. aeruginosa* at bloom level concentrations (approximately  $1 \times 10^6$  cells/ml) required a dose greater than 1 kGy to achieve an absorbance of 0 after culturing 11 days post-irradiation. The authors noted that there was no observed initial concentration dependence on the dose viability for controlling populations of any species. Further, the authors compared the results of the irradiated cultures to previously published work that treated cultures chemically (algicides or algistats) to prevent algal growth. They concluded that the significant variability seen between species and between cell concentration with various algicides was not seen with gamma treatment. Overall, this initial work by Morton and Derse suggested that cell growth could be prevented in *M. aeruginosa* and other cyanobacterial species using gamma irradiation.

A study published the following year by Kraus (1969) also used a  $\text{Co}^{60}$  gamma source for investigation of the resistance of 23 cyanobacterial strains (including *M. aeruginosa*) to irradiation.<sup>99</sup> In the study, Kraus determined cell viability based on a change in dry weight of pelleted cells due to differing cell morphologies. They also used a radiation-resistant bacterium, *Micrococcus radiodurans*, and a non-radiation resistant bacterium, *Sarcina lutea*, in co-culture with cyanobacterial species for comparison of resistance. Cultures were grown in a modified Chu medium with doubled nitrate content to discourage the cyanobacterial production of extracellular polysaccharides. Cell concentrations of irradiated cultures were not provided. Following irradiation, cultures were grown in fresh media for 15–21 days to monitor cell regrowth. Using the LD<sub>90</sub> determined from irradiated cultures, the authors categorized cyanobacterial resistance in

groups; low resistance ( $LD90 < 4 \text{ kGy}$ ), moderate resistance ( $4 \text{ kGy} < LD90 < 12 \text{ kGy}$ ), and high resistance ( $12 \text{ kGy} < LD90$ ). *M. aeruginosa* was considered “sensitive” and placed in the low resistance group. The authors also note that microscopic analysis of cells after ‘moderate’ exposures showed no abnormalities in cell division. After ‘high’ exposures there appeared to be distortion of the cell. However, this data was not provided.

Although recent research has improved methods for studying organism effects, these early studies provided a foundation for irradiation treatment of cyanobacteria and other microorganisms. Presumably unknown at the time that these studies were conducted, was the understanding that the presence of specific chemicals in solution can fundamentally alter the types of reactive species abundant in solution after radiation by virtue of their radical scavenging effects.<sup>100,101</sup> The addition of excess nitrate in media as performed by Kraus may have caused scavenging of aqueous electrons ( $e_{aq}^-$ ) reducing species as well as generation of  $NO_3^{2-}$  which may have affected cyanobacterial removal.<sup>76</sup>

There was a gap of approximately 38 years before the next gamma study was published focusing on *M. aeruginosa* and microcystins. This was published in 2007 by Zhang et al.<sup>102</sup> This study focused on the radiolysis of MC-LR and MC-RR by gamma irradiation, as well as the effect of additives on degradation. *M. aeruginosa* was cultured in BG-11 medium with additives being added directly to the culture medium in those studies. Microcystin concentrations were quantified using an HPLC with a UV diode array detector. The authors reported that degradation of both MCs increased with

increasing dose. A dose of 8 kGy resulted in a 98.8% degradation efficiency of MC-LR and a dose of 5 kGy was enough to remove all MC-RR. The authors then calculated  $D_{0.9}$  values (the required dose to reduce 90% of the initial concentration) resulting from the addition of additives to *M. aeruginosa* cultures. Presently, these values are referred to as  $D_{10}$  values to denote the reduction of the population by a factor of 10.  $\text{Na}_2\text{CO}_3$  and  $\text{H}_2\text{O}_2$  were seen to enhance both MC-LR and MC-RR degradation efficiency, whereas  $\text{NaNO}_2$ ,  $\text{NaNO}_3$ , and Triton X-100 were seen to inhibit degradation. They suggest that the presence of  $\text{CO}_3^{2-}$  quenches the  $\text{H}_3\text{O}^+$  created by gamma irradiation's radiolysis of water resulting in an increase in available  $e_{\text{aq}}^-$ . This would suggest a reductive process for MC breakdown. Oppositely, the authors also suggest the presence of  $\text{H}_2\text{O}_2$  could act as a source of hydroxyl radicals in solution promoting more oxidative processes. However, studies have shown that hydrogen peroxide may also act as a scavenger of hydroxyl radical.<sup>103</sup> Nitrate-containing compounds may react with both  $e_{\text{aq}}^-$  and  $\text{H}\cdot$  to inhibit the reduction process. Effects of all additives seemed more pronounced at lower irradiation doses.

Song et al. (2009) completed pulse radiolysis experiments and gamma irradiation studies on MC-LR.<sup>104</sup> In these studies, Microcystin was purified from *M. aeruginosa* cultures and purity was determined through HPLC. Radiolysis was performed using an 8 MeV Titan Beta model TBS-8/16-1S linear accelerator. Gamma irradiation was completed using a  $\text{Co}^{60}$  source with Fricke dosimetry. Breakdown of MCLR and degradation products were analyzed with LCMS. The authors began by conducting kinetic studies with 2–3 ns pulsed radiolysis at 3–5 Gy. By identifying experimental rate

constants, addition of HO· to the unsaturated hydrocarbons on MC-LR including the ADDA moiety benzene ( $1.03 (\pm 0.03) \times 10^{10} \text{ M}^{-1} \text{ s}^{-1}$ ), and ADDA moiety diene ( $10^9\text{-}10^{10} \text{ M}^{-1} \text{ s}^{-1}$ ), were determined to be the fastest reactions. Overall, the authors determined the rate constant for the reactions of hydroxyl radicals with MC-LR to be  $2.3 (\pm 0.1) \times 10^{10} \text{ M}^{-1} \text{ s}^{-1}$ . Hydrogen abstraction was seen to occur 1–2 magnitudes slower than the other reactions ( $10^8 \text{ M}^{-1} \text{ s}^{-1}$ ), however, more than 50 reaction sites exist on the MC-LR molecule making it a significant reaction pathway. The authors then modelled hydroxyl radical reactivity in respect to individual amino acids in MC-LR. Overall, a rate constant of  $2.1 \times 10^{10} \text{ M}^{-1} \text{ s}^{-1}$  was obtained by summation of these individual reaction sites which was approximately 10% lower than the observed experimental rate constant. They noted this was within experimental error and could be in part due to the exclusion of hydrogen abstraction pathways for the ADDA moiety. Next, Song et al. investigated transformation pathways using gamma irradiation. Samples were saturated with oxygen to encourage the reaction of  $e_{\text{aq}}^-$  and hydrogen atoms with dissolved oxygen. This in turn produced superoxide anions with much lesser reactivity than hydroxyl radicals. A dose of 1.8 kGy degraded MC-LR. Further, degradation products corresponding to hydroxylation of the benzene on the ADDA moiety and hydroxyl attack on the diene of the ADDA moiety were identified at 1011 m/z and 1029 m/z, respectively (Fig. 3). Overall, these studies suggest that the degradation products of MC-LR due to eBeam irradiation (as seen in the pulse radiolysis experiments) could undergo similar oxidative reactions to that of gamma irradiation.

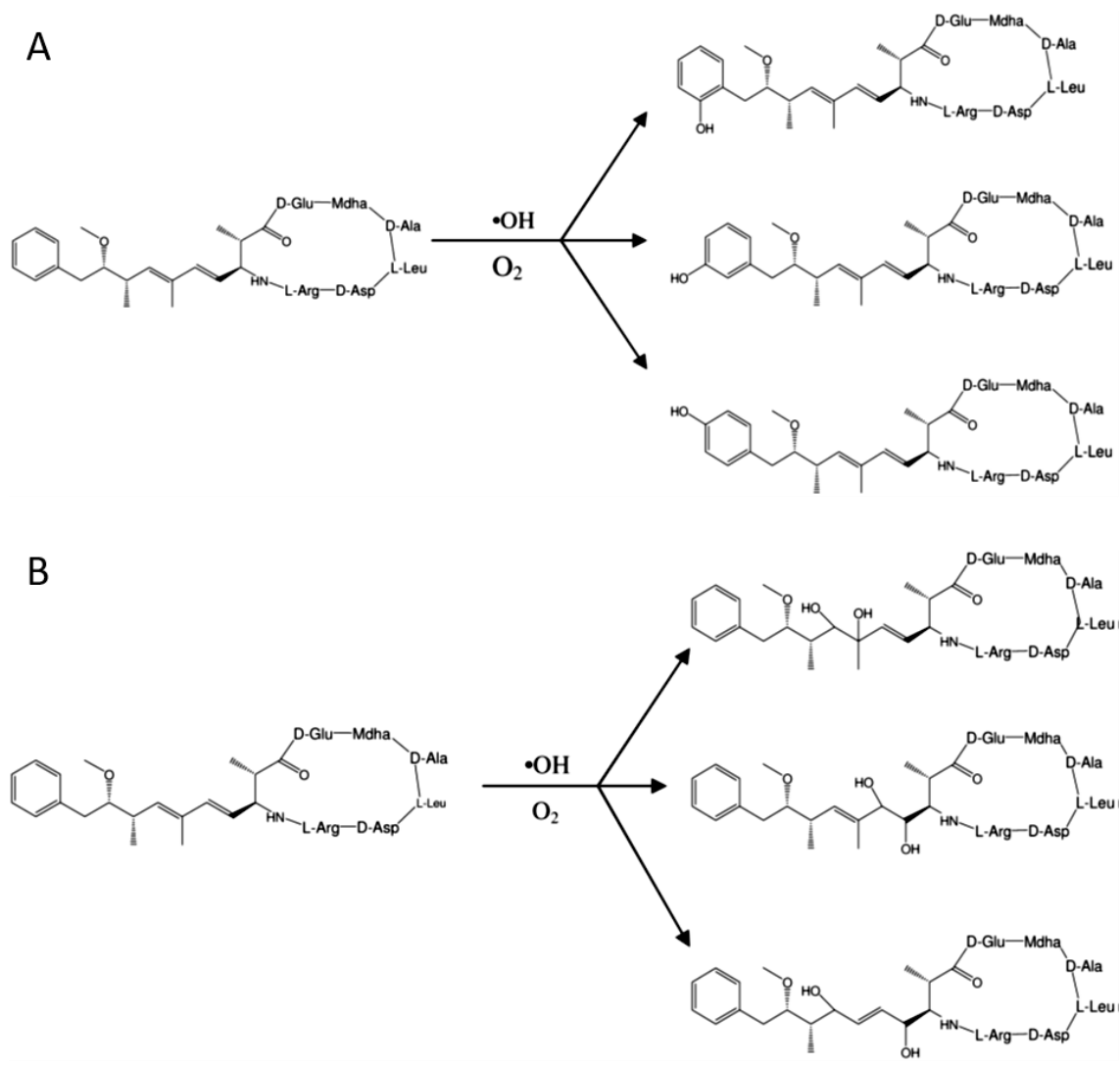


Figure 5. Reaction products for hydroxyl radical reaction with the A) benzene group and B) diene group of ADDA moiety of MC-LR. Reprinted (adapted) with permission from Song, Weihua, et al. "Radiolysis studies on the destruction of microcystin-LR in aqueous solution by hydroxyl radicals." *Environmental Science & Technology* 43.5 (2009): 1487–1492.<sup>104</sup> Copyright (2009) American Chemical Society.

Further, the breakdown of the molecule appears to be due to oxidative reactants rather than reductive as in the absence of reductive species, MC-LR degradation products were still identified.

Zheng et al. (2012) investigated the use of gamma irradiation to remove *M. aeruginosa* in water.<sup>105</sup> Various additives were also tested for their influence on cell removal. Cyanobacteria cultures were grown in BG-11 media and irradiated with a Co<sup>60</sup> gamma source. Cell growth was monitored using chlorophyll-a concentrations determined at 665 nm absorbance and carotenoid content determined at 615 and 652 nm absorbance. The antioxidants superoxide dismutase (SOD) and peroxidase (POD) were also monitored as a marker for oxidative stress in *M. aeruginosa*. Additives used included CH<sub>3</sub>OH, thiourea, and NO<sub>3</sub><sup>-</sup> and pH effects were measured. The authors report that a decrease in chlorophyll-a content was seen with increasing dose five days post-irradiation. Change in culture color was visually observed and a dose of 9 kGy resulted in a 98% chlorophyll-a removal efficiency. Similarly, carotenoids were greatly affected by irradiation with only 0.8% of control carotenoid content remaining after 9 kGy of irradiation. pH was also seen to impact removal efficiency with an increasing pH resulting in a decreased *M. aeruginosa* removal. The authors suggest this result could be due to H<sup>•</sup> readily reacting with OH<sup>-</sup> in alkaline conditions to produce more e<sub>aq</sub><sup>-</sup>. Further, recombination of e<sub>aq</sub><sup>-</sup> and OH<sup>•</sup> reduces hydroxyl radical concentrations and therefore decreases oxidative reactions in solution. However, *M. aeruginosa* has not shown to be adapted to high or low pH, suggesting that some observed cell death could have been due to culture pH and not only gamma irradiation. The authors then discussed the effect



of additives on *M. aeruginosa* removal. CH<sub>3</sub>OH addition resulted in a slight increase in chlorophyll-a content with increasing dose suggesting that removal of *M. aeruginosa* is reliant on OH·. Addition of thiourea also slightly increased the chlorophyll-a content suggesting H· and e<sub>aq</sub><sup>-</sup> are also involved in *M. aeruginosa* removal. Finally, addition of NO<sub>3</sub><sup>-</sup> also slightly decreased the removal efficiency of *M. aeruginosa*. Unfortunately, due to a lack of statistical significance, it was unclear which primary species were responsible for cell removal. The authors then reported changes in SOD and POD in irradiated cells. At low doses (2–5 kGy), SOD and POD activity was increased, caused by an increase in oxidative stress. High doses (6–9 kGy) reduced SOD and POD activity. The authors did not offer any explanation of the observed effects. However, at high doses, there may be increased DNA damage resulting in a dampened stress response and therefore reduced activity of SOD and POD. Lastly, Zheng et al. presented SEM images of *M. aeruginosa* cells irradiated at 9 kGy. Irradiated cells appeared to have depressions across the cell surface suggesting that irradiation could be affecting cellular morphology as well.

#### *Electron Beam Irradiation*

The first reported study to investigate eBeam as a possible treatment technique was a pilot project completed by Ho Kang in 2004 as a part of the International Atomic Energy Agency's (IAEA) coordinated research project on Remediation of Polluted Waters and Wastewater by Radiation Processing.<sup>106</sup> The study briefly investigated the use of eBeam to damage a variety of algal and cyanobacterial species including: *Chlorella sp.*, *Scenedesmus sp.*, *Microcystis sp.*, *Anabaena sp.*, *Oscillatoria sp.*,

*Prorocentrum micans*, *Prorocentrum minimum*, *Scrippsiella trochoidea*, *Lingulodinium polyedra*, and *Cochlodinium polykrikoides*. A Russian ELV-4 model electron beam accelerator was used to treat samples and samples were dosed from 1 to 10 kGy. The author reported that for *Microcystis*, a 40% reduction in photosynthetic activity was seen following a 3 kGy dose. A similar reduction was seen in marine red algae at approximately 1 kGy. However, no methods for chlorophyll-a measurement are mentioned in the study. The author also noted that after irradiation, freshwater algae leached soluble proteins from cells and a 'biopolymeric substance' that lead to bioflocculation of cells within two days of eBeam treatment. However, there was no data in the paper to support this claim.

Only two other papers have been identified in literature relating to eBeam treatment of *M. aeruginosa* and microcystin. The first was published by Liu et al. (2014) and investigated the effect of eBeam irradiation on *M. aeruginosa*.<sup>107</sup> *M. aeruginosa* cultures were grown in BG-11 media at a pH of 7.5. Samples were irradiated in a glass petri dishes in 100 ml volumes with a low energy linear accelerator (1.0 MeV and 1.0 mA). Chlorophyll-a was extracted using 90% acetone to determine photosynthetic ability and cell concentrations were monitored through optical density (OD<sub>680</sub>) measurements at 680 nm. The authors reported a removal efficiency based upon chlorophyll-a content of 43%, 83%, 86%, 91%, and 84% for doses of 1–5 kGy, respectively. OD<sub>680</sub> measurements decreased 34%, 71%, 74%, 85%, and 80% for doses 1–5 kGy, respectively. However, it was unclear if replicates were completed in the experiments. Additionally, the authors studied the effect of eBeam on cell morphology using a JEM-

1230 transmission electron microscope (TEM). Although images were provided for dosed cells, the authors only suggest that eBeam treatment can cause damage to integrity and morphology of *M. aeruginosa* cells. Next, they reported on decreases in photosynthetic rate of cultures following >2 kGy eBeam dose. Here, no method details were included to suggest how photosynthetic rates were obtained. The authors provide data on changes in SOD and POD enzymatic activity. Up to 7 days post irradiation, the authors saw an increase in POD activity, followed by a decrease up to 11 days. Similarly, up to 5 days post irradiation, the authors saw an increase in SOD activity, followed by a decrease up to 11 days. These results were attributed to oxidative damage caused by eBeam irradiation. Unfortunately, the experimental methods used for these studies were not disclosed.

Another study was published by the same group (Liu et al., 2015) and investigated the use of eBeam irradiation to control microcystin concentrations.<sup>108</sup> Similar to the previous publication, chlorophyll-a content and OD<sub>680</sub> were monitored and irradiation was completed in glass petri dishes using a low energy beam (1.0 MeV and 1.0 mA). After irradiation cultures were analyzed for intracellular and extracellular microcystin content. MC concentration was determined using an ELISA kit. The authors reported that for both intra- and extra-cellular MC-LR content, there was an increase in MC at approximately 4 days post irradiation for doses >1 kGy, followed by a sharp decrease up to 12 days. Although there is an increase, the authors conclude that an appropriate dose of eBeam irradiation can inhibit MC production. Liu et al. further presents total MC concentration data and reports that 37.2%, 60.8%, 59.6%, 60.2%, and

72.1% MC decreases were observed for doses of 1–5 kGy, respectively. It is unclear at what amount of time post irradiation these samples were taken. Finally, the authors tried to correlate MC concentration with algal growth using chlorophyll-a content. They found that chlorophyll-a content seemed to increase with increasing MC concentration for both control and irradiated samples. As with the previous publication, there was no mention of experimental replication.

A recent study was published by Liu et al. 2020 further investigating effects of eBeam irradiation on *Microcystis aeruginosa*.<sup>109</sup> Specifically, this study sought to investigate changes in proteins and exopolysaccharide production in *M. aeruginosa* cells. Cultures were grown in BG-11 media at a pH of 7.5 under a 14/10 hour light/dark cycle. Samples were irradiated in 100 ml petri dishes at doses between 1 and 5 kGy using a low energy linear accelerator (1.0 MeV, 1.0 mA, 3.5 kGy/sec dose rate). There was no mention whether experimental replicates were employed in this study. The authors determined pH and conductivity of cyanobacterial cultures as well as respiration rate using an equation involving chlorophyll-a concentrations and OD at 630, 645, 663, and 750 nm. *M. aeruginosa* cell structure was observed using atomic force microscopy. The authors give little information on their methods for extracting extracellular polysaccharides. Finally, the group determined protein content using Bradford's method and anthrone colorimetry.

The authors reported that pH decreased in irradiated cultures and continued to decrease following two days of incubation. The authors equated this decrease in pH with *M. aeruginosa* cells photosynthesizing and using up the media's CO<sub>2</sub>. They also reported

that a decrease in chlorophyll-a content in 2-5 kGy treated groups indicated a decrease in photosynthetic “level”. The authors further discussed that the conductivity of cultures was higher in irradiated groups than the controls. When investigating respiration, the authors reported that respiration rate initially increased in irradiated cultures following incubation (the authors did not define this time frame) but then declined following seven days of post-irradiation incubation. Liu et al. 2020 did not interpret these results. Next, the authors stated that an increase in extracellular polysaccharides (EPS) contributed to colony formation of *M. aeruginosa* cells in irradiated cultures. However, in doses greater than 1 kGy, EPS production decreased. They suggested that EPS secretion from cells is meant to scavenge ROS generated during irradiation and that cell death and lysis was observed due to a failure of the EPS to scavenge ROS. Finally, the authors observed total protein content decreasing with increasing irradiation dose above 1 kGy.

The author’s provide scant discussion about their findings. Overall, Liu et al. concludes that pH and conductivity increases in cultures with increasing dose which inhibits algal growth. They also conclude that eBeam treatment affects respiratory rates of cultures and decreases the soluble proteins inhibiting photosynthetic abilities. Finally, EPS is used by *M. aeruginosa* cells to resist irradiation damage. However, a decrease in EPS production was observed with increasing dose. The authors do not provide statistical significance in their paper.

### **Research Approach**

The studies published to date illustrate promising results for the use of ionizing radiation technologies for the breakdown and removal of MC-LR and *M. aeruginosa* in water.

Since gamma irradiation technology predates electron beam irradiation technology, there have been a larger volume of studies investigating its effectiveness for pollutant and organism treatment. Gamma irradiation could be a feasible treatment option for MC-LR and *M. aeruginosa* in water. However, the concept of utilizing radioactive cobalt-60 isotopes for the remediation of cyanotoxins, as well as other emerging water contaminants, is untenable from both a technology perspective as well as a homeland security perspective. Cobalt-60 is a high security material that requires extensive protection in transportation, handling, storage, and disposal. Agencies around the world are actively trying to reduce the commercial use of this technology.<sup>110-112</sup> Therefore, the need for radioactive materials makes widespread usage of gamma irradiation technology doubtful in today's security and environmentally conscious world.

There is a growing body of literature highlighting the value of eBeam technology for environmental remediation applications.<sup>72-74,76,113,114</sup> The preliminary data for eBeam irradiation as a water treatment technology for MC-LR and *M. aeruginosa* is promising. Electron beam technology utilizes a linear accelerator to generate its highly energetic electrons from commercial electricity. Therefore, this is a switch on and off technology without the security issues associated with radioactive sources. The U.S. Department of Energy has recognized the potential of this technology for energy and environmental applications.<sup>115</sup> Compact high energy (10 MeV) and high power (700 kW) linear

accelerators capable of treating extremely large volumes of water are commercially available today. However, there is a lack of published articles related to eBeam technology and the degradation of cyanobacteria and their toxins.

There is a critical need for pursuing research on cyanobacteria and cyanotoxin remediation on multiple fronts. One key objective should be to understand the breakdown products associated with MC-LR degradation. It is important to understand the extent of breakdown of the toxin molecule that is achievable at varying eBeam doses and under varying experimental conditions such as pH, total organic carbon content, presence of extraneous biomass, and chemical composition, etc. A deep understanding of the generation of toxin breakdown products under varying eBeam doses will help in predicting possible toxicity associated with these by-products. These studies can also shed light on whether the by-products would undergo autolysis or will be metabolized by the microbial community. *In vitro* and *in vivo* toxicity studies focusing on the eBeam degradation products are a necessary compliment to the above described studies.

Another research focus should be to understand the cellular effects of eBeam doses on *M. aeruginosa* and other toxin-producing cyanobacteria. It is important to confirm whether or not the cell undergoes morphological changes. It is now known that in bacterial cells, eBeam irradiation does not cause cell lysis but nevertheless causes inactivation.<sup>89</sup> Experimental approaches should include microscopy as well as the use of membrane integrity dyes and nucleic acid stains. Microscopic studies should be performed at specific time points post-eBeam irradiation exposure as well as after incubation at varying conditions. A clear understanding of how the cells respond to

varying eBeam doses will help in developing post treatment cell filtration/separation strategies.

A third avenue of research should revolve around understanding how the genome, transcriptome, proteome, and the metabolome of *M. aeruginosa* respond to varying eBeam doses and incubation periods post-irradiation. It is unknown at this time whether the DNA in cyanobacterial cells undergo multiple single and double strand breaks, and, therefore, DNA fragmentation studies should be performed to determine whether there are “hot-spots” in the DNA that are more susceptible to eBeam irradiation damage. Omic technologies such as transcriptomics, proteomics, and metabolomics should be employed to better understand how cyanobacterial cells respond to varying eBeam doses under differing experimental conditions. It is also important to determine whether inactivated cyanobacterial cells continue to produce toxins post irradiation. The potential for pre-formed toxins to be released from inactivated cells, as well as those potentially formed post-irradiation, must be understood. This information is imperative when designing an eBeam technology-based remediation strategy for the water industry.

Finally, there is a need to conduct research to enable the designing of an eBeam technology-based treatment train for the drinking water industry. These studies should focus on demonstrating the degradation of the toxin and inactivation of the cyanobacterial cells in actual environmental surface water samples. Electron beam technology, if proven to be capable of inactivating the cyanobacterial cells and degrading the toxin molecule, can be used to remediate toxin containing drinking water in the treatment plants as well as detoxify drinking water treatment plant residuals



containing cyanotoxins and toxin-producing cyanobacteria. The ability to treat such residuals can facilitate the disposal of hazardous wastes. Therefore, research should focus on identifying the doses required to attain specific toxin limits to facilitate disposal.

Overall, while there are promising results for the use of ionizing radiation technologies for the removal of MC-LR and *M. aeruginosa* in water, additional research is crucial in order to implement these technologies. The research conducted as part of these studies were meant to address the above mentioned research needs.

## CHAPTER III

### RESPONSE OF *M. AERUGINOSA* AND MICROCYSTIN-LR TO ELECTRON BEAM IRRADIATION\*

#### **Abstract**

Harmful cyanobacterial blooms (cyanoHABs) pose threats to human and animal health due to the production of harmful cyanotoxins. *Microcystis aeruginosa* is a common cyanobacterium associated with these blooms and is responsible for producing the potent cyclic hepatotoxin microcystin-LR (MC-LR). Concerns over the public health implications of these toxins in water supplies have increased due to rising occurrence of these blooms. High energy electron beam (eBeam) irradiation technology presents a promising strategy for the mitigation of both cyanobacterial cells and cyanotoxins within the water treatment process. However, it is imperative that both cellular and chemical responses to eBeam irradiation are understood to ensure efficient treatment. We sought to investigate the effect of eBeam irradiation on *M. aeruginosa* cells and MC-LR degradation. Results indicate that doses as low as 2 kGy are lethal to *M. aeruginosa* cells and induce cell lysis. Even lower doses are required for degradation of the parent MC-LR toxin. However, it was observed that there is a delay in cell lysis after irradiation where *M. aeruginosa* cells may still be metabolically active and able to synthesize microcystin. These results suggest that eBeam may be suitable for cyanoHAB mitigation in water treatment if employed following cell lysis.

\*Adapted with permission from: "Response of *Microcystis aeruginosa* and Microcystin-LR to electron beam irradiation doses" by Folcik, A. M., Klemashevich, C., Pillai, S. D., 2020. *Radiation Physics and Chemistry*, 109534, Copyright 2021 by Elsevier.

## **Introduction**

The underlying hypothesis for this study was that when *M. aeruginosa* cells are exposed to lethal eBeam doses, the cyanobacterial cells would be unable to further synthesize microcystin. However, we also postulated that both intra- and extra-cellular microcystin would be degraded after eBeam exposure. Therefore, the specific research questions we pursued were a) to identify the eBeam dose that would be able to achieve inactivation of *M. aeruginosa* cells and degradation of extra-cellular MC-LR, b) determine the structural integrity of the eBeam-inactivated cells post eBeam exposure, and c) determine whether the intra-cellular MC-LR would be degraded with eBeam exposure.

## **Materials and Methods**

### *Laboratory Propagation of M. aeruginosa*

*M. aeruginosa* (LB 2385, UTEX Culture Collection of Algae, origin: Little Rideau Lake, Ontario, Canada) were cultured in a modified Bold 3N medium (without soil-water extract) under a 12/12 day/night cycle at ~20°C on an orbital shaker at ~100 rpm. The cultures were also maintained on Bold 3N agar plates under identical light and temperature conditions. The cell titers were determined using chlorophyll absorbance (680 nm) read on a Synergy H1 Hybrid Multi-Mode Microplate Reader (Biotek, Winooski, VT) using Gen5 Microplate Reader and Imager software. An initially prepared standard curve was used for quantification. Cell titers were also determined microscopically just prior to experiments and throughout using a hemocytometer.

### *Quantification of Microcystin-LR*

Pure microcystin-LR (purity  $\geq$  95%) was obtained commercially (Cayman Chemical, Ann Arbor, MI). Microcystin-LR concentrations in experimental samples were analyzed analytically at the Integrated Metabolomic Analysis Core (IMAC) at Texas A&M University. Supernatant samples were filtered through a 0.2  $\mu$ m syringe filter and subjected to further methanol extraction. Cyanobacterial cell pellet samples were weighed (for wet weight normalization) and extracted using a methanol:chloroform:water based extraction method. Briefly, 800  $\mu$ l ice cold methanol:chloroform (1:1, v:v) was added to cyanobacterial cell samples in a Precellys bead-based lysis tube (Bertin, Rockville, MD). Samples were extracted on a Precellys 24 (Bertin) tissue homogenizer for 30 seconds at a speed of 6000. The supernatant was then collected and samples were homogenized a second time with 800  $\mu$ l ice-cold methanol:chloroform. Following, 600  $\mu$ l of ice-cold water was added to the combined extract, vortexed for 30 sec, and centrifuged for 10 minutes at 4000 rpm at 4 °C. The upper aqueous layer was filtered through a 0.2  $\mu$ m nylon filter (Merck Millipore, Burlington, MA). 500  $\mu$ l of the filtrate was then purified using a 3 kDa cutoff column (Thermo Scientific, Waltham, MA) and flow through collected for analysis.

Untargeted liquid chromatography high resolution accurate mass spectrometry (LC-HRAM) analysis was performed on a Q Exactive Plus orbitrap mass spectrometer (Thermo Scientific) coupled to a binary pump HPLC (UltiMate 3000, Thermo Scientific). Full MS spectra were obtained at 70,000 resolution (200 m/z) with a scan range of 100-1500 m/z. Full MS followed by ddMS2 scans were obtained at 35,000 resolution (MS1) and 17,500 resolution (MS2) with a 1.5 m/z isolation window and a

stepped NCE (20, 40, 60). Samples were maintained at 4°C before injection. The injection volume was 10 µl. Chromatographic separation was achieved on a Synergi Fusion 4µm, 150 mm x 2 mm reverse phase column (Phenomenex, Torrance, CA) maintained at 30°C using a solvent gradient method. Solvent A was water (0.1% formic acid). Solvent B was methanol (0.1% formic acid). The gradient method used was 0-5 min (10% B to 40% B), 5-7 min (40% B to 95% B), 7-9 min (95% B), 9-9.1 min (95% B to 10% B), 9.1-13 min (10% B). The flow rate was 0.4 mL min<sup>-1</sup>. Sample acquisition was performed with Xcalibur (Thermo Scientific). Data analysis was performed with Compound Discoverer 3.1 (Thermo Scientific).

#### *Electron Beam Treatment*

The eBeam treatments were performed at Texas A&M University's National Center for Electron Beam Research in College Station, TX. A high energy (10 MeV), 15 kW pulsed S-band linear accelerator was used (dose rate 3 kGy/sec). Industry standard alanine (L- $\alpha$ -alanine) dosimeters and EPR based spectroscopy using the Bruker e-scan reader (Billerica, MA) were used to confirm delivered dose. Preliminary dose-mapping studies were performed on vials used for irradiation to confirm a dose uniformity of one. Studies involving pure microcystin were performed using 2 ml glass screw-thread vials (VWR International, Radnor, PA). Larger 30 ml glass round-bottom screw cap culture tubes (Corning Inc., Corning, NY) were used for irradiation studies involving cyanobacterial cultures.

#### *Response of M. aeruginosa Cells to Varying eBeam Doses*

High titers of *M. aeruginosa* cells (approximately  $9 \times 10^6$  cells/ml) were irradiated at target doses of 0, 0.6, 2, and 5 kGy. Actual doses received were 0.6, 2.1, and 4.9 kGy. Control and eBeam-treated cultures were then incubated for 14 days in 23 ml of fresh Bold 3N media in 125 ml Erlenmeyer flasks. Every 24 hours, 1 ml aliquots were removed and cell concentrations were determined using the absorbance methods described above.

#### *Microscopic Examination of Structural Integrity*

*M. aeruginosa* cells that received a lethal 5 kGy dose were observed microscopically using brightfield and fluorescence microscopy using a FITC filter. An Olympus BX50 microscope (Olympus, Shinjuku City, Tokyo, Japan) was used for this purpose. Images were captured using an Olympus Q color 3 camera and Qcapture pro 7 software (Teledyne QImaging, Surrey, British Columbia, Canada).

#### *Stability and Residual Toxicity of Microcystin-LR Exposed to Varying eBeam Doses*

Commercially purchased microcystin-LR was used in these studies. MC-LR was suspended in 2 ml of deionized water (0.5 mg/L) in 2 ml glass vials. This starting concentration of MC-LR was chosen to be a magnitude greater than the center of the standard curve of the EPA preferred ADDA-specific ELISA kit (Eurofins Abraxis inc., Warminster, PA) to allow for analytical detection. The ELISA kit standard curve ranged from 0.15 - 5.0  $\mu\text{g/L}$ . These MC-LR samples were initially exposed to target eBeam doses of 5, 15, 25, 35, and 50 kGy. Following no detection of MC-LR, samples were then exposed to target doses of 0, 0.3, 0.4, 0.65, 2, and 5 kGy. Actual doses received were 0.29, 0.39, 0.64, 2.1, and 5.1 kGy. Quantification of MC-LR after irradiation was

determined biologically using the EPA preferred ADDA-specific ELISA kit (Eurofins Abraxis) as well as analytically via LC-HRAM as described previously. This ELISA test kit follows guidelines set forth in the EPA method 546 for determination of total microcystins and nodularins in drinking water.<sup>116</sup> A protein phosphatase 2A inhibition kit (Eurofins Abraxis) was used as a basis for determining toxicity. The PP2A inhibition kit standard curve ranged from 0.25 – 2.5 µg/L. The underlying principle of this assay is that samples containing MC-LR will inhibit the PP2A enzyme proportionally to the amount contained in the sample. Normally, PP2A is able to hydrolyze a substrate that is detectable at 405 nm. MC-LR present in solution will inhibit the PP2A enzyme and prevent hydrolysis of the substrate.

#### *Potential of Microcystin-LR Release from eBeam Exposed M. aeruginosa Cells*

Experiments were performed to determine whether lethally eBeam irradiated *M. aeruginosa* were capable of releasing MC-LR into the surrounding environment. For these experiments, turbid *M. aeruginosa* cultures (~10<sup>7</sup> cells/ml) were exposed to target dose of 5 kGy which was determined earlier to achieve complete inactivation. Actual dose received was 5.4 kGy. The control and eBeam treated samples were incubated following treatment for 48 hours. At periodic time intervals (0, 16, 24, and 48 hours) 1 ml aliquots of culture were removed and centrifuged (5 min; 5000 x g) to separate the cell pellets from the culture supernatant. The supernatant and the cell pellets were independently analyzed for the presence and concentrations of microcystin-LR according to methods described above. To preclude any possibility of cyanobacterial cells in the supernatant samples, the supernatant samples were syringe-filtered (0.2 µm)

prior to methanol extraction for microcystin determination. The cell pellets were also weighed and extracted for microcystin determination.

#### *Data Analysis*

All *M. aeruginosa* experiments were performed using biological triplicate samples. Additionally, the colorimetric assays also included technical (n=3) replicates. The data was statistically analyzed and visualized using commercially available GraphPad (GraphPad Software, San Diego, CA). Shapiro-Wilks tests and qq-plots were used to verify normality of data. According to these results, a one-way ANOVA was used followed by the Dunnett's multiple comparisons test. The tests were performed with a significance of 95% ( $p < 0.05$ ).

### **Results and Discussion**

#### *Cyanobacterial Inactivation*

We first began by investigating the response of *M. aeruginosa* cells to electron beam irradiation. Figure 7 shows the response of *M. aeruginosa* cells in liquid suspensions when exposed to varying eBeam doses which were then monitored over the course of 14 days using chlorophyll absorbance. The *M. aeruginosa* cells exposed to 2.1 and 4.9 kGy doses resulted in no cell multiplication over the 14-day monitoring period. This suggests that *M. aeruginosa* cells (at  $10^5$  cells/mL) are sensitive to eBeam irradiation doses even as low as 2 kGy and that doses  $>2$  kGy are lethal doses. When exposed to 0.6 kGy, viable cells remained in the population which multiplied during the 14-day incubation period. However, the growth rate of the 0.6 kGy treated cultures were lower than that of the 0 kGy un-treated control and did not show an increase in chlorophyll absorbance



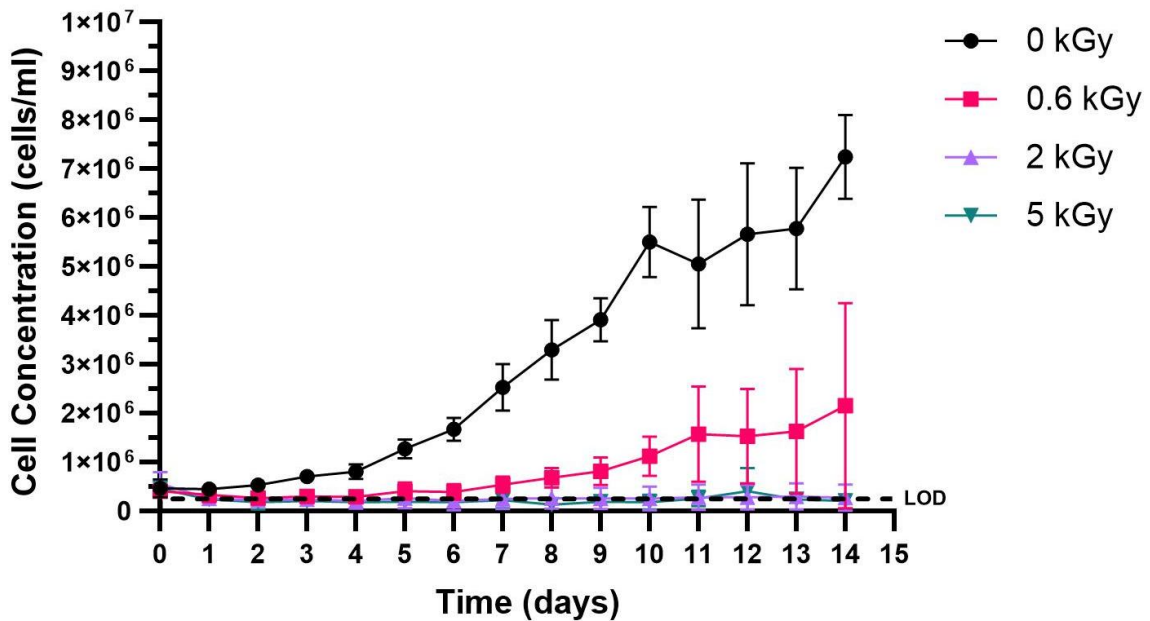


Figure 6. Response of *M. aeruginosa* cells to 0, 0.6, 2.1, and 4.9 kGy eBeam irradiation doses over 14 days. (Error bars represented as standard deviation, Limit of detection (LOD) =  $2.5 \times 10^5$  cells/ml).

until 5 days of incubation following irradiation treatment. Therefore, there was sub-lethal injury at 0.6 kGy as evidenced by the reduced growth rate.

Cultures irradiated at 0.6, 2.1 and 4.9 kGy also all exhibited a visually detectable color change over time (Figure 7). This color change implied a decline of chlorophyll pigments indicative of cell degradation.<sup>105,117</sup> To investigate this further, brightfield and fluorescent microscopic images were taken of the *M. aeruginosa* cells when exposed to the 4.9 kGy dose (Figure 8). The 4.9 kGy dosed cells were chosen for imaging because this was determined to be a lethal dose. Immediately after irradiation, *M. aeruginosa* cells still appeared structurally intact, however, there was slight discoloring in the centers of the cells indicating some internal or membrane damage. Cells were then imaged following 24 hours of incubation after eBeam exposure at 4.9 kGy.



Figure 7. Irradiated cultures exhibited a visibly detectable color change over time following irradiation. From left to right: 0, 0.6, 2.1, and 4.9 kGy.

After 24 hours, the cyanobacterial cells appear to undergo lysis implying loss of structural integrity. The red hue in the 24-hour auto-fluorescent micrograph is indicative of free chlorophyll fluorescing on the slide due to cell lysis.

The observed sensitivity of prokaryotic cells to eBeam doses is not surprising and has been reported extensively. This is the basis for the adoption of ionizing radiation, and eBeam in particular, for commercial pasteurization and sterilization applications in the food and medical devices industries.<sup>118-120</sup> However, the cell lysis

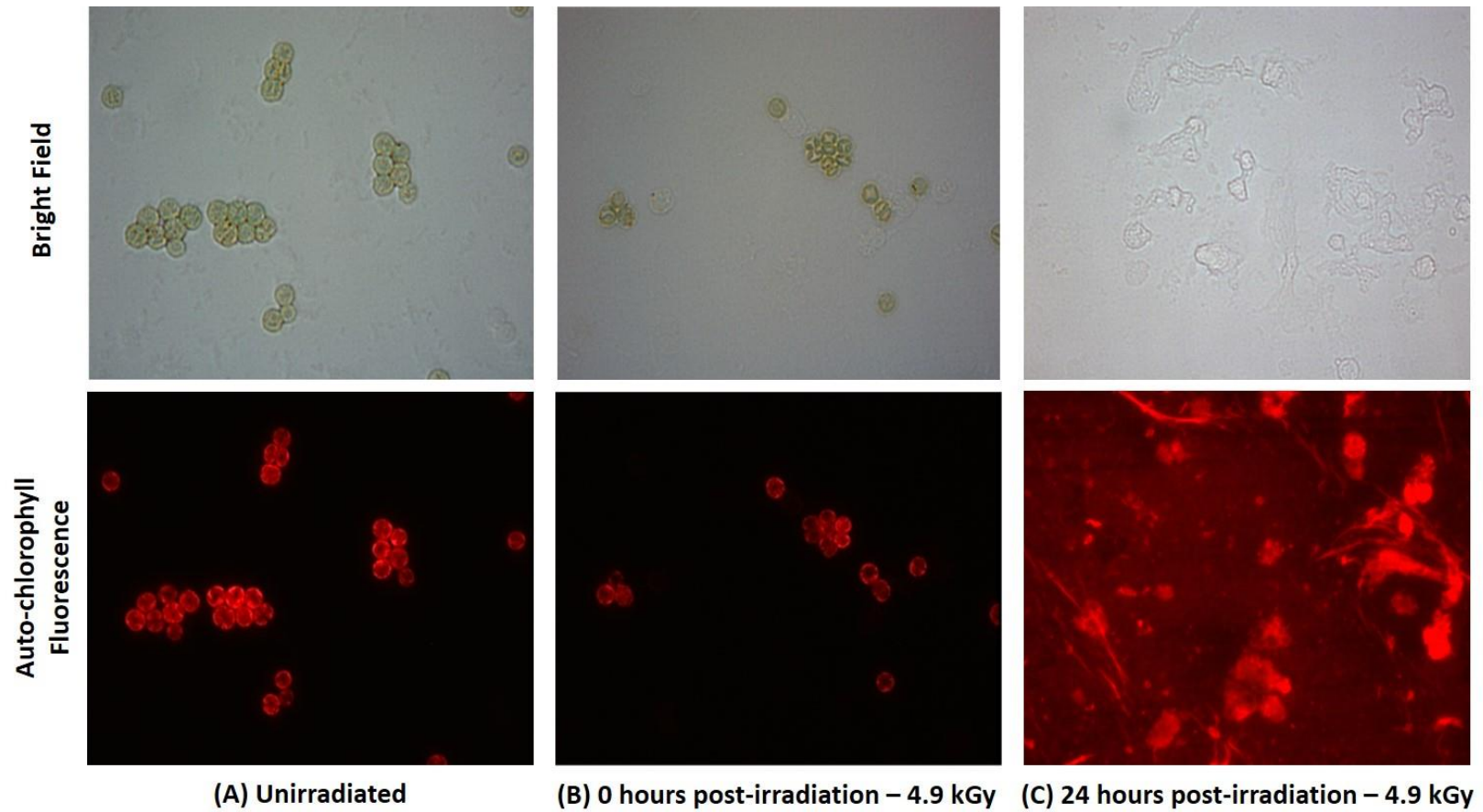


Figure 8. Brightfield and auto-chlorophyll fluorescence microscopy images of *M. aeruginosa* cells. A) Unirradiated cells. Cells appear normal and intact; B) Cells immediately after irradiation at 4.9 kGy. Cells are still structurally intact but have slight discoloring in the center of the cells indicating possible internal or membrane damage; C) Cells 24 h after irradiation at 4.9 kGy. Cells have completely lysed and free chlorophyll is fluorescing on the slide.

seen in the irradiated cyanobacterial cells was surprising because other prokaryotes, such as *Salmonella enteritidis*, do not exhibit a decline in cell turbidity over time post-ionizing irradiation exposure.<sup>89</sup> Only one other study identified completed by Agarwal et al. (2008) observed similar results in *Anacystis nidulans* exposed to gamma irradiation (Co<sup>60</sup>).<sup>121</sup> They observed significant alterations to the cyanobacterial cell ultrastructure and thylakoids following irradiation and 24 hours of light exposure which they attributed to possible increases in glycogen deposits. Previous studies suggest that structural damage to photosynthetic machinery promotes cell death in photosynthetic organisms.<sup>121–123</sup> Due to the necessity of photosystem function for cyanobacterial cell survival, it is possible that a similar mechanism is responsible for the unexpected cell lysis of eBeam exposed *M. aeruginosa* cells.

#### *Stability and Residual Toxicity of Microcystin-LR*

Following the investigation of the cellular effects of eBeam irradiation treatment on *M. aeruginosa*, we studied the effects of eBeam doses on the toxin, MC-LR. The response of pure MC-LR (0.5 mg/L) suspended in laboratory grade distilled water to 0, 0.29, 0.39, 0.64, 2.1 and 5.1 kGy is shown in Figure 9. During preliminary studies, we had exposed 0.5 mM MC-LR to relatively high doses (between 5 kGy and 50 kGy) and attempted to detect the presence of the toxin molecule using LC-HRAM. However, all these doses resulted in the MC-LR concentrations dropping below the quantification limits (data not shown).

Figure 9A depicts resulting MC-LR concentrations determined analytically using LC-HRAM. Samples irradiated at 0.29 kGy (290 Gy) resulted in an 85% reduction of

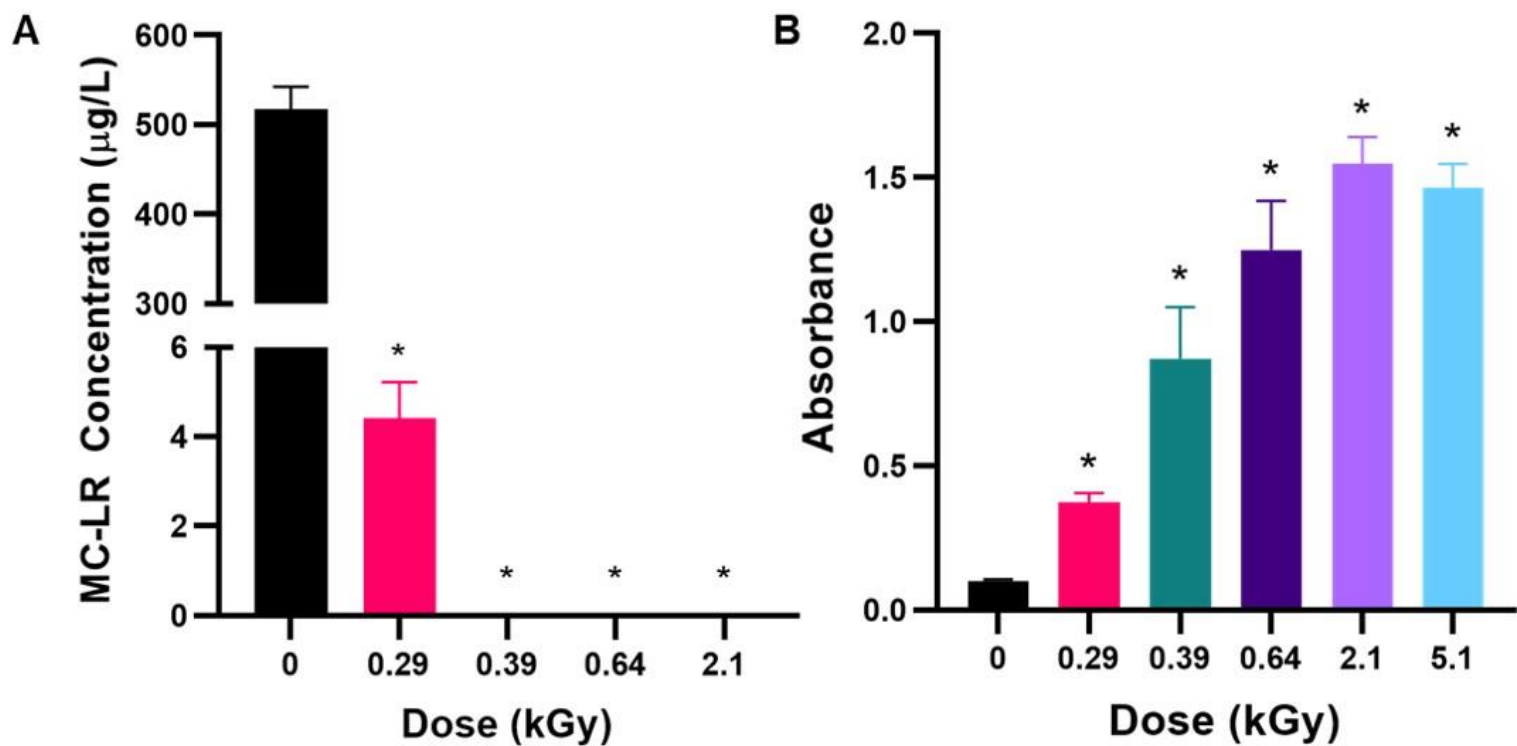


Figure 9. Degradation of MC-LR after 0, 0.29, 0.39, 0.64, 2.1, and 5.1 kGy eBeam irradiation treatment. A) Analytical determination of remaining MC-LR using LC-HRAM after eBeam treatment. B) MC-LR remaining after eBeam irradiation as determined by EPA method 546 ADDA-specific ELISA. Increasing absorbance corresponds to a decrease in binding of MC-LR to the detection antibody. (\* =  $p \leq 0.05$ ; error bars represent standard deviation).

the parent MC-LR concentration. At doses exceeding 0.29 kGy, MC-LR concentrations were below the limit of quantification (1 ng/L). Figure 9B shows the remaining MC-LR following eBeam irradiation as determined biologically using the ADDA-specific ELISA kit (Eurofins Abraxis).<sup>116</sup> Similarly to analytical identification, all eBeam treatment doses resulted in a significant decrease in binding within the assay suggesting degradation of the MC-LR parent molecule after eBeam irradiation treatment. These results suggest that minimal eBeam doses may be sufficient to breakdown extracellular MC-LR molecules in water samples.

We then investigated the ability of MC-LR irradiation degradation products to exhibit toxicity using a colorimetric PP2A inhibition bioassay as previously described.

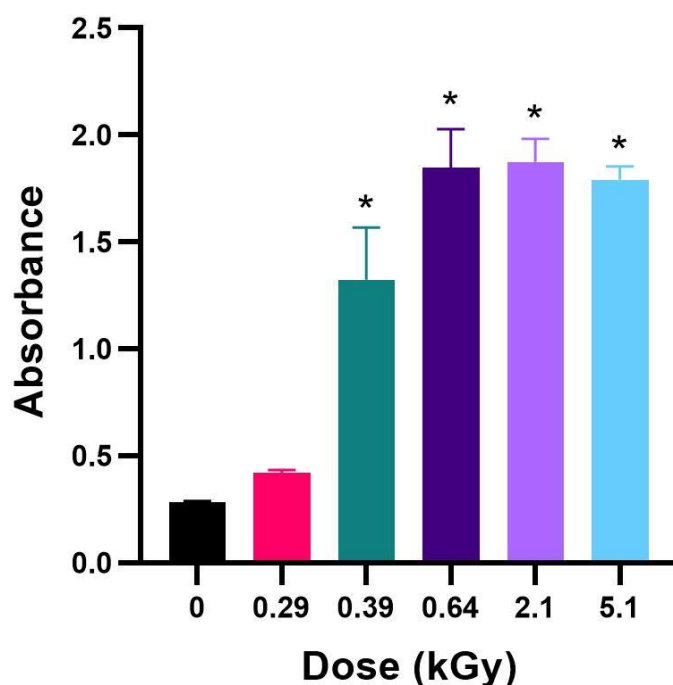


Figure 10. Protein phosphatase 2A inhibition assay toxicity of MC-LR after 0, 0.29, 0.39, 0.64, 2.1, and 5.1 kGy eBeam irradiation treatment as determined using a protein phosphatase 2A inhibition assay. (\* =  $p \leq 0.05$ ; error bars represent standard deviation).

We observed an increased absorbance corresponding to a decrease in PP2A inhibition at all doses (Figure 10). This suggests that even at doses as low as 0.39 kGy, there is a significant reduction in toxicity. Samples treated with doses 0.64 kGy or greater resulted in similar levels of PP2A function. We were unable to use this assay quantitatively due to the MC-LR concentrations of irradiated samples falling below the kit's standard curve concentrations. Nevertheless, these results indicate a significant reduction in PP2A inhibition in irradiated samples.

A portion of toxicity caused by MC-LR is associated with the binding and inhibition of protein phosphatases.<sup>47,50</sup> This binding is thought to be largely due to the ADDA moiety of MC-LR molecule binding irreversibly to the enzyme.<sup>49</sup> The gradual reduction of toxicity observed between 0.29 kGy and the 0.64 kGy treated MC-LR suggests that eBeam irradiation is resulting in possible structural damage to the ADDA moiety. Studies to understand the structure of the degradation products are currently underway.

Studies show that eBeam irradiation does cause both direct and indirect damage to biomolecules such as DNA and proteins.<sup>84,124</sup> It is understood that there is an inverse relationship between ionizing radiation doses required for degradation and the molecular weight of the target molecule.<sup>79,125</sup> Due to proteins being much smaller in size than DNA, our MC-LR degradation results were surprising. At present, little research has been done to identify the degradation products of MC-LR resulting from ionizing radiation treatment. Of these, a study completed by Song et al. (2009) identified two main possible reaction pathways of MC-LR degradation by gamma irradiation.<sup>104</sup> The

first suggested pathway was the hydroxylation of the aromatic ring of the ADDA moiety, and the second was hydroxyl attack at the diene bond also on the ADDA group. However, in their studies, the solution was saturated with oxygen creating a more oxidative environment with the conversion of hydrated electrons to superoxide radical. Also, as mentioned above, there are fundamental differences in the form of ionizing radiation used. Further, it is unclear whether these degradation products of MC-LR will lack toxicity. The experiments that we have performed do not permit us to postulate whether the damage to the ADDA molecule is due to direct or indirect damage specifically. Studies are ongoing to determine residual toxicity of these degradation products in mammalian cells.

In comparison with our previous data on cyanobacterial cell response to eBeam irradiation, much lower dose is required for the degradation of the MC-LR toxin. However, although Figure 9 suggests doses >290 Gy are enough to breakdown MC-LR below quantification limits, it appears that the dose still leaves residual toxicity that is detectable by the PP2A inhibition bioassay (Figure 10). This result emphasizes the higher sensitivity of bioassays compared to analytical assays.<sup>126,127</sup> Moreover, this result suggests that water utilities should include toxicity bioassays to determine residual toxicity rather than just relying on analytical determinations.

It is also important to note that these results utilize laboratory grade distilled water and cannot be extrapolated directly to the minimum dose required to achieve complete breakdown on 0.5 mM MC-LR concentration in drinking water supplies. This is because drinking water sample parameters can vary, primarily in terms of pH and



alkalinity.<sup>25,76,128</sup> Nevertheless, the results suggest that at the pH of the laboratory distilled water (~7), low eBeam was sufficient to achieve significant breakdown. This result also suggests that the mechanism of breakdown is primarily hydroxyl radical mediated rather than the solvated electrons. To confirm the exact mode of MC-LR breakdown, the sequential use of radical scavengers needs to be employed.<sup>101</sup>

#### *Potential of Microcystin-LR Release from eBeam-exposed M. aeruginosa Cells*

It is recognized that eBeam inactivation of microorganisms results in the cells entering a MAyNC state.<sup>89,91,129</sup> In order to understand the ability of eBeam irradiation to mitigate both cyanobacteria and cyanotoxins in water, it is also important to understand if *M. aeruginosa* is capable of retaining its metabolic activity. As noted above, it was observed that there is a delay in cell lysis following eBeam irradiation exposure. Therefore, we sought to investigate if MC-LR was present in cell culture following treatment. This was done by monitoring cultures post-irradiation over a 48-hour time period and separating intra-cellular MC-LR from extra-cellular MC-LR for analysis.

Figure 11 shows the intracellular and extracellular concentrations of MC-LR in *M. aeruginosa cells* after exposure to a lethal dose of 5.4 kGy and incubation in growth permissive Bold 3N medium. The intra-cellular and extra-cellular concentrations were based on the MC-LR concentrations in cell pellet and supernatant fractions, respectively. The MC-LR concentration in the untreated (0 kGy) cell pellet remained relatively constant over the 48 hours. The MC-LR concentration in the untreated supernatant increased ~97% over 48 hours due to normal cell turnover. In the lethally exposed (5.4 kGy) cell pellets, concentrations of MC-LR dropped below the limit of quantification at

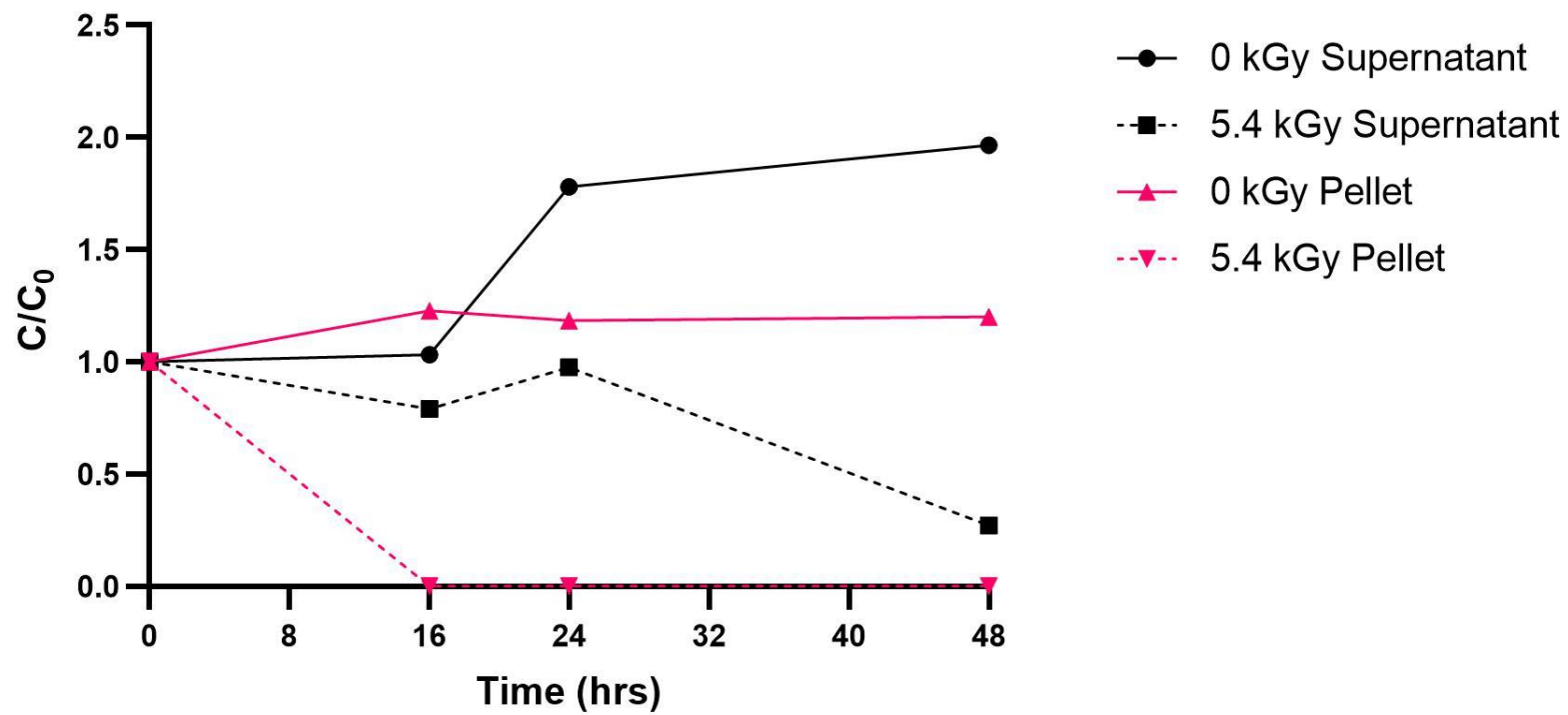


Figure 11. Time course study of intracellular MC-LR (pellet) and extracellular MC-LR (supernatant) at 0 and 5.4 kGy eBeam treatment

16 hours and remained below quantification limits up to 48 hours. This drop in intracellular MC-LR was assumed to be indicative of cell lysis. On the other hand, the MC-LR concentration in the supernatant of cells exposed to lethal eBeam doses showed a gradual decline over 48 hours but was not eliminated.

The presence of MC-LR in lethally exposed cell cultures suggests the possibility that *M. aeruginosa* is still metabolically active prior to cell death. During this time, synthesis of MC-LR may continue. The precise reasons why *M. aeruginosa* cells produce MC-LR and how these toxin molecules are transported out of cells is still unknown. It is also unclear whether *M. aeruginosa* has the ability to actively transport MC-LR out of the cell or if MC-LR release is reliant on cell lysis.<sup>130,131</sup> Figure 8 indicates that when *M. aeruginosa* cells are exposed to a 4.9 kGy eBeam dose, the cells lyse within 24 hours of eBeam exposure. Therefore, regardless of a mechanism of active transport, all remaining MC-LR is released into the surroundings. In Figure 11, the increase of MC-LR concentrations in the supernatant of 5.4 kGy exposed cells (as compared to supernatant of unexposed cells) after lysis suggests that the majority of toxin release occurs during cell lysis. However, it is unknown if the presence of MC-LR after irradiation is a result of synthesis by the inactivated cells or remaining toxin that was not degraded in treatment. Further, there is a gradual decline of MC-LR in the 5.4 kGy eBeam treated supernatant over time. This could suggest that MC-LR produced by irradiated cells may be less stable than normal MC-LR or that changes to media composition after irradiation induce MC-LR degradation. This data then supports our hypotheses that *M. aeruginosa* cells are ‘inactivated’ and that extra-cellular microcystin

is degraded. However, the presence of MC-LR in post-irradiated cell cultures contradicts our original predictions that no further synthesis would occur.

It is important to note that although resulting eBeam treatment concentrations of MC-LR in this study are lower than necessary for acute toxicity effects, chronic toxicity has been associated with prolonged MC-LR consumption. MC-LR is a potent acute toxin with an intraperitoneally administered LD<sub>50</sub> of 25-150 ug/kg of body weight in mice.<sup>33,132</sup> However, epidemiological studies have suggested increased risk of liver cancers following prolonged exposure to microcystin in drinking water.<sup>58</sup> A study completed by Zhou et al. (2002) also suggests there is an association between chronic microcystin exposure and colorectal cancer.<sup>133</sup> Therefore, understanding degradation and cellular effects are important for protecting the public's clean water supply.

The finding that lethally inactivated *M. aeruginosa* cells could accumulate and release MC-LR into the surrounding medium prior to lysis is significant in terms of developing a drinking water treatment train for drinking water treatment plants. It is possible that with just a single lethal eBeam dose, the inactivated cells could still accumulate the toxin and release it into the surrounding water. Therefore, in addition to inactivating the cyanobacterial cells, a secondary eBeam exposure a few days post the initial exposure may be warranted. This is because residual MC-LR may remain in the water supply without proper downstream treatment and pose further economic and public health ramifications. Alternatively, eBeam treatment may be deployed at the end of the drinking water treatment process following prior treatment that lyses the cyanobacterial cells. In this case, eBeam would be sufficient to remove free MC-LR

from the water. However, a deeper understanding of *M. aeruginosa* cell's metabolic activity post irradiation is necessary for development of effective treatment trains. Studies are on-going to understand the molecular mechanisms of how *M. aeruginosa* responds to eBeam irradiation treatment.

## **Conclusion**

Ionizing technologies are utilized for a variety of applications due to their ability to reduce bioburden by damaging DNA and cell membranes in microorganisms. Often used for medical device sterilization or phytosanitation, ionizing technologies present useful additions to water treatment processes to reduce both microbial loads as well as harmful toxins.<sup>118-120,134</sup> eBeam technology, in particular, is an electricity based and chemical free treatment strategy that could be effective at mitigating cyanoHABs and their toxins within the water treatment process.

In order for adequate treatment, it is imperative to understand the fundamental biology and chemistry associated with ionizing radiation doses on the various target microorganisms and pollutants. In summary, this study shows that eBeam technology can achieve significant reduction of MC-LR in pure water at neutral pH. Residual degradation products of MC-LR are unable to inhibit protein phosphatase activity suggesting an alleviation of toxicity. eBeam doses are also able to inactivate *M. aeruginosa* cells by inducing cell lysis. To our knowledge, this response has not been previously reported in cyanobacteria following eBeam exposure. However, cell lysis occurs after a time delay after exposure to ionizing doses. Additionally, *M. aeruginosa*

cells enter a MAyNC state during this time and may have the ability to synthesize more microcystin prior to cell lysis.

While full scale eBeam technology platforms for environmental remediation and water treatment are still in their infancy, this study demonstrates the utility of eBeam technologies for cyanotoxin and cyanobacteria degradation. In comparison with conventional and AOP technologies, eBeam technology can degrade both toxins and organisms in water samples.

## CHAPTER IV

### TOXICITY AND POSSIBLE ELECTRON BEAM MEDIATED DEGRADATION

#### MECHANISMS OF MICROCYSTIN-LR

##### **Abstract**

The degradation and residual toxicity of high energy electron beam (eBeam) treated microcystin-LR (MC-LR) were studied. Complete degradation of MC-LR was achieved in pure water in the presence of all radical scavengers employed (t-butanol, nitrogen sparging, and pH 13). Samples amended with t-butanol resulted in the most abundant degradation products suggesting that hydroxyl radicals play a significant role in MC-LR degradation by eBeam irradiation. LC/MS identified degradation products of treated MC-LR in pure water resulted in degradation products all below 303.155 m/z. MALDI TOF/TOF identified degradation products of treated MC-LR in pure water suggest the cleavage of the bioactive ADDA moiety in eBeam irradiated samples. These results were confirmed in vitro using the HEPG2 cell line. eBeam treated MC-LR eliminated toxicity in hepatocytes. Overall, MC-LR degradation by eBeam treatment appears mediated by reductive reactive species resulting in the elimination of toxicity of the parent MC-LR toxin.

##### **Introduction**

We had previously shown that eBeam technology was able to degrade MC-LR in water at low irradiation doses.<sup>135</sup> Thus, the purpose of this study was to investigate the effect of eBeam dose on the toxicity of MC-LR and to identify its possible degradation mechanisms. Our central hypothesis was that eBeam degrades MC-LR into non-toxic

byproducts. To test this hypothesis, we sought to investigate degradation products using radical scavengers, multiple analytical methods, as well as to investigate treated MC-LR cytotoxicity using an *in vitro* approach.

## **Materials and Methods**

### *Quantification of Microcystin-LR*

Pure microcystin-LR (purity  $\geq 95\%$ ) was obtained commercially (Cayman Chemical, Ann Arbor, MI). Microcystin-LR concentrations in experimental samples were quantified at the Integrated Metabolomics Analysis Core (IMAC) at Texas A&M University.

### *In Vitro Toxicity Assay*

Human hepatocellular carcinoma HEPG2 (HB-8065) purchased from ATCC (Manassas, Virginia) were grown in Dulbecco modified eagle medium (DMEM) (Corning Inc., Corning, NY) supplemented with 10% fetal bovine serum (Corning Inc., Corning, NY) and 1% antibiotic-antimycotic (Gibco, Thermo Fisher Scientific, Waltham, MA) at 37°C in 5% CO<sub>2</sub>. The cells were used between passages 8 and 10.

Cell proliferation and survival was assessed using the Cell Counting Kit-8 (CCK-8) (ApexBio Technology, Houston, TX). HEPG2 cells were seeded at  $5 \times 10^3$  per well in 96 well cell culture-treated plates. Cells were allowed to adhere for 24 hours in a CO<sub>2</sub> incubator (5% CO<sub>2</sub>, 37°C). After adhesion, media was removed and replaced with media containing test concentrations: 200  $\mu$ M MC-LR, 5 kGy treated 200  $\mu$ M MC-LR, 0  $\mu$ M MC-LR (negative control), 20% DMSO (positive control), and a blank (media without cells). A 1 mM stock of MC-LR was irradiated and diluted to test concentration for cell



culture application. The measured eBeam dose was 5.48 kGy. The cells were then incubated for 24, 48, 72, or 96 hours in the CO<sub>2</sub> incubator. Following incubation, 10 µl of CCK-8 solution was added to each well and then incubated for 2 hours. Absorbance was measured at 450 nm using a Synergy H1 Hybrid Multi-Mode Microplate Reader (Biotek, Winooski, VT) using Gen5 Microplate Reader and Imager software. The MC-LR cytotoxicity tests were performed using biological and technical triplicates.

#### *Electron Beam Treatment*

eBeam treatments were performed at Texas A&M University's National Center for Electron Beam Research in College Station, TX. A high energy (10 MeV), 15 kW pulsed S-band linear accelerator was used (dose rate 3 kGy/sec). EPR based spectroscopy using the Bruker e-scan reader (Billerica, MA) and alanine (L- $\alpha$ -alanine) dosimeters and were used to confirm delivered dose. Preliminary dose-mapping studies were performed on vials to ensure dose uniformity. All eBeam dosings were performed using 2 ml glass screw-thread vials (VWR International, Radnor, PA).

#### *Scavenger Study*

The roles of oxidative and reductive species on MC-LR degradation were assessed using three chemical additives. T-butanol was utilized to scavenge hydroxyl radicals (HO $\cdot$ ) and samples were prepared containing 0.2 g/L t-butanol ( $\geq 99\%$ , Sigma Aldrich), pH = 7, and 0.5 µg/L MC-LR in deionized water.<sup>136</sup> Nitrogen sparging was utilized to shift radiolytic species yield towards aqueous electrons (e<sub>aq</sub><sup>-</sup>).<sup>136</sup> Samples were prepared in an oxygen free enclosure, sparged with N<sub>2</sub> gas, and prepared at a concentration of 0.5 µg/L MC-LR in deionized water. Finally, samples were adjusted to

pH 13 using 1 N NaOH in order to alter the hydrogen/hydroxide ion ratio, creating a more reductive atmosphere.<sup>134,136</sup> All samples were irradiated at target doses of 0, 0.2, and 1 kGy. The measured doses were 0.18 kGy and 1.15 kGy.

#### *MC-LR Degradation Product Analysis*

MC-LR degradation was assessed using three different analytical methods namely 1) untargeted liquid chromatography high resolution accurate mass spectrometry (LC-HRAMS) – run in the positive mode, 2) hydrophobic interaction chromatography coupled to a Q Extractive HF mass spectrometry (HILIC QE HF MS/MS) – run in positive and negative mode, and 3) matrix-assisted laser desorption/ionization coupled to time-of-flight mass spectrometry (MALDI TOF/TOF MS). HILIC QE HF MS (Thermo QE HF. Thermo Scientific) analysis using was performed by the West Coast Metabolomics Center at the University of California, Davis. LC-HRAMS (Thermo Scientific) and MALDI TOF/TOF MS (Bruker Ultraflex extreme, Bruker Corporation) analysis were completed by IMAC at Texas A&M.

#### *Data Analysis*

Untargeted analytes in scavenging experiments and degradation experiments using LC-HRAMS were analyzed by IMAC at Texas A&M University. Briefly, sample acquisition was performed by Xcalibur (Thermo Scientific) and data analysis was performed with Compound Discoverer 3.1 (Thermo Scientific). Identified products based upon peaks areas were deemed significant if they were present at a >2 fold increase ( $p \leq 0.05$ ) as compared to the control (0 kGy) samples.

Untargeted analytes in degradation experiments using HILIC QE HF MS were analyzed by the West Coast Metabolomics Center at the University of California, Davis. Briefly, sample acquisition was completed using their in-house MS-Dial software (version 4.6). Data were normalized to a sum of internal standards and identified products based upon peak heights were deemed significant if they were >2 fold increase as compared to the blank.

These analytical methods are based on the assumption that breakdown products ionize well. It is important to note that potential products that are not easily ionized may not be detected with these techniques.

## **Results and Discussion**

### *Radiolytic Species Responsible for eBeam MC-LR Degradation*

We sought to investigate potential radiolytic species primarily responsible for the degradation of MC-LR during eBeam treatment. It is known that eBeam induced degradation of pollutants is caused by both oxidative and reductive radical species. Oxidative species, primarily hydroxyl radicals (HO<sup>\*</sup>), are believed to be the most important radical species for degradation of MC-LR in other studies.<sup>22,23,104</sup> Therefore, we employed three different radical scavengers (t-butanol, N<sub>2</sub> purging, and pH 13 to retard hydroxyl radical formation as much as possible) to understand whether it was the oxidative or reductive radiolytic species responsible for MC-LR eBeam degradation.

Samples containing 0.5 μM MC-LR were individually amended with t-butanol, purged with N<sub>2</sub> to remove oxygen, or adjusted to pH 13, and then exposed to target eBeam doses of 0, 0.2, or 1 kGy. These doses were chosen based on our previous studies

indicating that very low doses of eBeam treatment were sufficient to degrade MC-LR.<sup>135</sup> The MC-LR concentrations in all treated samples were below limit of detection (<LOD) for all additives (data not shown). To assess the scavenger effects, the breakdown products in the 200 Gy and 1 kGy treated samples were compared with the control (0 kGy) samples to identify differential products present in treated samples. These products were deemed significant if they were present at a >2 fold increase ( $p \leq 0.05$ ) as compared to the control (0 kGy) samples.

Based on the LC-HRAMS, in 200 Gy t-butanol amended samples, 22 products were identified as significant and 29 products were identified at 1 kGy (Figure 12 and 13). Using Compound Discoverer Software (Thermo Fisher Scientific), spectra of treated samples were compared to the mzCloud and ChemSpider databases for possible structure identification. In the 200 Gy treated t-butanol amended samples, 2 of the 22 significant peaks could be structurally assigned, and in the 1 kGy treated t-butanol amended samples, 4 of the 22 peaks were structurally assigned (Table 4 and 5). In the N<sub>2</sub> purged samples, 2 significant products were identified in the 200 Gy treated samples (Figure 14; Table 6). The mzCloud and ChemSpider database searches did not yield any matches for either compound. No significant products were identified in the 1 kGy treated samples. Finally, in the pH 13 adjusted samples, one (1) product was found to be significant for both the 200 Gy and 1 kGy treated samples (Figure 15 and 16; Table 7 and 8). Neither compound could be structurally identified.

T-butanol is known to scavenge hydroxyl radicals in solution as it has a high reactivity rate constant ( $3.8-7.6 \times 10^8 \text{ M}^{-1} \text{ s}^{-1}$ ).<sup>137,138</sup> The presence of a greater number of

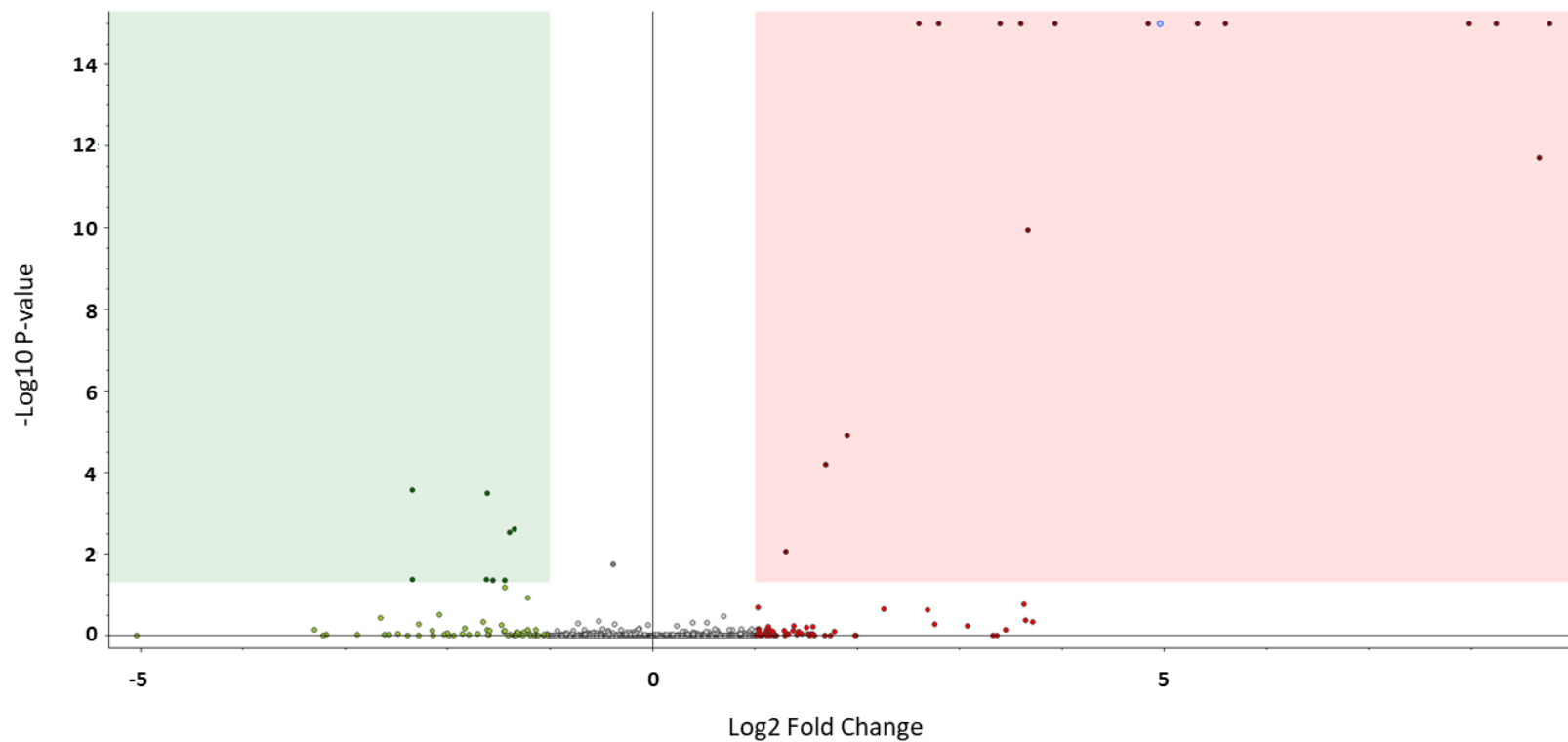


Figure 12. Products identified as significant (in red) in 0.18 kGy t-butanol amended samples vs. 0 kGy t-butanol amended samples (>2 fold change;  $p \leq 0.05$ ).

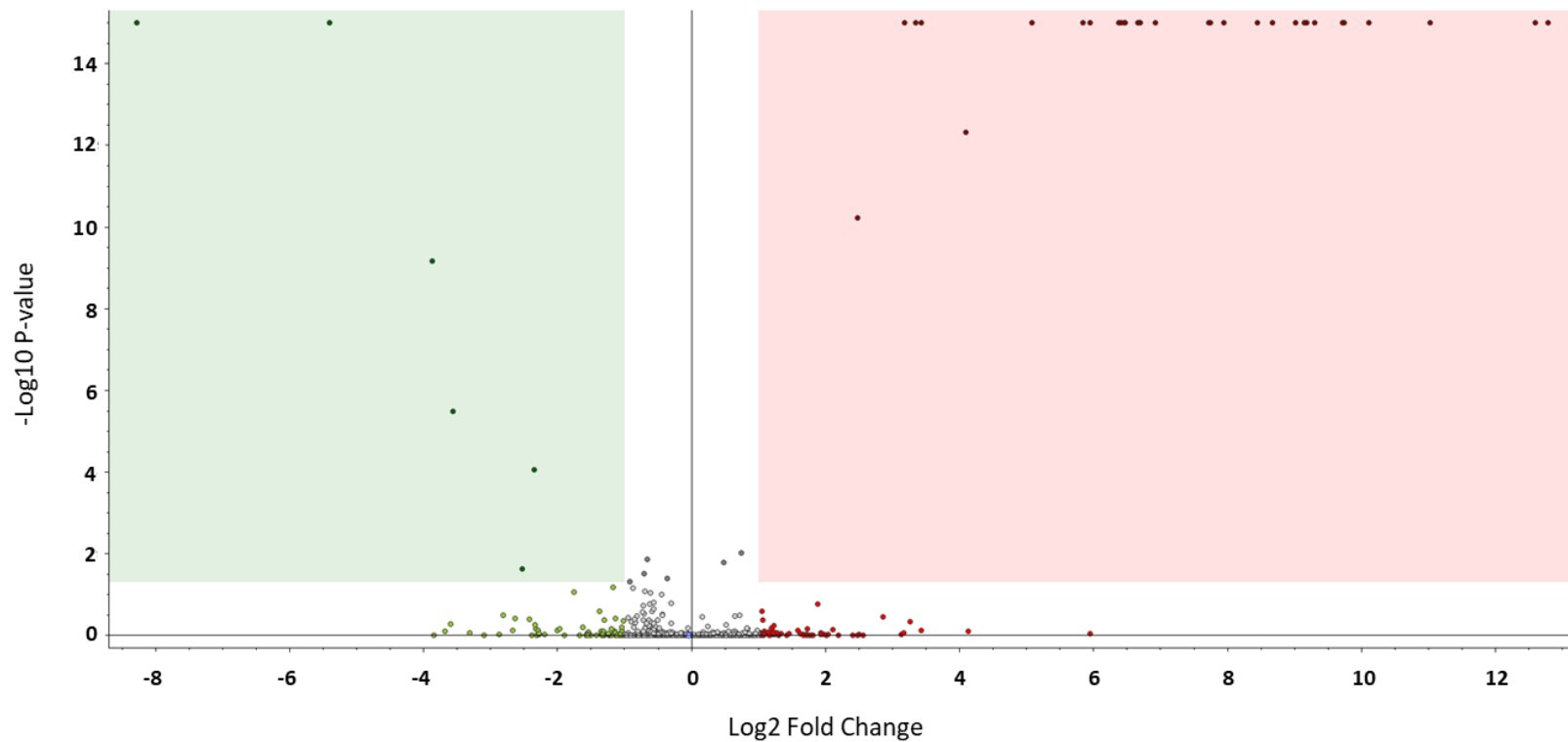


Figure 13. Products identified as significant (in red) in 1.15 kGy t-butanol amended samples vs. 0 kGy t-butanol amended samples (>2 fold change;  $p \leq 0.05$ ).

Table 4. Significant products in 0.18 kGy t-butanol amended samples vs. 0 kGy t-butanol amended samples (>2 fold change; p ≤ 0.05) identified by LC-HRAM. Suggested compound names identified by mzCloud or ChemSpider Databases.

Suggested Compound	Chemical Formula	mzCloud Annotation	ChemSpider Annotation	Molecular Weight (g/mol)	RT [min]
1733342	C8 H14	No results	Full match	110.1098	5.735
		No results	No results	154.0969	5.328
	C6 H12 N6	No results	No results	168.1125	5.734
	C5 H7 N2 O3 P	No results	No results	174.0203	1.762
	C8 H19 N O3	No results	No results	177.1363	2.386
	C6 H12 N6 O	No results	No results	184.1074	3.604
	C5 H8 N4 O2 S	No results	No results	188.036	2.26
	C6 H7 Cl N2 O3	No results	No results	190.0153	1.524
HLK	C18 H32 N6 O4	Invalid mass	Invalid mass	198.123	5.458
	C6 H12 N6 O2	No results	No results	200.1023	5.809
	C6 H11 N2 O4 P	No results	No results	206.0465	2.26
	C6 H5 N6 O P	No results	No results	208.0258	2.077
	C7 H16 O5 S	No results	No match	212.0722	5.744
	C8 H13 N2 O3 P	No results	No match	216.0672	5.324
	C9 H15 N2 O3 P	No results	No results	230.0828	5.739
	C8 H15 N2 O4 P	No results	No results	234.0777	5.329
	C4 H13 N8 O2 P	No results	No results	236.0889	5.732
	C9 H17 N2 O4 P	No results	No results	248.0932	5.736
	C11 H15 N6 P	No results	No results	262.109	5.735
	C9 H17 N2 O5 P	No results	No results	264.088	1.781
	C17 H33 N2 O5 P	No results	No results	376.2133	5.732
	C29 H39 N4 O2 P	No results	No match	506.2799	7.861

Table 5. Significant products in 1.15 kGy t-butanol amended samples vs. 0 kGy t-butanol amended samples (>2 fold change; p ≤ 0.05) identified by LC-HRAM. Suggested compound names identified by mzCloud or ChemSpider Databases.

Suggested Compound	Chemical Formula	mzCloud Annotation	ChemSpider Annotation	Molecular Weight (g/mol)	RT [min]
1733342	C8 H14	No results	Full match	110.1098	5.735
		No results	No results	154.0969	5.328
(1S,4aS)-1,4a-Dimethyl-1,2,3,4,4a,5,6,8a-octahydronaphthalene	C12 H20	No results	Full match	164.1564	7.456
	C6 H12 N6	No results	No results	168.1125	5.734
	C5 H7 N2 O3 P	No results	No results	174.0203	1.762
	C8 H19 N O3	No results	No results	177.1363	2.386
	C6 H12 N6 O	No results	No results	184.1074	3.604
10-Undecenoic acid	C11 H20 O2	No results	Full match	184.1462	7.665
	C5 H8 N4 O2 S	No results	No results	188.036	2.26
HLK	C18 H32 N6 O4	Invalid mass	Invalid mass	198.123	5.458
	C6 H12 N6 O2	No results	No results	200.1023	5.809
	C6 H11 N2 O4 P	No results	No results	206.0465	2.26
	C8 H13 N2 O3 P	No results	No match	216.0672	5.324
	C9 H15 N2 O3 P	No results	No results	230.0828	5.739
	C8 H15 N2 O4 P	No results	No results	234.0777	5.329
	C9 H17 N2 O4 P	No results	No results	248.0932	5.736
	C10 H17 N2 O4 P	No results	No results	260.0933	5.456
	C11 H15 N6 P	No results	No results	262.109	5.735
	C7 H23 N9 O7	No results	No match	345.1722	5.733
	C15 H29 N2 O5 P	No results	No results	348.182	5.328
	C17 H33 N2 O5 P	No results	No results	376.2133	5.732
	C28 H53 N O7 S	No results	No results	547.3569	7.295
	C27 H53 N5 O9	No results	No results	591.3828	7.404
	C32 H61 N O9 S	No results	No results	635.4088	7.485



Table 5. Continued

<b>Suggested Compound</b>	<b>Chemical Formula</b>	<b>mzCloud Annotation</b>	<b>ChemSpider Annotation</b>	<b>Molecular Weight (g/mol)</b>	<b>RT [min]</b>
	C28 H59 N4 O6 P3	No results	No results	640.3639	7.488
	C26 H61 N7 O13	No results	No results	679.435	7.552
	C36 H71 N O9 P2	No results	No match	723.4611	7.608
	C36 H65 N9 O9	No results	No results	767.4872	7.657
	C35 H76 N9 O6 P3	No results	No match	811.5133	7.697

untargeted peaks in t-butanol amended samples, as compared to differently amended samples, suggests that the lack of hydroxyl radicals in solution alters normal eBeam degradation of MC-LR at the doses employed in this study. However, the presence of t-butanol did not inhibit overall MC-LR degradation. In deaerated solutions ( $N_2$  purged), the predominant radical species present are expected to be aqueous electrons ( $e_{aq}^-$ ) as well.<sup>139,140</sup> The presence of hydroxyl radicals and hydrogen radicals are also expected under these conditions. Similar to the t-butanol amended samples, we observed complete degradation of the parent MC-LR compound at both 200 Gy and 1 kGy doses in deaerated samples. However, in these samples there were fewer identified significant products when compared to the t-butanol amended samples suggesting a more complete breakdown of MC-LR. This may be a result of hydroxyl radicals still present, albeit in smaller amounts, or the action of primary damage from the irradiation. In the experimental samples at pH 13, abundant hydroxide ions encourage the conversion of hydroxyl radicals to oxide radical anions, a reductive species.<sup>141</sup> The lack of identified products in pH 13 adjusted samples may suggest a similar MC-LR eBeam degradation mechanism to deaerated samples, or that reductive species may also play a role in the absence of hydroxyl radicals. Overall, this data suggests that eBeam degradation of MC-LR is primarily an oxidative process, but that reductive species may also contribute to degradation at neutral pH.

#### *MC-LR Degradation Products*

Following investigation of radical species responsible for MC-LR degradation using eBeam treatment, we sought to identify possible structures of these degradation

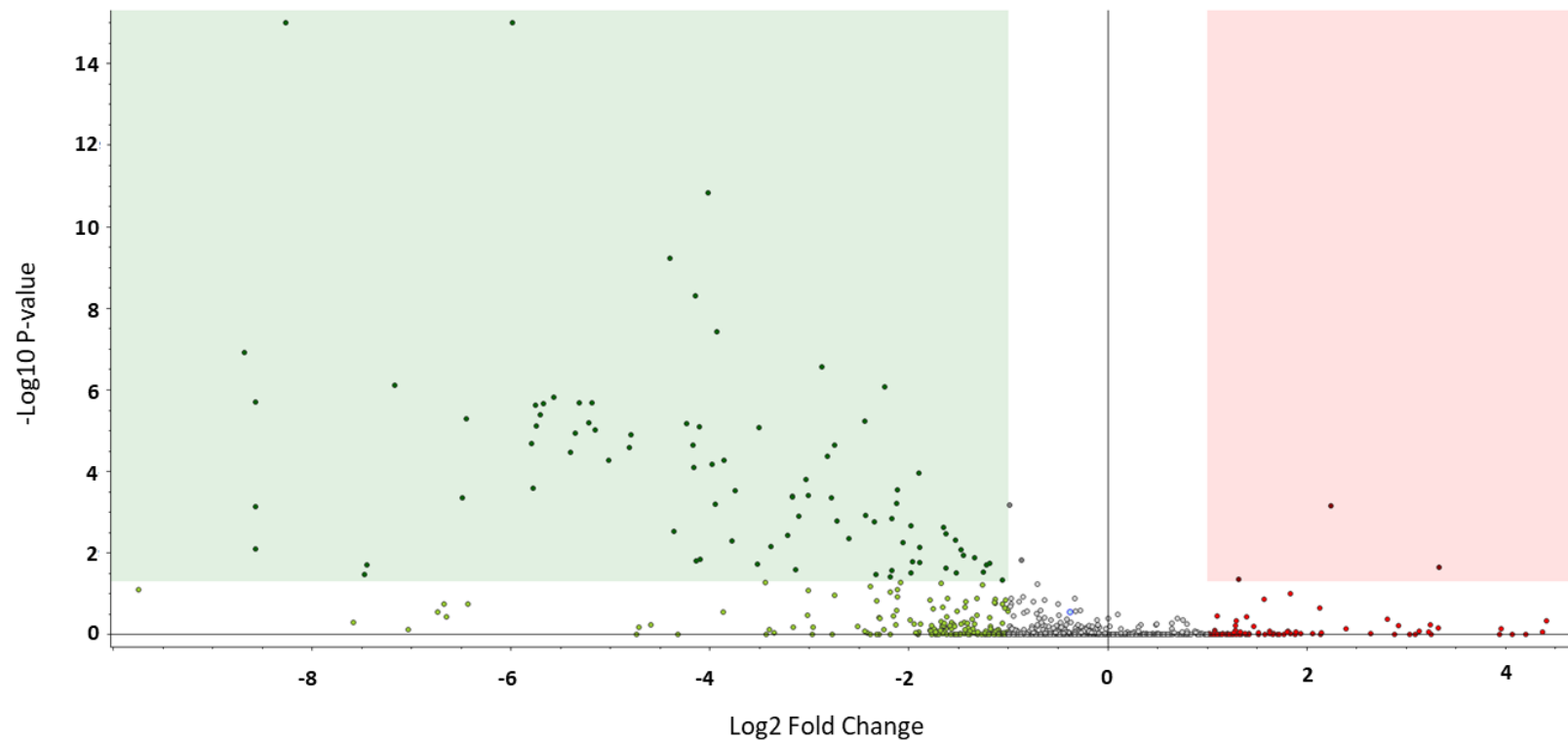


Figure 14. Products identified as significantly upregulated (in red) in 0.18 kGy N<sub>2</sub> sparged samples vs. 0 kGy N<sub>2</sub> sparged samples (>2 fold change;  $p \leq 0.05$ ).

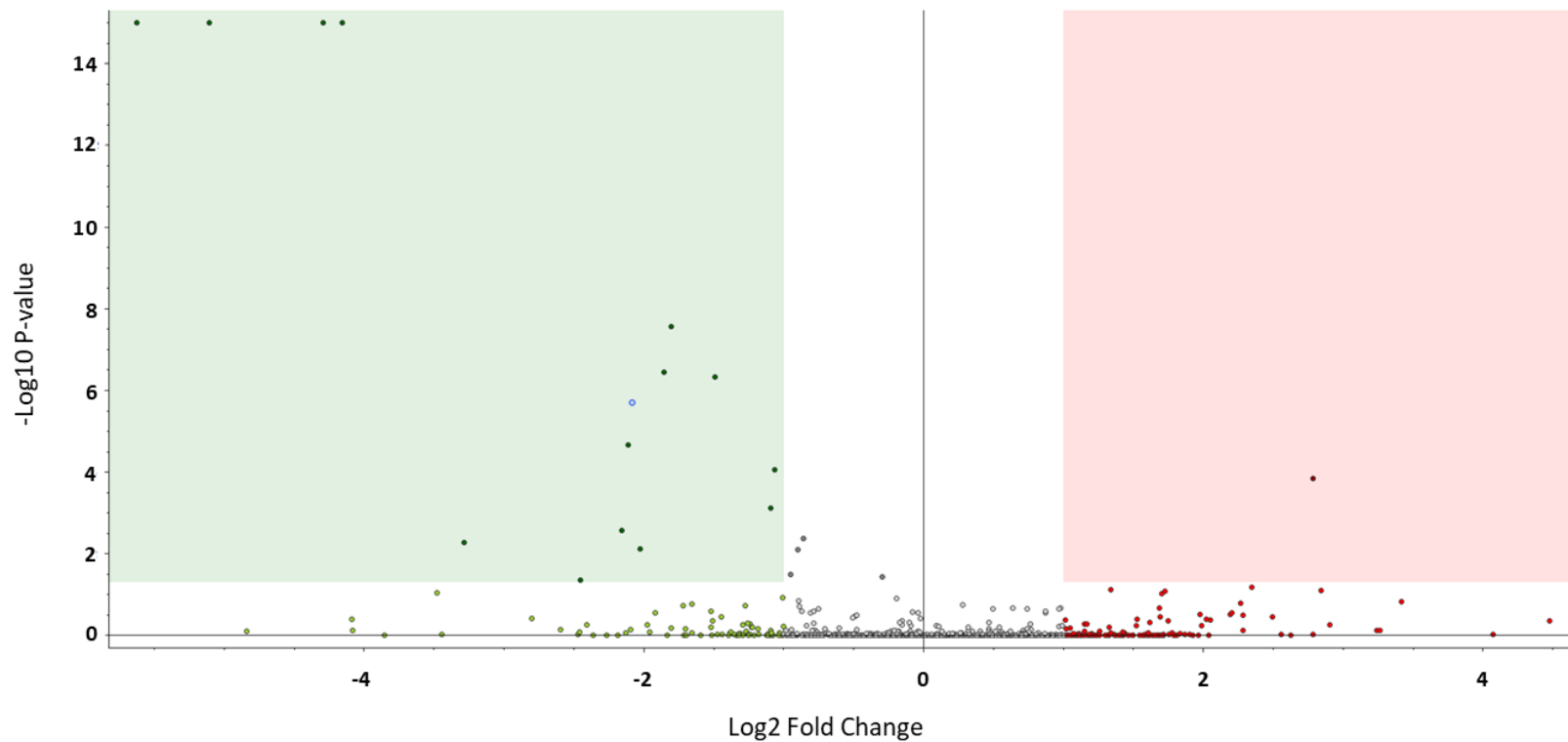


Figure 15. Products identified as significant (in red) in 0.18 kGy pH 13 adjusted samples vs. 0 kGy pH 13 adjusted samples (>2 fold change;  $p \leq 0.05$ ).

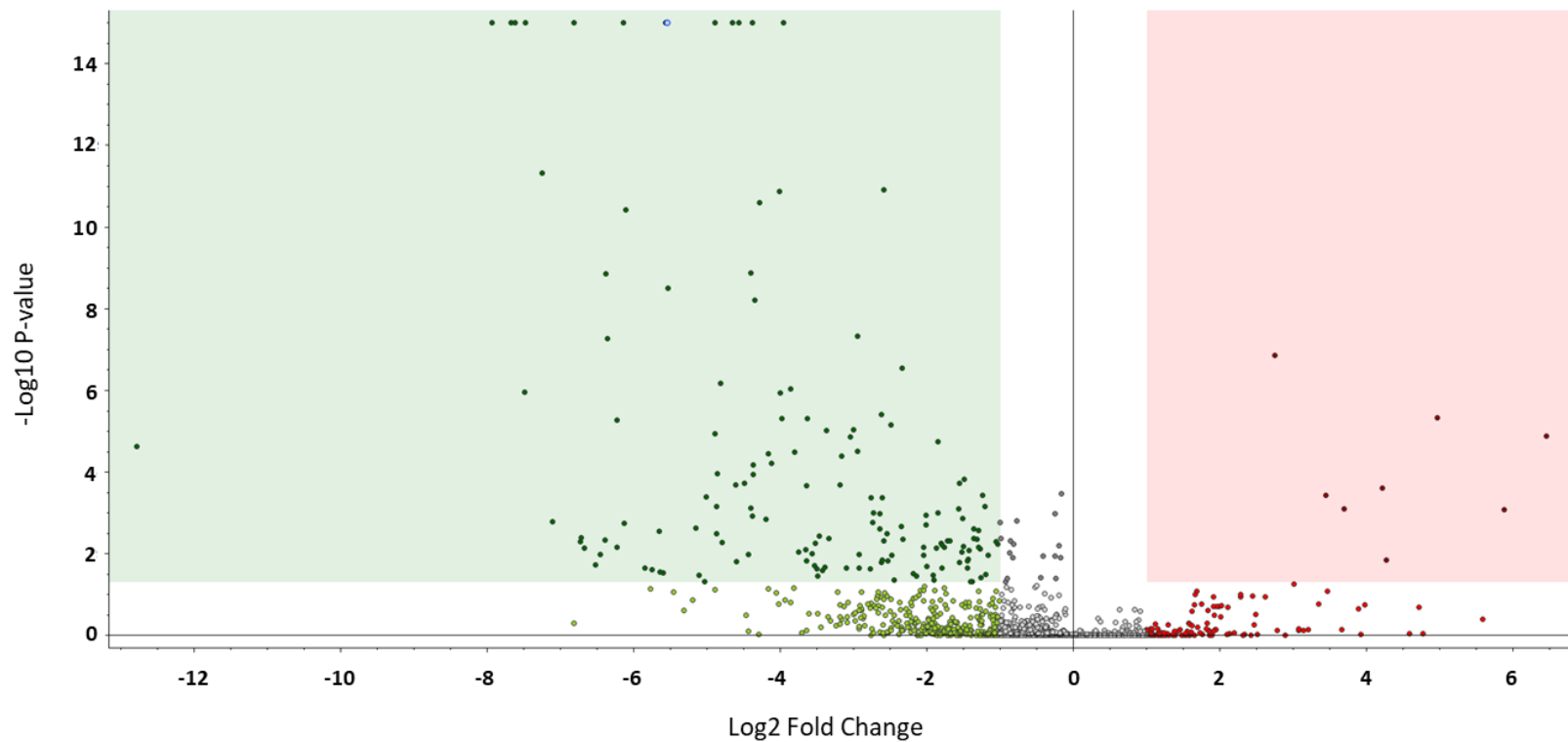


Figure 16. Products identified as significant (in red) in 1.15 kGy pH 13 adjusted samples vs. 0 kGy pH 13 adjusted samples (>2 fold change;  $p \leq 0.05$ ).

Table 6. Significant products in 0.18 kGy N<sub>2</sub> sparged samples vs. 0 kGy N<sub>2</sub> sparged samples (>2 fold change; p ≤ 0.05) identified by LC-HRAM. Suggested compound names identified by mzCloud or ChemSpider Databases.

<b>Suggested Compound</b>	<b>Chemical Formula</b>	<b>mzCloud Annotation</b>	<b>ChemSpider Annotation</b>	<b>Molecular Weight (g/mol)</b>	<b>RT [min]</b>
	C4 H4 O7 P2	No results	No match	225.9439	1.282
	C5 H4 N2 O13 P2	No results	No results	361.9181	1.365

Table 7. Significant products in 0.18 kGy pH 13 adjusted samples vs. 0 kGy pH 13 adjusted samples (>2 fold change; p ≤ 0.05) identified by LC-HRAM. Suggested compound names identified by mzCloud or ChemSpider Databases.

<b>Suggested Compound</b>	<b>Chemical Formula</b>	<b>mzCloud Annotation</b>	<b>ChemSpider Annotation</b>	<b>Molecular Weight (g/mol)</b>	<b>RT [min]</b>
	C5 H9 O2 P S	No results	No results	164.0061	1.636

Table 8. Significant products in 1.15 kGy pH 13 adjusted samples vs. 0 kGy pH 13 adjusted samples (>2 fold change; p ≤ 0.05) identified by LC-HRAM. Suggested compound names identified by mzCloud or ChemSpider Databases.

<b>Suggested Compound</b>	<b>Chemical Formula</b>	<b>mzCloud Annotation</b>	<b>ChemSpider Annotation</b>	<b>Molecular Weight (g/mol)</b>	<b>RT [min]</b>
	C2 H4 N2 O10 S	No results	No results	247.9594	1.092

products. Three different analytical methods were employed to examine degradation products: LC-HRAMS, MALDI TOF/TOF MS, and HILIC QE HF MS.

We began using untargeted LC-HRAMS with a scan range of 100-1500 m/z. Initial studies were completed with 0.5  $\mu$ M MC-LR in pure water at doses ranging from 300 Gy – 5 kGy. No degradation products were identified in these samples (data not shown).

Following these studies, we increased sample concentrations to 5  $\mu$ M and samples were treated at target doses of 2 and 5 kGy. Measured eBeam doses received were 2.14 and 5.03 kGy. Significant products (>2 fold change;  $p \leq 0.05$ ) were identified between untreated and treated samples with 8 products being identified in both the 2 and 5 kGy treated samples, respectively (Table 9 and 10). As with scavenging experiments, mzCloud and ChemSpider Databases were utilized for possible structure identification. The databases identified possible structures for 1 product (8-Azaguanine) in 2 kGy treated samples, and 2 products (8-Azaguanine and epsilon-Caprolactone) in 5 kGy treated samples. However, neither of these compounds appeared to be degradation products of MC-LR.

Following a lack of identifiable products using LC-HRAMS, we attempted MALDI tandem time of flight analysis to aid in breakdown product further identification. Samples containing 0.5  $\mu$ M MC-LR in pure water were irradiated at target doses of 300 Gy and 5 kGy. Actual doses received were 0.29 and 5.1 kGy. Initial MS1 spectra obtained for 0.3 kGy treated samples identified a significant peak at 789.110 m/z (Figure 17A). In 5 kGy treated samples, MS1 spectra identified a second significant peak at 699.057 m/z (Figure 17B). MALDI TOF/TOF utilizes a high energy ionizing

Table 9. Significant products in 2.14 kGy treated samples vs. 0 kGy untreated samples (>2 fold change;  $p \leq 0.05$ ) identified by LC-HRAM. Suggested compound names identified by mzCloud or ChemSpider Databases.

<b>Suggested Compound</b>	<b>Chemical Formula</b>	<b>mzCloud Annotation</b>	<b>ChemSpider Annotation</b>	<b>Molecular Weight (g/mol)</b>	<b>RT [min]</b>
	C4 H9 N3 O	No results	No results	115.075	1.01
		No results	No results	124.014	1.779
8-Azaguanine	C4 H4 N6 O	No results	Full match	152.045	1.927
	C3 H4 N8	No results	No results	152.056	1.547
	C3 H6 O7 S	No results	No results	185.984	1.771
	C4 H6 O9	No results	No results	198.001	1.616

Table 10. Significant products in 5.03 kGy treated samples vs. 0 kGy untreated samples (>2 fold change;  $p \leq 0.05$ ) identified by LC-HRAM. Suggested compound names identified by mzCloud or ChemSpider Databases.

<b>Suggested Compound</b>	<b>Chemical Formula</b>	<b>mzCloud Annotation</b>	<b>ChemSpider Annotation</b>	<b>Molecular Weight (g/mol)</b>	<b>RT [min]</b>
Epsilon-Caprolactone	C6 H10 O2	No results	Full match	114.0684	3.108
	C4 H4 N6	No results	No results	136.0501	3.106
	C4 H6 N6	No results	No results	138.0658	3.311
8-Azaguanine	C4 H4 N6 O	No results	Full match	152.0451	1.927
	C3 H4 N8	No results	No results	152.0563	1.547
	C4 H6 N6 O	No results	No results	154.0607	2.257



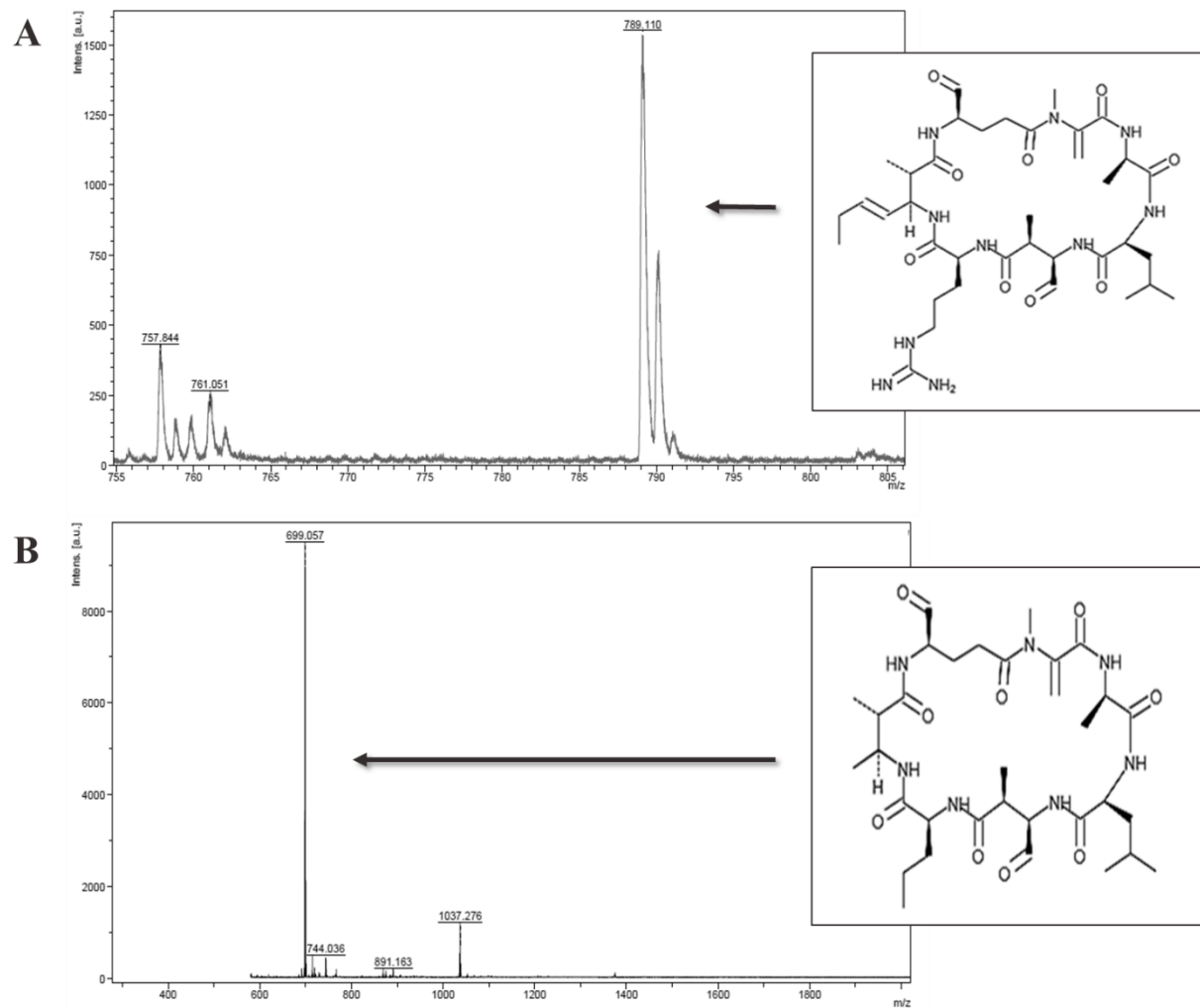


Figure 17. MALDI TOF/TOF spectra. A) Spectra of 0.5  $\mu\text{M}$  MC-LR irradiated at 0.29 kGy. Peak identified at 789.110 m/z and possible chemical structure. B) Spectra of 0.5  $\mu\text{M}$  MC-LR irradiated at 5.1 kGy. Peak identified at 699.057 m/z and possible chemical structure.

technique via lasers to ionize compounds of interest. This is beneficial for certain compounds that require higher energy for ionization. However, it is known that it can cause a secondary fragmentation of parent compounds and/or degradation products. To understand if the 699.057 m/z peak could be a degradation product or fragmentation caused by MALDI TOF/TOF, the 789.110 m/z was re-fragmented. However, re-fragmentation did not yield a peak at 699.057 m/z, suggesting this compound originated as a result of MC-LR being exposed to a 5 kGy eBeam dose. The possible structures of these compounds were estimated (Figure 17).

A final analytical method, HILIC QE HF MS, was attempted for MC-LR degradation product analysis. HILIC QE HF MS differs from LC-HRAMS analysis due to different LC methods for compound separation. Samples containing 1  $\mu$ M MC-LR were irradiated at target doses of 50, 150, and 350 Gy with actual doses received being 41, 126, and 343 Gy. A total of 87 compounds were identified as being significant degradation products in treated samples when compared to non-treated samples (data not shown). Of these 87 compounds, only two could be structurally identified. In the 50 Gy treated samples, a total of 10 compounds were identified as being significant. However, of these 10 compounds, only one (1) compound (200.9491 m/z) was present in all three replicates (Table 11). In 150 Gy treated samples, 31 compounds were identified, but only 5 products were present in all three replicates (232.7636, 160.0241, 162.0871, 303.1548, and 200.9491 m/z). Finally, in 350 Gy treated samples, a total of 66 compounds were identified as being significant when compared to the untreated control. However, only 11 of these compounds were identified in all three replicates. Between all

Table 11. Degradation products in 41 Gy, 126 Gy, and 343 Gy treated samples vs. 0 Gy untreated samples identified by HILIC QE HF MS. Shaded ions exhibit a dose response with increasing treatment dose.

m/z	Average Peak Height		
	50 Gy	150 Gy	350 Gy
154.0473			96627
160.0241		1867	121983
162.0871		1887	148715
181.0468			84243
190.0531			54838
199.0242			108778
200.9491	18376	58725	310425
221.0661			13979
231.0121			69200
232.7636		34512	
242.8918			95246
303.1548		6375	100502

Table 12. MC-LR identified by HILIC QE HF MS as [M+2H]<sup>2+</sup> ion at different sample doses.

Annotation	Species	m/z	Average Peak Height			
			0 kGy	50 Gy	150 Gy	350 Gy
Microcystin-LR	[M+2H] <sup>2+</sup>	498.281	590032	298285	153260	0

doses, 10 individual compounds were identified in treated samples. Four of these compounds, 160.0241, 162.0871, 200.9491, and 303.1548 m/z, exhibited a dose response with increasing irradiation dose. The 200.9491 m/z ion was present in all three treated samples and showed increasing peak height with increasing dose. This was seen inversely for the parent MC-LR compound (identified as  $[M+2H]^{2+}$ ) as peak height declined with increasing dose, signaling degradation (Table 12).

Few studies have investigated the degradation of MC-LR by ionizing radiation, and none have been published on degradation products resulting from eBeam irradiation. Most similarly, a study by Song et al. (2009) researched the destruction of MC-LR by hydroxyl radicals using both pulse radiolysis and radiolysis induced by gamma irradiation.<sup>104</sup> The main oxidative reaction sites identified were hydroxylation of the aromatic ring (1011 m/z) and hydroxyl radical attack of the ADDA (3-amino-9-methoxy-2,6,8-trimethyl-10-phenyldeca-4,6-dienoic acid) diene bond (1029 m/z) determined via LC/MS. Similar degradation identification studies utilizing treatments such as ozone, Fenton reagent, and UV/H<sub>2</sub>O<sub>2</sub>, yielded similar results.<sup>22,23,142</sup> However, neither of our LC/MS methods used identified any potential degradation products greater than 303.1548 m/z, even with a scan range up to 1500 m/z. This may suggest that eBeam MC-LR degradation may not only be mediated with hydroxyl radicals and/or that degradation of the parent compound is more complete with eBeam irradiation. However, it is important to note that the downfalls of all these analytical methods is the assumption that breakdown products ionize well. Potential products that are not easily ionized may not be detected with these techniques.

Using MALDI TOF/TOF, we were able to identify two potential degradation products of MC-LR of greater size than those detected via LC/MS. MC-LR is known to cause toxicity in mammalian hepatocytes primarily through the inhibition of protein phosphatases 1 and 2A (PP1 and PP2A).<sup>45</sup> Studies looking at MC-LR conformation and structure have shown that stereochemistry of the ADDA moiety is essential for biological activity and toxicity and that simple alterations in the double bonds of the ADDA group produce non-toxic stereoisomers.<sup>143</sup> From structures proposed using MALDI TOF/TOF analysis, the two identified degradation products may fully lack this ADDA moiety (Figure 17). Our previous work has shown that irradiated MC-LR is no longer able to bind in an ADDA-specific ELISA test or PP2A inhibition assay, further corroborating this idea.<sup>135</sup>

#### *Effect of eBeam Treated MC-LR on Target Cell Viability*

HEPG2 cells were used to investigate the hepatotoxic effects of eBeam treated MC-LR. Initially, a preliminary dose response was completed to assess the cytotoxic concentration range. MC-LR was added at a concentration range of 0 - 200  $\mu$ M and monitored for 24-120 hours using the CCK-8 assay (Figure 18). A concentration of 200  $\mu$ M MC-LR was the only dose that showed a decline in cell viability over time, resulting in a ~95% decline in cell viability at 120 hours. Therefore, this MC-LR concentration was chosen for further studies.

To determine if eBeam irradiation treatment could reduce MC-LR toxicity, MC-LR was irradiated at a target dose of 5 kGy (Figure 19). The actual dose received was 5.48 kGy. Cultures dosed with 5 kGy treated MC-LR showed no significant decline in

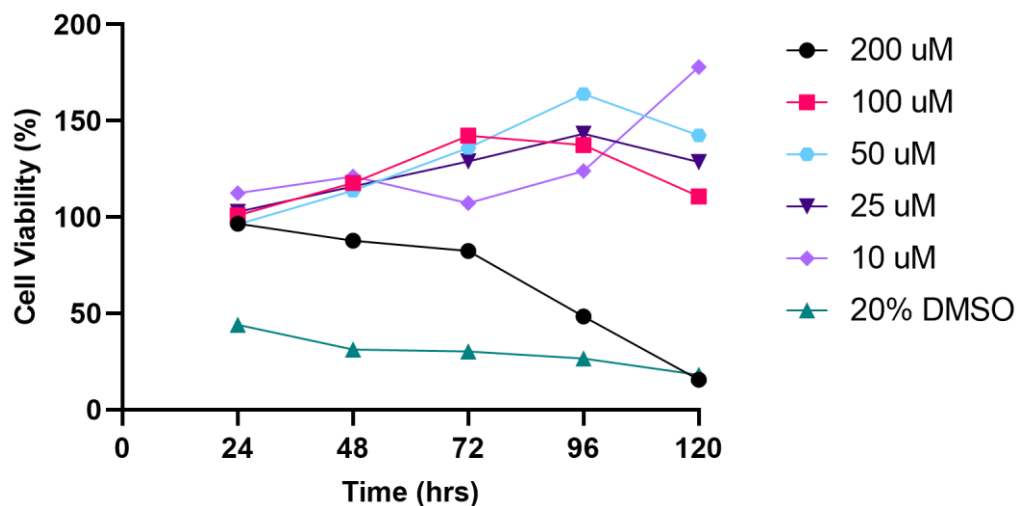


Figure 19. Initial dose response of MC-LR on HEPG2 cells over 120 hours using the CCK-8 assay. (No error bars are shown as this was a preliminary study with technical replicates only.)

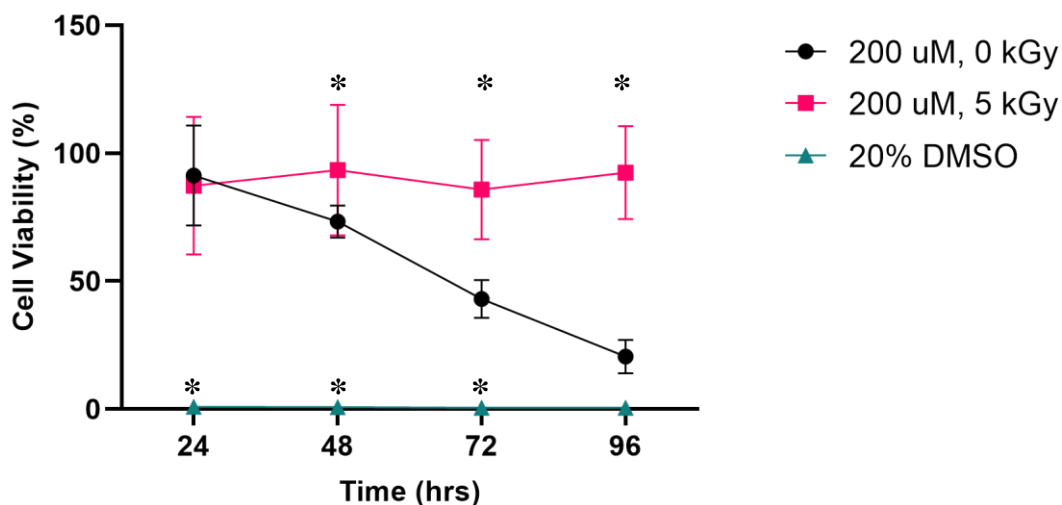


Figure 18. Change in cell viability in HEPG2 cells dosed with 5.48 kGy irradiated or 0 kGy non-irradiated MC-LR over 96 hours using the CCK-8 assay. (Error bars represented at standard deviation; \* =  $p \leq 0.05$  determined via Tukey's multiple comparisons test)

cell viability over the 96-hour test window. Unirradiated MC-LR dosed cells showed significant declines in cell viability over the same 96-hour window with cell viability decreasing 19.66, 52.77, and 77.47% for 48, 72, and 96 hours respectively.

As discussed previously, the MC-LR ADDA side chain has been linked to the biologic activity of these cyanotoxins. The lack of this ADDA functional group in MALDI TOF/TOF identified degradation products may indicate a reduction in toxicity of irradiated MC-LR. The *in vitro* results support the hypothesis that alteration and/or cleavage of this moiety occurs after exposure to 5.48 kGy eBeam dose with its resulting lack of toxicity. The lack of cell death in HEPG2 cells also suggests that degradation products formed during eBeam irradiation do not exhibit residual toxicity.

## **Conclusion**

Electron beam technology is a promising addition to water treatment strategies for the treatment of various environmental pollutants.<sup>144-147</sup> Cyanotoxins are an emerging class of drinking water contaminants that require effective removal strategies for the protection of human health. Previous work has demonstrated analytically, and in bioassays, that eBeam treatment is able to degrade the cyanotoxin MC-LR.<sup>135</sup> In this study, we investigated the possible degradation mechanisms of eBeam treated MC-LR, as well as the ability of eBeam treatment to reduce the toxicity of MC-LR.

Three chemical additives were used to investigate possible radiolytic species responsible for MC-LR degradation. Degradation of the parent MC-LR compound occurred in all amended samples. Samples amended with t-butanol resulted in the greatest number of significant products suggesting that hydroxyl radicals play a large

role in MC-LR degradation. Deaerated and pH 13 amended samples resulted in fewer identified significant products further corroborating an oxidative breakdown mechanism. Still, the degradation of the parent MC-LR compound in all samples suggests that reductive species may still play a role in MC-LR breakdown, especially in less oxidative conditions.

Three different analytical chemistry methods were employed to identify degradation product structures of MC-LR following eBeam treatment. Unlike studies completed with other AOPs, our LC/MS methods did not identify products with hydroxyl addition or substitution on the ADDA moiety. Instead, various ions ranging from 114.068 - 303.155 m/z were detected, but chemical structures could not be elucidated. MALDI TOF/TOF investigation of irradiated MC-LR identified two potential degradation products at 788.110 m/z and 699.057 m/z. The proposed structures for these compounds suggest eBeam treatment may result in cleavage of the ADDA moiety.

As the ADDA moiety of MC-LR is responsible for its biologic activity, cytotoxicity of irradiated MC-LR was assessed in vitro using HEPG2 cells. Irradiation of MC-LR at 5 kGy reduced cell death in HEPG2 cells as compared to non-irradiated MC-LR. This suggests that MC-LR is degraded by eBeam treatment and that degradation products also lack toxicity. Further, lack of toxicity in vitro also agrees with lack of the ADDA moiety present on MC-LR eBeam irradiation byproducts. Overall, this study demonstrates the ability of eBeam irradiation technology to reduce the toxicity of MC-LR in water and that the degradation of MC-LR is primarily an oxidative process.



## CHAPTER V

### MOLECULAR RESPONSES OF *MICROCYSTIS AERUGINOSA* TO VARYING ELECTRON BEAM DOSES

#### **Abstract**

Electron beam (eBeam) technology is a promising addition to drinking water treatment for the removal of the cyanotoxins, microcystins. However, the molecular response(s) of cyanobacteria following exposure to eBeam doses still needs to be understood. In this study, the effect of eBeam doses on *M. aeruginosa* was studied as it relates to both amount of dose and incubation period after exposure to eBeam doses. Cell concentrations in treated cultures declined following two hours of incubation after treatment. However, extracellular microcystin-LR (MC-LR) increased significantly in both 2 and 5 kGy treated cultures and continued to increase over time. DNA fragmentation was more extensive in eBeam-treated cultures than untreated cultures suggesting that eBeam irradiation does do damage the DNA of these organisms. Global gene expression was investigated using transcriptomics. The primary genes affected by eBeam treatment were related to photosystem function and DNA repair. Differences in expression of both photosystem I and II genes and *mcy* cluster genes were seen between 2 and 5 kGy eBeam exposed cultures. The data suggests that MC-LR synthesis may indeed be occurring following irradiation, but at a lesser extent than in untreated cultures. Furthermore, cell lysis of *M. aeruginosa* cells appears to be due to light damage following irradiation rather than damage to DNA.

#### **Introduction**

This study aimed to investigate the molecular responses of *M. aeruginosa* to eBeam irradiation treatment. We hypothesized that following eBeam exposure, the *M. aeruginosa* cells will continue to synthesize the MC-LR toxin prior to cell lysis. We also postulated that extensive DNA damage accrued from ionizing radiation ultimately results in cell death. Therefore, the specific research questions we pursued were a) to determine intracellular and extracellular MC-LR production over time following irradiation, b) to investigate DNA fragmentation patterns as a function of eBeam dose and incubation time following irradiation, and c) to investigate transcriptomic responses in *Microcystis aeruginosa* over specific time points post eBeam exposure.

## **Materials and Methods**

### *Laboratory Propagation of M. aeruginosa*

*M. aeruginosa* (LB 2385, origin: Little Rideau Lake, Ontario, Canada) was purchased from UTEX Culture Collection of Algae in Austin, TX. The cyanobacteria were cultured in a modified Bold 3N medium (without soil-water extract) under a 12/12 day/night cycle at ~20°C on an orbital shaker at ~100 rpm. Cell titers were determined using chlorophyll absorbance (680 nm) read on a Synergy H1 Hybrid Multi-Mode Microplate Reader (Biotek, Winooski, VT) using Gen5 Microplate Reader and Imager software using an initially prepared standard curve.

### *Electron Beam Treatment*

eBeam dosing treatments were performed at the National Center for Electron Beam Research at Texas A&M University in College Station, TX as described previously in Chapter III. Cultures were exposed to eBeam doses in 30 ml round-bottom

screw cap culture tubes (Corning Inc., Corning, NY) following preliminary dose-mapping studies were to confirm dose uniformity.

### *Experimental Design*

Previous studies have suggested that there is a time delay between eBeam treatment and *M. aeruginosa* cell lysis.<sup>135</sup> Therefore, we sought to understand the effect of both time and irradiation dose on *M. aeruginosa* cells. All samples in this study were taken from the same experimental cultures to create matching datasets (Figure 20). First, turbid *M. aeruginosa* cultures were exposed to target doses of 0, 2, or 5 kGy in biological triplicate. Actual doses received were 2.02 and 5.03 kGy. Samples were collected following treatment at 0, 2, 4, 6, 24, and 48 hours post irradiation. Cultures were analyzed for cell growth, MC-LR production, DNA fragmentation, and transcriptomics.

### *Quantification of Microcystin-LR*

Microcystin-LR concentrations in culture samples were analyzed analytically at the Integrated Metabolomic Analysis Core (IMAC) at Texas A&M University using LC-HRAMS as described previously in Chapter IV.<sup>135</sup>

### *DNA Extraction and Fragmentation Analysis*

DNA extraction was completed using the DNeasy UltraClean Microbial Kit (Qiagen, Germantown, MD). DNA samples were quantified using the DropletQuant (PerkinElmer, Waltham, MA) on DropletViewer/cDrop Software version 3.2.0.128 (PerkinElmer). Fragment size was then analyzed using the Agilent Fragment Analyzer 5300 (Agilent, Santa Clara, CA) and data was evaluated using Agilent ProSize Data

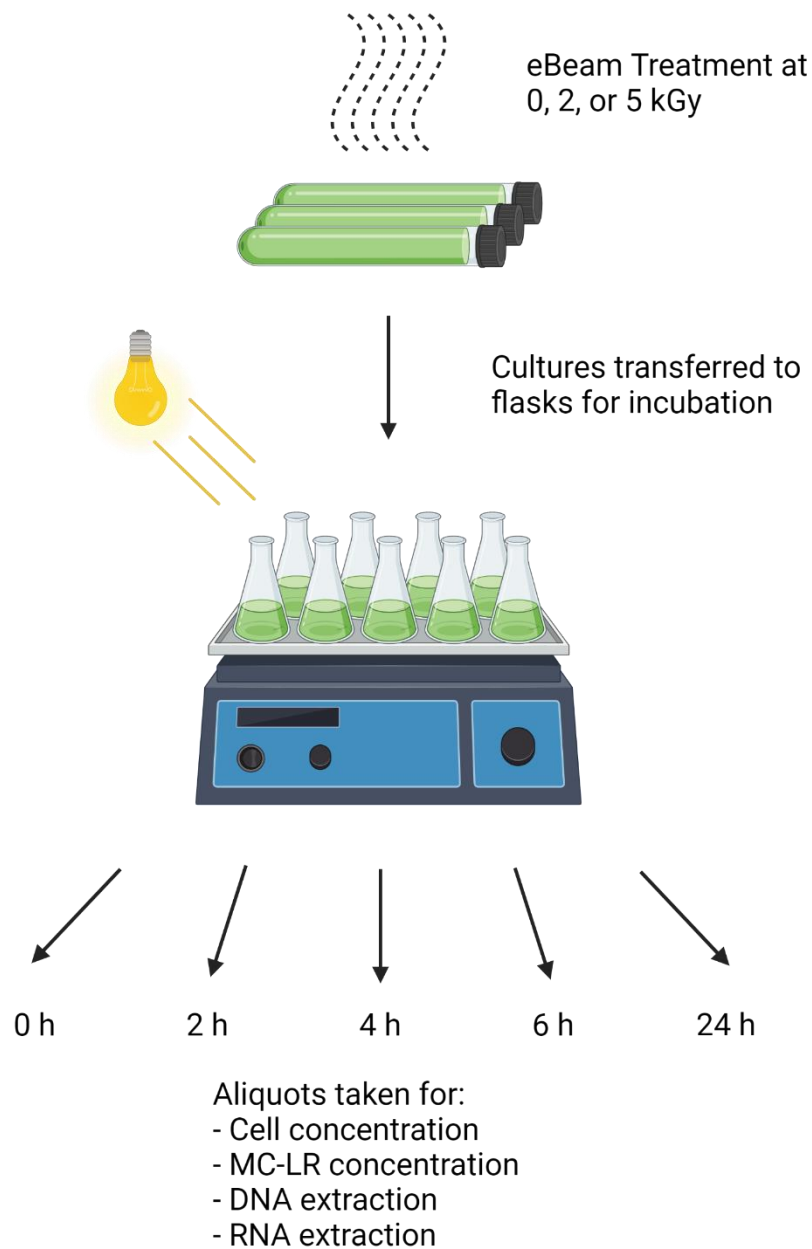


Figure 20. Experimental design for timed experiment. *M. aeruginosa* cultures were irradiated in 30 ml screw cap vials at 0, 2.02, or 5.03 kGy. Following irradiation, cultures were transferred to flasks and incubated in lighted conditions on an orbital shaker. Sampling aliquots were taken at 0, 2, 4, 6, and 24 hours post eBeam exposure for further analysis. Schematic created with BioRender.

Analysis Software version 4.0.0.3.

### *Transcriptomic Analysis*

#### *RNA Extraction*

RNA extraction was completed using the RNeasy Mini Kit with RNeasy Protect Bacteria Reagent (Qiagen, Germantown, MD). Briefly, total RNA was extracted using the RNeasy Protect Bacteria Reagent kit protocol 1: Enzymatic Lysis of Bacteria. This was followed by protocol 7: Purification of total RNA from Bacterial Lysate Using RNeasy Mini Kit.

#### *Library Preparation and RNAseq*

RNA samples were quantified using the Qubit High Sensitivity Fluorometric Assay (Thermo Fisher Scientific, Waltham, MA) and RNA quality was assessed using the Agilent TapeStation RNA Tapes (Agilent Technologies). RNA was normalized to between 50-100 ng of input into the NEBNext rRNA Depletion Kit (Bacteria) kit to deplete the bacterial rRNA before preparation of sequencing libraries using the NEBNext Ultra II Directional RNA Library Preparation Kit for Illumina (New England BioLabs, Ipswich, MA). Each sample was uniquely indexed then pooled in an equimolar concentration for sequencing on an Illumina NovaSeq 6000 2x150 S4 flow cell to generate approximately 20 million read pairs for each sample.

#### *Bioinformatic Analysis*

RNAseq data was analyzed using Zymo Research RNAseq service pipeline, which was originally adapted from nf-core/rnaseq pipeline v1.4.2 (<https://github.com/nf-core/rnaseq>).<sup>148</sup> Briefly, quality control of raw reads was carried out using FastQC

v0.11.9 (<http://www.bioinformatics.babraham.ac.uk/projects/fastqc>). Adapter and low-quality sequences were trimmed from raw reads using Trim Galore! v0.6.6 ([https://www.bioinformatics.babraham.ac.uk/projects/trim\\_galore](https://www.bioinformatics.babraham.ac.uk/projects/trim_galore)). Trimmed reads were aligned to the reference genome *Microcystis aeruginosa* NIES-298 using STAR v2.6.1d (<https://github.com/alexdobin/STAR>).<sup>149</sup> BAM file filtering and indexing was carried out using SAMtools v1.9 (<https://github.com/samtools/samtools>).<sup>150</sup> RNAseq library quality control was implemented using RSeQC v4.0.0 (<http://rseqc.sourceforge.net/>) and QualiMap v2.2.2-dev (<http://qualimap.conesalab.org/>).<sup>151,152</sup> Duplicate reads were marked using Picard tools v2.23.9 (<http://broadinstitute.github.io/picard/>).<sup>153</sup> Library complexity was estimated using Preseq v2.0.3 (<https://github.com/smithlabcode/preseq>).<sup>154</sup> Duplication rate quality control was performed using dupRadar v1.18.0 (<https://bioconductor.org/packages/dupRadar/>).<sup>155</sup> Reads overlapping with exons were assigned to genes using featureCounts v2.0.1 (<http://bioinf.wehi.edu.au/featureCounts/>).<sup>156</sup> Differential gene expression analysis was carried out using DESeq2 v1.28.0 (<https://bioconductor.org/packages/DESeq2/>).<sup>157</sup> Quality control and analysis results plots were visualized using MultiQC v1.9 (<https://github.com/ewels/MultiQC>).<sup>158</sup>

KEGG annotation of the reference genome was obtained using BlastKOALA (<https://www.kegg.jp/blastkoala/>) and annotation of the microcystin biosynthesis (*mcy*) gene cluster were manually curated. Expression patterns of photosystem I/II and *mcy* genes were plotted using DESeq2-normalized read counts and were based on these KEGG annotations. Mean normalized read counts among replicates were calculated,

log<sub>2</sub>-transformed, centered on the mean of all dosage-time combinations, and plotted in heatmaps.

## Results

### *M. aeruginosa* Cell Growth

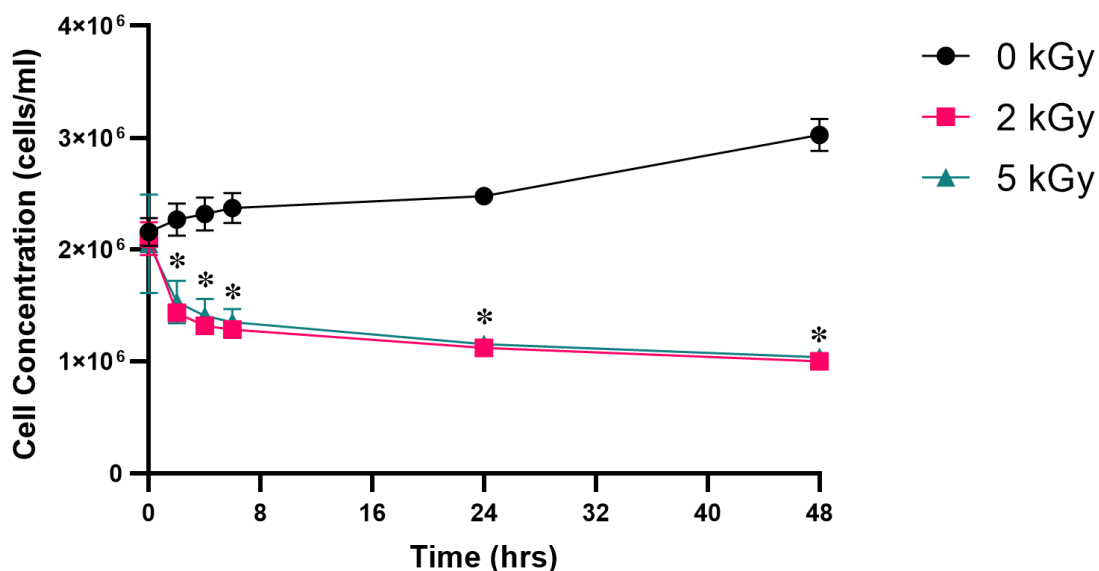


Figure 21. Response of *M. aeruginosa* cells to 0, 2.02, and 5.03 kGy eBeam irradiation doses. (Error bars are represented as standard deviation; \* =  $p \leq 0.05$  determined via Tukey's multiple comparisons test).

*M. aeruginosa* cell growth was monitored over time after eBeam treatment at 0, 2, or 5 kGy. Figure 21 shows the response of the cells over 48 hours following irradiation. At hour 0 (immediately following irradiation), cell concentrations were approximately  $2 \times 10^6$  cells/ml in both treated and non-treated cultures. Following 2 hours of incubation, both 2 and 5 kGy treated culture cell concentrations significantly decreased by 31.4% and 26.1%, respectively. Cell concentrations in untreated cultures increased gradually over time signifying normal cell growth. However, cell

concentrations continued to decline in treated cultures throughout the 48-hour sampling time frame.

#### *M. aeruginosa Toxin Production*

To investigate MC-LR production, intracellular and extracellular MC-LR concentrations were monitored over time (Figure 22). Intracellular MC-LR consisted of MC-LR extracted from the cellular fraction of the cultures, and the extracellular MC-LR consisted of MC-LR extracted from the supernatant fraction of the cultures. In untreated cultures, intracellular MC-LR gradually increased over time with culture growth (Figure 22A). In 2 kGy treated cultures, intracellular MC-LR fell below limits of quantification (<LOQ) after the 2-hour time point. At 2 hours, 2 kGy cultures contained more intracellular MC-LR ( $3.05 \pm 0.75 \mu\text{g/L}$ ) than untreated cultures ( $1.62 \pm 0.45 \mu\text{g/L}$ ). In 5 kGy treated cultures, all sampling time points had concentrations of MC-LR <LOQ. In 0 kGy untreated cultures, extracellular MC-LR fluctuated between quantifiable amounts and values <LOQ (Figure 22B). This could be due to overall biologic variability between cultures and a small amount of cell turnover. In 2 and 5 kGy treated cultures, extracellular MC-LR trends were the inverse of intracellular MC-LR trends. At 0 hours, the 2 kGy extracellular MC-LR was <LOQ. However, all other time points showed increases in extracellular MC-LR. Similarly, 5 kGy also had elevated levels of extracellular MC-LR at all sampling time points. Overall, extracellular MC-LR in 2 and 5 kGy samples were approximately 3 times higher than those measured in untreated cultures.

#### *eBeam Induced DNA Fragmentation*



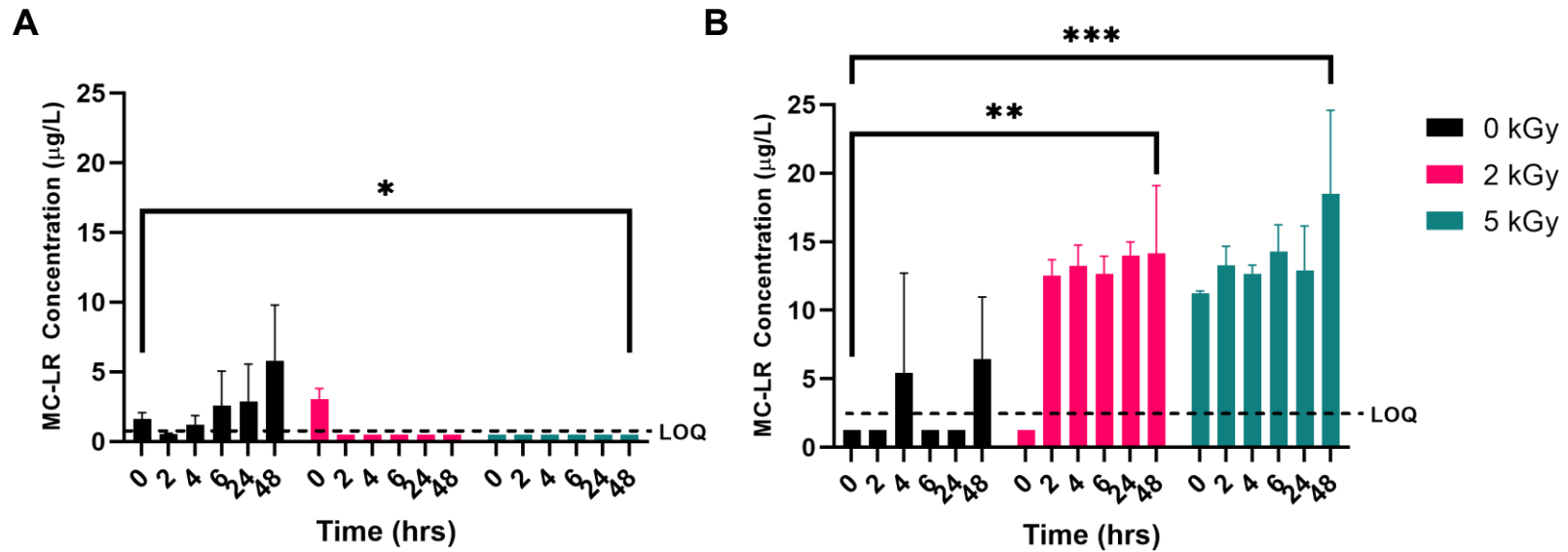


Figure 22. Intracellular and extracellular MC-LR concentrations following eBeam treatment at 0, 2.02 and 5.03 kGy over time. A) Intracellular MC-LR concentration. B) Extracellular MC-LR concentration. (Error bars represented as standard deviation; Intracellular limit of quantification (LOQ) = 1  $\mu\text{g/L}$ ; Extracellular LOQ = 2.5  $\mu\text{g/L}$ ; \* =  $p \leq 0.05$ ; \*\* =  $p \leq 0.01$ ; \*\*\* =  $p \leq 0.001$ )

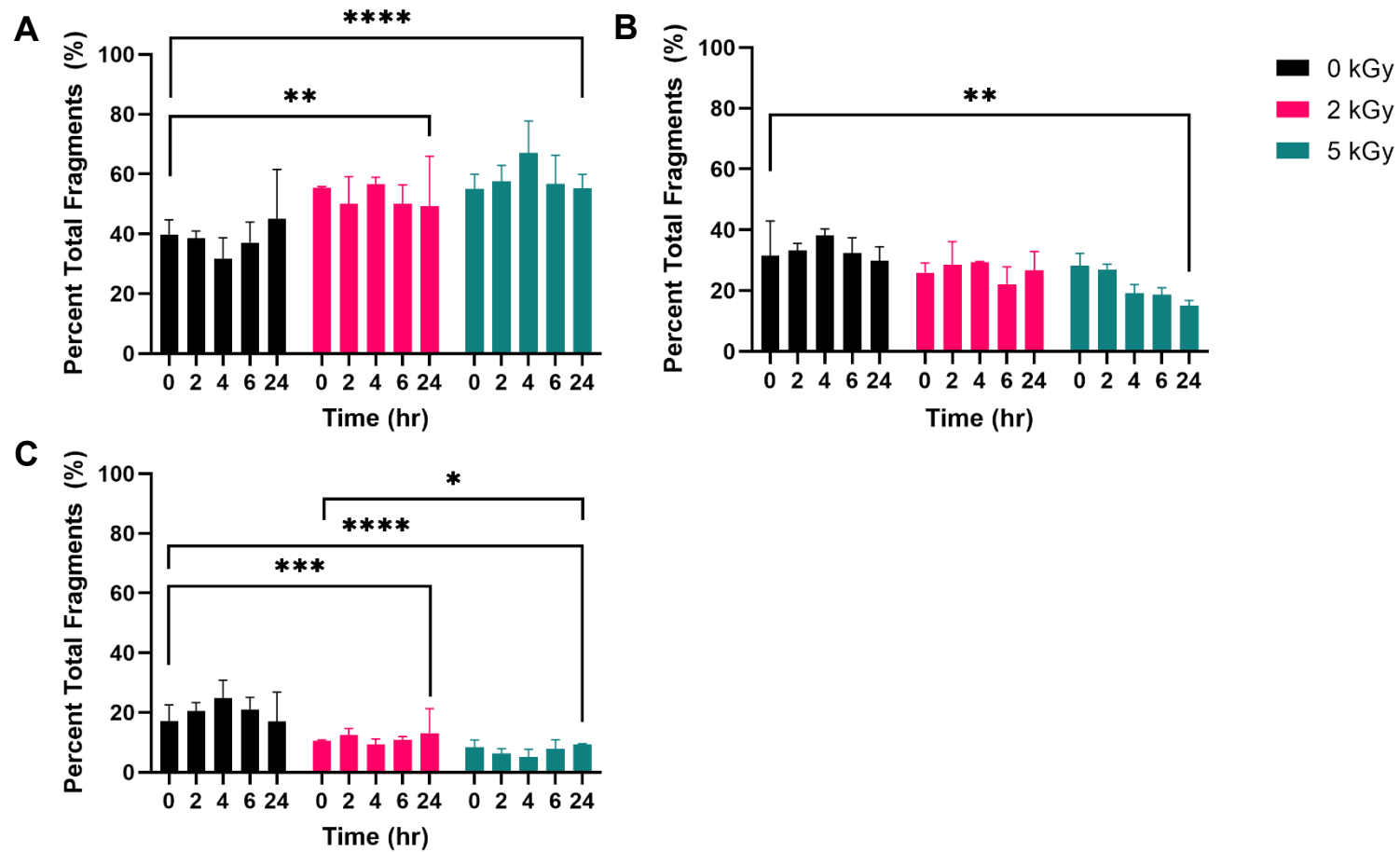


Figure 23. DNA fragmentation as a percent of total DNA fragments in 0 kGy, 2.02 kGy, and 5.03 kGy eBeam exposed *M. aeruginosa* cultures over time. A) 50 – 10,000 bp length fragments; B) 10,000 – 20,000 bp length fragments; C) 10,000 – 30,000 bp length fragments.

We sought to investigate the effect of eBeam treatment on *M. aeruginosa* cell's DNA condition as it related to dose, as well as if DNA repair was able to occur following irradiation and prior to cell death. To aid in data analysis, the DNA fragmentation patterns were binned into fragment sizes. Figure 23 shows the percent of DNA fragments binned by fragment size in 0, 2, and 5 kGy treated cultures. Overall, 2 and 5 kGy eBeam treated cultures showed a significantly greater percentage of shorter fragments (50 – 10,000 bp length) than nontreated cultures (Figure 23A). Conversely, 2 and 5 kGy treated cultures contained a significantly smaller percentage of longer fragments (20,000 – 30,000 bp length) when compared to nontreated cultures (Figure 23C). In the intermediate fragment size bin (10,000 – 20,000 bp length), significant differences in percent of total fragments were only observed between 5 kGy treated and untreated cultures (Figure 23B). It is important to note that mechanical shearing is natural and expected during DNA extraction, which is why fragmentation is still present in untreated cultures.<sup>159</sup> No trends discernable were observed when comparing fragment sizes over the sampling time points within either dose.

#### *eBeam Induced Changes in M. aeruginosa Global Gene Expression*

Global changes in gene expression of *M. aeruginosa* cells were investigated as a function of both eBeam dose and time following exposure using RNAseq analysis. Overall, dose was seen to be the main factor influencing gene expression in cultures. Figure 24 displays the pattern of separation among all samples. eBeam treated samples were distinctly clustered by dose regardless of incubation period. Untreated cultures did display time dependence in genes expressed, which could be associated with day:night

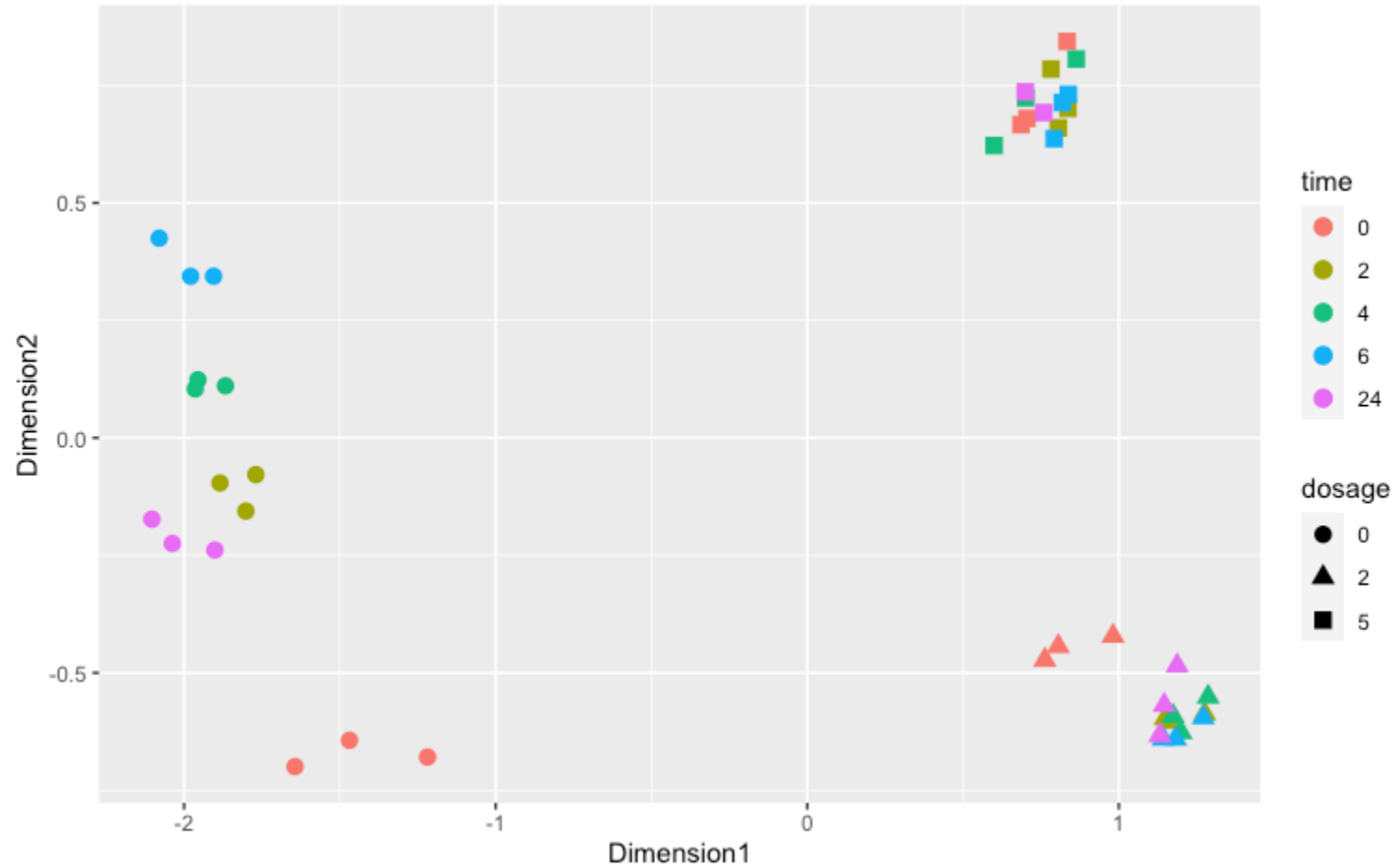


Figure 24. Multidimensional scaling (MDS) plot of all *M. aeruginosa* samples. Samples appear clustered by eBeam treatment dose. Shapes indicate doses of 0, 2.02, and 5.03 kGy. Colors indicate time following eBeam treatment at 0, 2, 4, 6, and 24 hours. Untreated cultures also showed clustering across sample timepoints (circle shape).

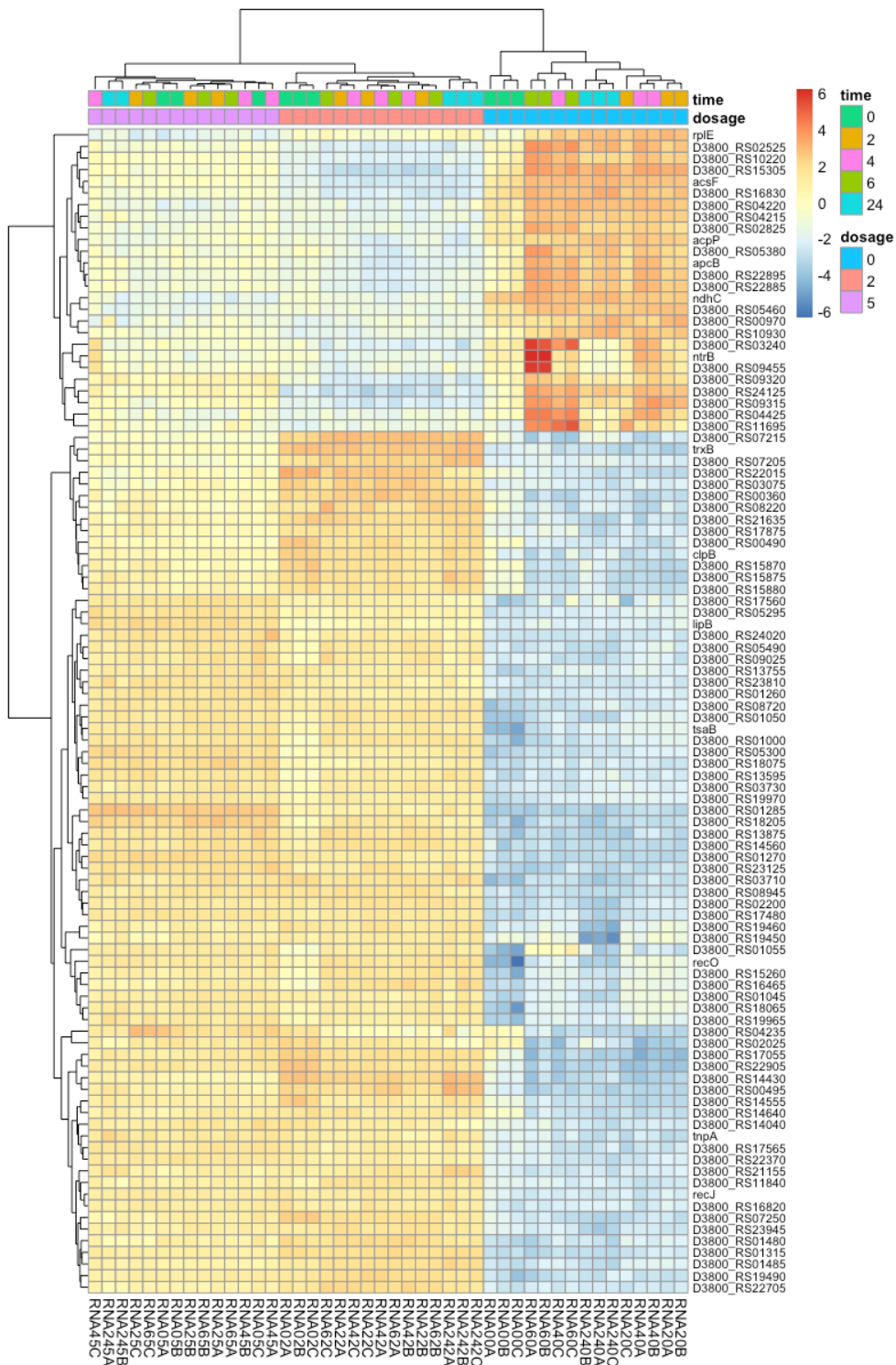


Figure 25. Heatmap of expression patterns of top 100 differentially expressed genes with greatest variance in eBeam treated and untreated *M. aeruginosa* cultures.

cycling (as seen by the circle shapes). In the 2 kGy dose group, there was a distinction between expression of samples at 0 hours and the remaining timepoints (as seen by the red triangle shapes). This aligns with the MC-LR concentration data discussed above (Figure 22) and may indicate an increase in metabolic activity prior to cell death. In 5 kGy eBeam treated samples, there were no distinctions between any time points (as seen by the square shapes).

The top 100 genes with the greatest variance in differential expression across all samples are displayed in Figure 25. Unfortunately, due to gaps in genome annotation, many genes were unidentified. Gaps in annotation may occur at regions that are highly repetitive, regions that have low coverage, or due to a full annotation not being completed for the selected reference genome.<sup>160</sup> The reference genome selected for this project was ASM1019642v1 (<https://bit.ly/3rpqbm7>) as it had the lowest percentage of non-mapped reads when tested on our samples. Figure 25 shows distinct clustering between gene expression patterns and dose. The majority of differentially expressed genes were unchanged or upregulated in 2 and 5 kGy treated cultures but downregulated in untreated cultures. Approximately 25% of the top differentially expressed genes showed downregulation in 2 and 5 kGy cultures but upregulation in untreated cultures.

#### *Influence of Incubation Period Post eBeam Exposure on Gene Expression*

A total of 3,216 genes were differentially expressed between at least 2 time points in non-treated cultures. Figure 26 displays the expression patterns of the top 100 genes differentially expressed in non-treated cultures at all time points. eBeam treatment of *M. aeruginosa* cultures at 2 kGy resulted in a total of 2,276 differentially expressed

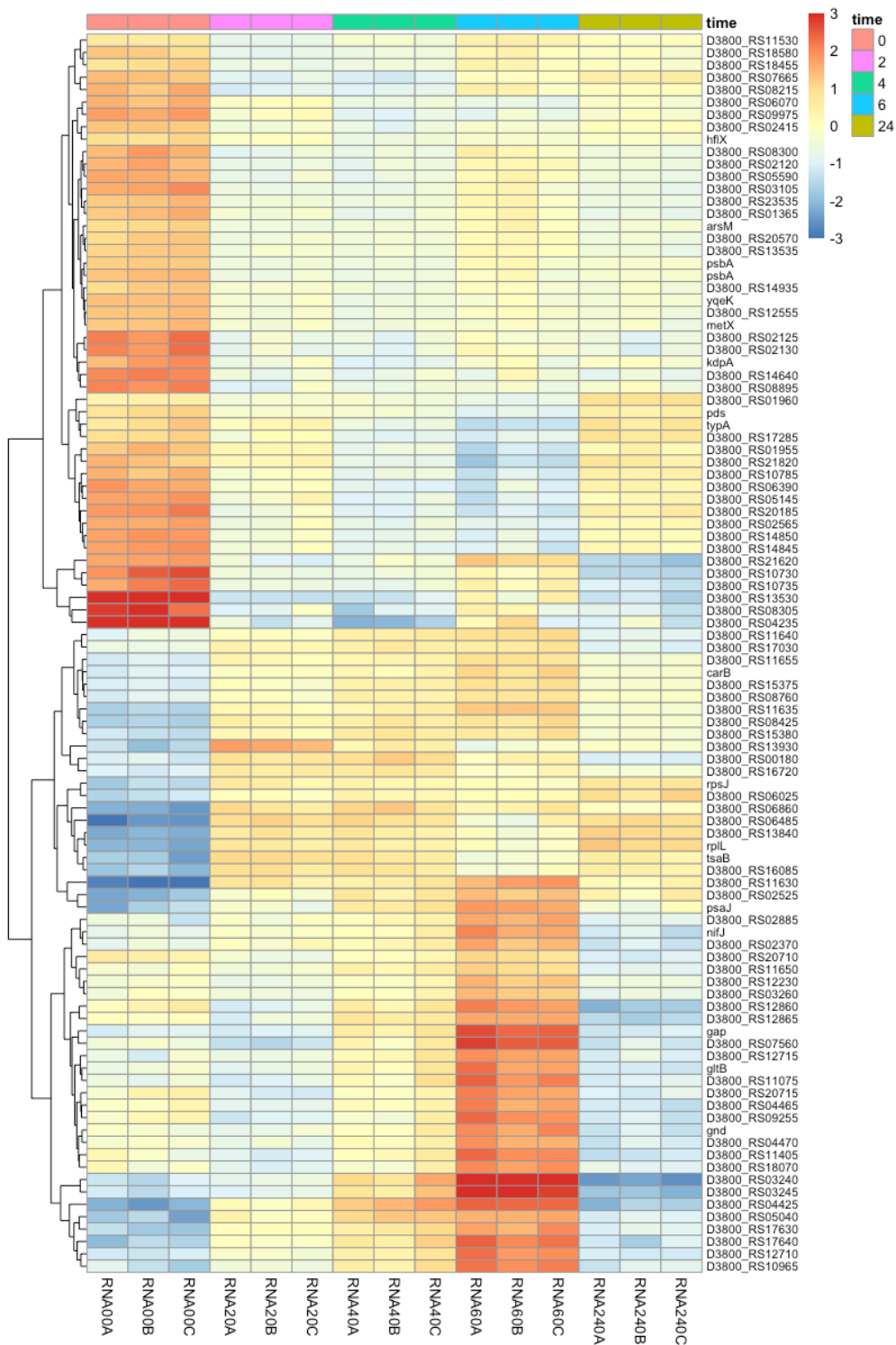


Figure 26. Heatmap showing expression patterns of top 100 genes with the smallest false discovery rate (FDR) in untreated *M. aeruginosa* cultures. Each three-column group represents incubation time as indicated by color.

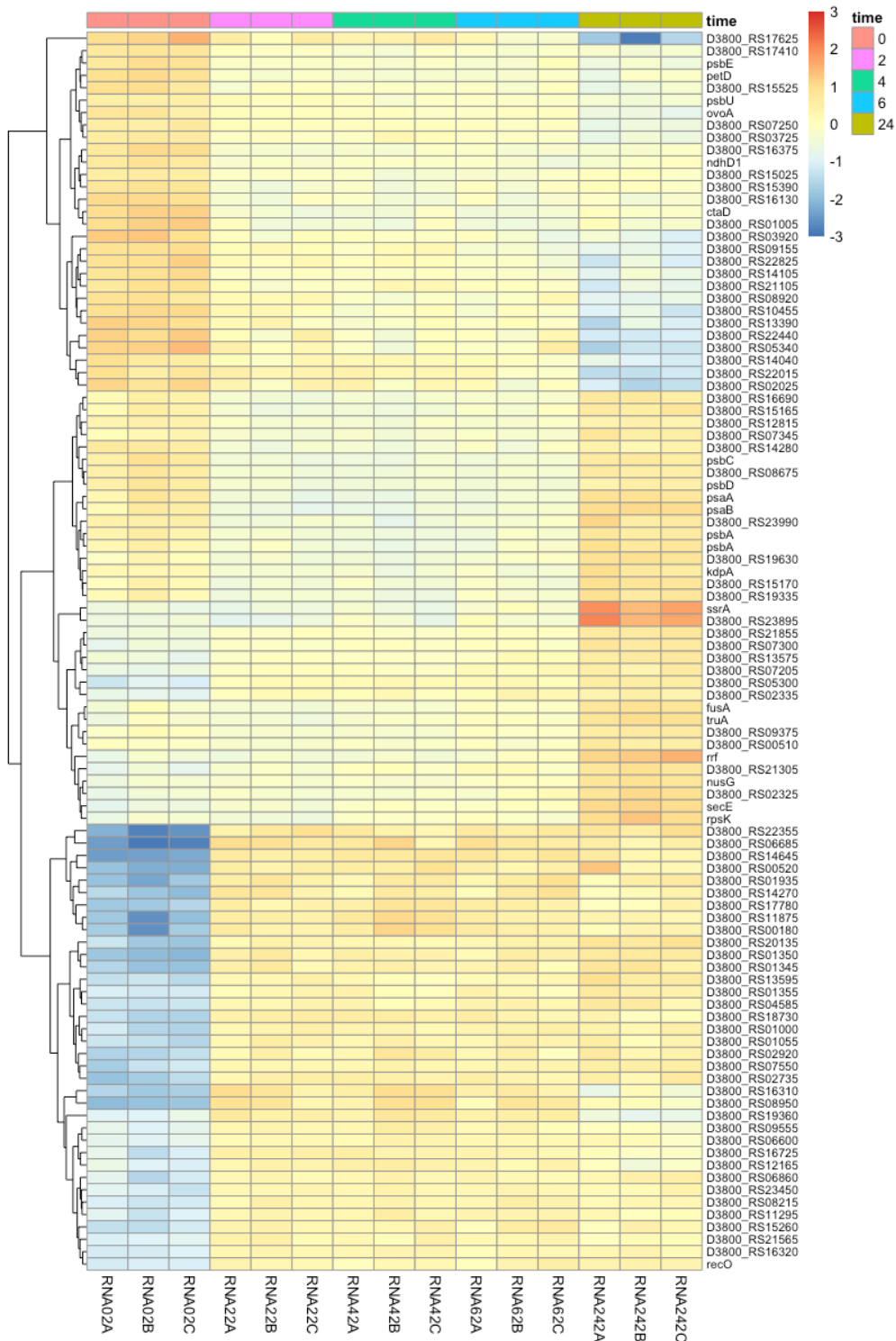


Figure 27. Heatmap showing expression patterns of top 100 genes with the smallest false discovery rate (FDR) in 2.02 kGy eBeam treated *M. aeruginosa* cultures. Each three-column group represents incubation time as indicated by color.





Figure 28. Heatmap showing expression patterns of top 100 genes with the smallest false discovery rate (FDR) in 5.03 kGy eBeam treated *M. aeruginosa* cultures. Each three-column group represents incubation time as indicated by color.

genes between at least two time points. The majority of genes identified showed differential expression between sample time 0 and all other time points. Figure 27 displays the expression patterns of the top 100 genes differentially expressed in 2 kGy treated cultures. *M. aeruginosa* cultures receiving 5 kGy eBeam treatment resulted in a total of only 343 genes differentially expressed between at least two time points. In these samples, the majority of genes identified showed differential expression between the 24-hour sample time and all other timepoints. Figure 28 displays the expression patterns of the top 100 genes differentially expressed in 5 kGy treated cultures.

#### *eBeam Induced Changes in M. aeruginosa Photosystem Gene Expression*

To analyze the influence of eBeam exposure on photosynthesis, gene expression of photosystems I and II (PSI/PSII) were compared across time and eBeam dose (Figure 29 and 30). Similar to global expression, eBeam treatment dose appeared to be the influential gene expression factor rather than time as 2 and 5 kGy treated cultures showed overall downregulation or no change in PSI and II genes, but untreated cultures showed overall upregulated expression of PSI and II genes. However, some time dependence was observed in both PSI and II in untreated *M. aeruginosa* cultures as reflected by the MDS plot (Figure 24). Metabolic periodicities of photosynthesis and MC-LR synthesis over diurnal cycles have been observed in various cyanobacterial species suggesting that healthy cultures couple various physiological activities to a biological clock.<sup>161-163</sup> These activities allow adaptation to fluctuations in the environment. This is reflected in changes in gene expression for many photosystem genes, especially in PSI, over the time duration of this experiment in untreated cultures.

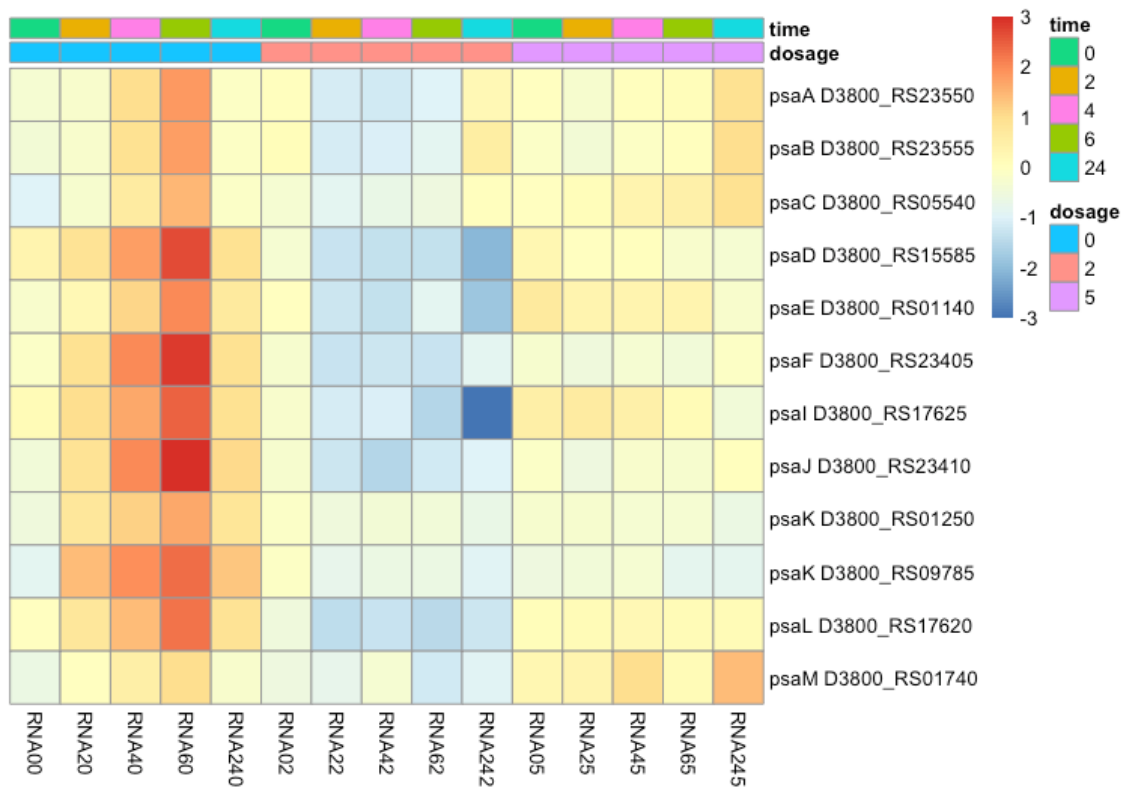


Figure 29. Heatmap showing expression patterns of photosystem I (PSI) genes in *M. aeruginosa* exposed to 0, 2.02, and 5.03 kGy eBeam doses over time following irradiation. Values plotted are log2 fold changes against mean values.

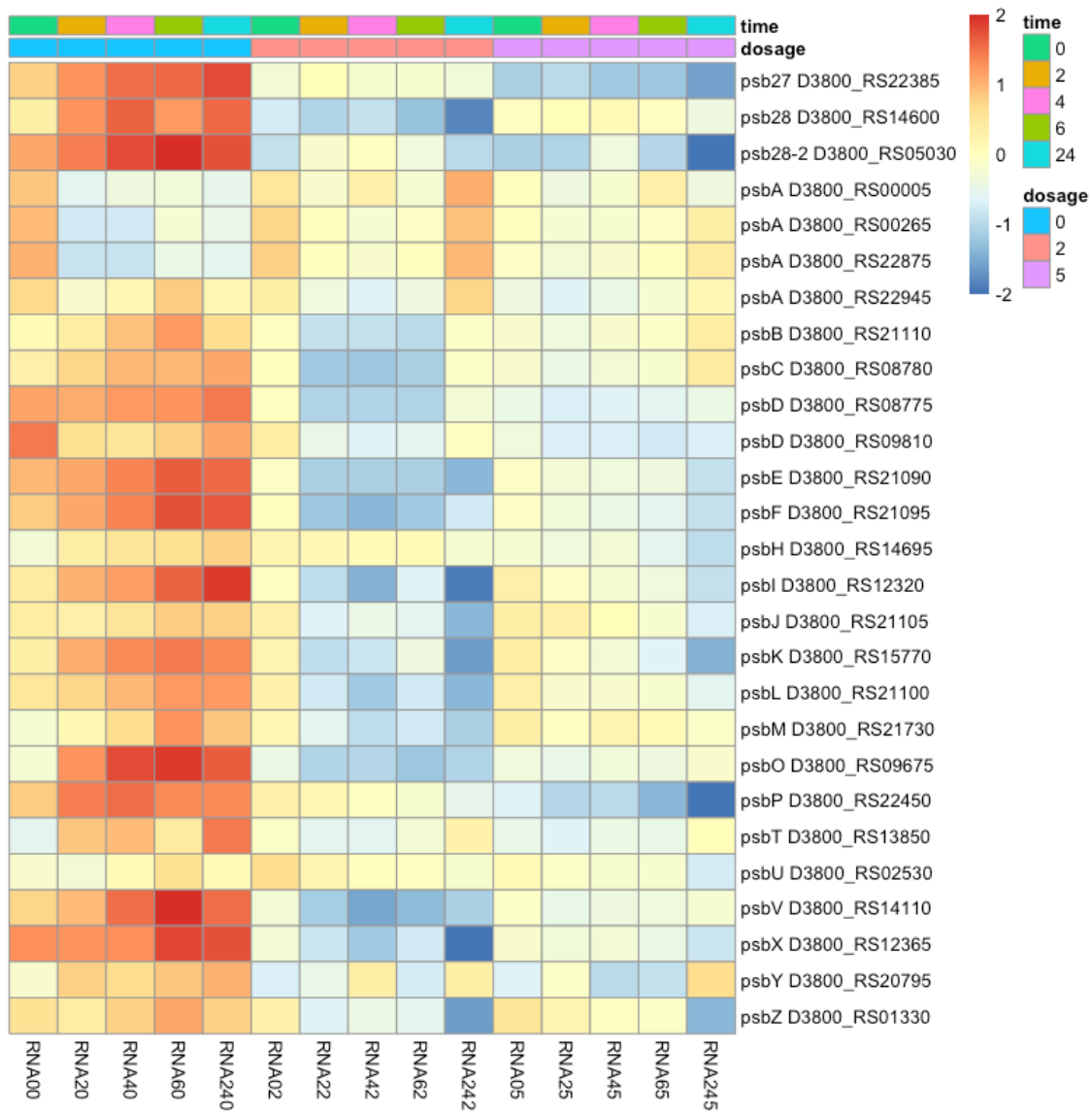


Figure 30. Heatmap showing expression patterns of photosystem II (PSII) genes in *M. aeruginosa* exposed to 0, 2.02, and 5.03 kGy eBeam doses over time following irradiation. Values plotted are log<sub>2</sub> fold changes against mean values.

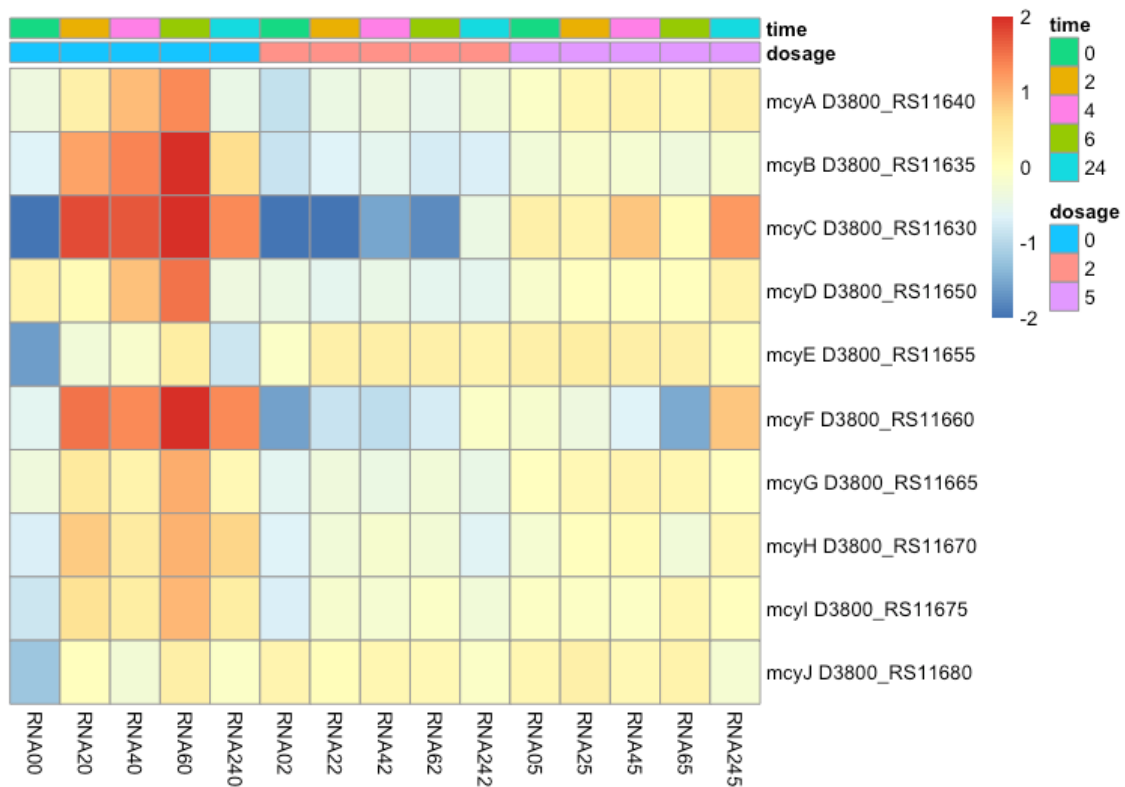


Figure 31. Heatmap showing expression patterns of the *mcy* gene cluster in *M. aeruginosa* exposed to 0, 2.02, and 5.03 kGy eBeam doses over time following irradiation. Values plotted are log<sub>2</sub> fold changes against mean values.

In 2 kGy treated cultures, general expression of PSI and II genes were downregulated in comparison to untreated cultures. The exception appeared to be *psbA* (PSII P680 reaction center D1 protein) which was downregulated in untreated cultures, but slightly upregulated (~fold change of 1) in 2 kGy eBeam treated cultures (Figure 30). In 5 kGy eBeam treated cultures, overall gene expression of PSI genes were unchanged when compared to untreated and 2 kGy treated *M. aeruginosa* cultures (Figure 29). In PSII genes, a small number of genes were downregulated (Figure 30). These included *psb27*, *psb28-2*, *psbD*, and *psbP* – all related to stabilization or assembly of PSII.

#### *eBeam Induced Changes in M. aeruginosa mcyA-J Gene Expression*

Patterns observed for *mcy* genes were overall very similar to that of PSI and II genes. In untreated cultures, there was observed time dependence in some *mcy* genes, especially at 0 hours compared to other time points (Figure 31). eBeam treatment of *M. aeruginosa* cultures require removing them from light incubation conditions during treatment for transport to the eBeam facility. The initial down regulation of *mcy* genes in untreated cultures may be a reflection of this light absence if *mcy* genes are indeed associated with photosynthetic function. At all other time points, *mcy* genes in untreated cultures ranged from no change to highly upregulated. *mcyB*, *mcyC*, and *mcyF* showed the greatest upregulation in untreated cultures. In 2 kGy eBeam treated cultures, overall trends were in the downregulation of *mcy* genes. *mcyC* and *mcyF* were the most significantly downregulated. Finally, in 5 kGy treated cultures, overall gene expression was unchanged.

## **Discussion**

### *M. aeruginosa* Cell Growth and Toxin Production

Previous research on the response of prokaryotic cells to eBeam treatment have identified the presence of a metabolically active yet non-culturable (MAyNC) state. In this state, bacterial cells such as *Salmonella typhimurium* and *E. coli* O26:H11, maintain cell membrane integrity and retain metabolic activity following irradiation treatment.<sup>91,164</sup> Pathway analysis of differentially expressed metabolites in eBeam treated cells suggest that key differentially expressed pathways include those associated with overall stress response in the cells but exclude pathways involved in cell structure, corroborating these observations.<sup>91</sup> Oppositely, following treatment with ionizing radiation, declines in cyanobacterial cell concentration and chlorophyll absorbance as well as eventual cell lysis, have been reported.<sup>105,107,135</sup> This influence on cell membrane integrity has been postulated to be a result of thylakoid membrane damage as oxidative stress is known to result in photoinactivation in photosynthetic organisms.<sup>121</sup> However, as mentioned previously, a time delay in cell lysis following irradiation has been observed. This indicates the potential for metabolic activity to continue until cell lysis occurs. In this study, both 2 and 5 kGy doses resulted in significant declines in cell concentration as early as 2 hours following treatment (Figure 21). This suggests that *M. aeruginosa* cell lysis at these treatment doses occurs as early as 2 hours following treatment and that the window for potential metabolic activity is brief. Still, it is critical to understand if additional MC-LR synthesis occurs during this metabolically active, albeit short, period of two hours.

Microcystins are energetically expensive for cyanobacteria to synthesize. Still, the reason for MC-LR production by *M. aeruginosa* remains unclear.<sup>131</sup> A recent review by Omid et al. (2018) summarizes the research to date on the purpose of microcystin production.<sup>165</sup> Of interest to irradiation treatment of *M. aeruginosa* and MC-LR is the possibility of MC involvement in protection from oxidative stress. Studies have shown that under conditions of oxidative stress, microcystin production was stimulated.<sup>166,167</sup> It is postulated that under increased oxidative stress conditions, MCs may be able to bind to proteins to prevent their dimerization in these conditions.<sup>165</sup> If this is the case, then the increase in MC-LR observed in 2 and 5 kGy treated cultures could be postulated to be a result of stress induced via eBeam (ionizing radiation) exposure (Figure 22). At present, MCs are considered endotoxins, with only 10% of toxins constituting extracellular fractions in *M. aeruginosa* cultures.<sup>131,165</sup> Therefore, the increase of extracellular MC-LR in 2 and 5 kGy treated cultures primarily occurs due to cell lysis following eBeam treatment. Nevertheless, from a drinking water treatment plant/public health perspective, the increase in MC-LR following eBeam treatment of *M. aeruginosa* can be problematic.

*eBeam Induced DNA Fragmentation*

For decades, DNA has been assumed as the primary biomolecule targeted by ionizing radiation and in microbes irradiation damage has been associated with single and double stranded breakage of the organism's DNA.<sup>84,168</sup> The amount of DNA damage accrued is proportional to the size of the organism's genome. More recently, proteins have also been proposed as the primary target molecules.<sup>169</sup> However, regardless of proteome damage, DNA strand breakage will ultimately lead to cell death when accrued



in high numbers. Interestingly, even with the accumulation of DNA strand breaks, studies have shown that bacterial cells still enter the MAyNC state and can even host bacteriophage growth following lethal irradiation doses.<sup>170</sup> In 2 and 5 kGy treated *M. aeruginosa* cultures, overall fragment sizes were smaller than in unirradiated cultures suggesting that eBeam treatment indeed induced DNA strand breakage in this organism (Figure 23). In the largest fragment size bin, significance was even seen between 2 kGy and 5 kGy doses suggesting that dosage influences the amount of fragmentation occurring (Figure 23C). Previous work in our lab conducted with *Clostridium perfringens* similarly observed a decrease in average fragment size, and at comparable percentages, in cultures irradiated at 10 kGy.<sup>171</sup> *C. perfringens* was also observed to enter a MAyNC state like previous bacterial species discussed. Given that DNA fragmentation patterns appear relatively consistent across these two organisms, DNA fragmentation accrued by *M. aeruginosa* cells does not appear to be the driver for cell lysis.

#### *eBeam Induced Changes in M. aeruginosa Global Gene Expression*

Of the top identified genes in our global transcriptomic analysis, two trends were apparent. In untreated cultures, genes associated with photosynthesis and biosynthesis of secondary metabolites were upregulated as opposed to these genes being downregulated in both 2 and 5 kGy eBeam treatments (Figure 25). These downregulated genes included; *rplE* (encoding for the 50S ribosomal protein L5), *acsF* (encoding for an oxidoreductase responsible for chlorophyll metabolism), *acpP* (encoding for an acyl carrier protein), *apcB* (encoding for an allophycocyanin beta subunit), *ndhC* (encoding

for an NAD(P)H-quinone oxidoreductase), and *ntrB* (encoding for a nitrate ABC transporter permease). In a similar study investigating the response of *M. aeruginosa* to electromagnetic radiation, the expression of the *ndh* gene family was also downregulated after treatment.<sup>172</sup> NAD(P)H-quinone oxidoreductase is involved in a number of energy reactions including cyclic electron flow around photosystem I (PSI).<sup>172</sup> The observed downregulation in eBeam treated cultures suggests consequences in a variety of physiological processes within the cell related to photosystem function.

Concurrently, there were seven annotated genes identified as downregulated in untreated cultures, but overall upregulated in 2 and 5 kGy eBeam treated cultures. These genes were related to overall DNA repair mechanisms (*recO* and *recJ*), translation (*tsaB*), and photosynthetic function (*trxB* and *clpB*).<sup>173,174</sup> No trends were observed when compared over time. This data suggests that following eBeam treatment, *M. aeruginosa* cells do attempt to repair accrued DNA damage. However, as photoprotection related genes were upregulated, this indicates that there is damage to photosynthetic machinery following irradiation.

#### *eBeam Induced Changes in M. aeruginosa Photosystem Gene Expression*

It is known that light can become lethal when the light energy exceeds the photosynthetic capacity of cyanobacteria.<sup>175</sup> ROS are a general byproduct of electron transport in photosynthesis but may become damaging under light damaging conditions. In 2 kGy treated cultures, *psbA* (PSII P680 reaction center D1 protein) was upregulated as compared to downregulated in untreated cultures (Figure 30). The D1 protein complex represents a vital pigment-protein complex in PSII.<sup>176</sup> It has been observed that

photoinhibition of cyanobacteria occur when the rate of damage exceeds the synthesis of new D1 subunits.<sup>177</sup> Therefore, this slight increase in expression in 2 kGy eBeam treated cultures could represent an attempt of *M. aeruginosa* to counteract light damage following irradiation.

There was little expression change in PSI genes in 5 kGy treated *M. aeruginosa* (Figure 29). However, the downregulated PSII genes in 5 kGy treated cultures further suggest photosystem damage (Figure 30). *psb27* encodes for a cyanobacterial lipoprotein (located in the thylakoid membrane) associated with the assembly of the water splitting site of PSII and that is also highly involved in the repair cycle of PSII.<sup>178</sup> The *psb28* gene in *M. aeruginosa* has two annotated homologs, *psb28-1* and *psb28-2*. *Psb-1* has been associated in the recovery of PSII and *psb28* overall appears related to chlorophyll synthesis.<sup>179–181</sup> The *psbD* gene encodes for the PSII D2 protein, also associated with light protection.<sup>175</sup> Finally, the *psbP* gene encodes for a PSII extrinsic protein that has been seen to drastically change PSII efficiency and its repair system when expression changes.<sup>182</sup> The downregulation of these genes reflect the inability of eBeam treated *M. aeruginosa* cultures to counteract photoinhibition following eBeam exposure due possibly to accrued damage to DNA.

#### *eBeam Induced Changes in M. aeruginosa mcyA-J Gene Expression*

A theory for MC-LR production in *M. aeruginosa* is for their use in photo protection.<sup>165</sup> Therefore, following investigation of photosystem gene expression changes, we sought to analyze gene expression patterns in microcystin synthesis. Biosynthesis of MC-LR in *M. aeruginosa* occurs nonribosomally (ie. via nonribosomal

peptide synthetases) and is controlled by the *mcy* gene cluster. The cluster is 55 kb long and includes 10 open reading frames (*mcyA-J*).<sup>183,184</sup> The gene cluster is formed by two polycistronic operons (*mcyABC* and *mcyDEFGHIJ*) that are transcribed bidirectionally.<sup>185</sup> *mcyABC* encodes for non-ribosomal peptide synthetases (NRPS), *mcyD* encodes a polyketide synthase (PKS), *mcyEG* encodes for a mixed PKS-NRPS, and *mcyF* encodes for racemase. Additionally, *mcyH-J* appear downstream of *mcyDEFG* and are involved in microcystin synthesis and transportation.<sup>184</sup> *mcyD* is proposed to be involved in the synthesis of the bioactive ADDA moiety.<sup>166</sup>

Differentially expressed gene trends observed for *mcy* genes were similar to that of PSI and II genes (Figure 31). Several studies have investigated the effects of light and other stressors on *mcy* gene expression. However, these studies have generally focused on monitoring one or two *mcy* genes rather than the whole cluster.<sup>166,186-188</sup> As expression of the various *mcy* genes in this study were different, monitoring only select genes may result in study biases. The ability to look at the entire cluster in response to stressors may give us greater information on gene cluster function. The significant up or down regulation in *mcyC* and *mcyF* between treated and nontreated cultures may indicate a susceptibility of these genes to eBeam treatment or light. Tillet et al. (2000) was the first to describe the biosynthesis pathway of MC-LR of *M. aeruginosa* PCC7806.<sup>184</sup> In their study, they determined that *mcyC* encodes a 147,781 Da peptide synthetase with a carboxy-terminal thioesterase and that the domain may be involved in cyclization of the molecule.<sup>184</sup> *mcyF* encodes for a glutamate racemase and is thought to

be involved in the addition of D-glutamate in position 6 of MC-LR.<sup>189</sup> However, it is not known what would make these genes more susceptible to eBeam exposure.

Based upon our previous work, we hypothesized that *M. aeruginosa* cells would be able to further synthesize MC-LR following eBeam treatment, but before cell lysis. This data suggests that MC-LR synthesis is decreased following eBeam treatment in 2 kGy treated cultures. Little change in overall expression of *mcy* genes was observed in 5 kGy treated cultures, but this could be due to cells losing metabolic functioning faster than 2 kGy treated cells. Further, if MC-LR is involved in photo protection, a decrease in MC-LR synthesis may be due to the cells inability to protect itself from light damage following eBeam treatment.

## **Conclusion**

In this study, the response of *M. aeruginosa* to eBeam treatment was studied in regard to both dose of irradiation and time following irradiation. Cell growth was retarded in both 2 and 5 kGy eBeam treated cultures. The decline in cell concentration occurred as early as 2 hours post eBeam treatment. Intracellular MC-LR concentrations declined in both 2 and 5 kGy treated cultures, but extracellular MC-LR concentration increased in the treated cultures over time. Overall DNA fragmentation patterns were observed to be similar to other organisms known to enter a MAyNC state following eBeam treatment. There was a greater percentage of smaller fragments in 2 and 5 kGy treated cultures when compared to untreated and there were a smaller percentage of larger fragments in 2 and 5 kGy treated cultures when compared to untreated. Global gene expression of untreated and treated cultures appeared to be clustered by dose, rather

than time following irradiation. Many top genes affected were related to photosystem function and DNA repair. Cultures treated with 2 kGy eBeam dose showed overall downregulation in PSI and II genes, as well as certain mcy genes. Cultures treated with 5 kGy eBeam dose had relatively unchanged expression for the same genes. Overall, this data suggests that MC-LR synthesis may indeed be occurring following irradiation, however, this is occurring at a lower rate than untreated cultures. The similarity of fragmentation patterns to other bacterial species suggests that DNA damage is not the culprit of cell lysis but is instead due to photo damage accrued during culturing following treatment. Further, this data supports the idea of microcystins being involved in photodamage in *M. aeruginosa* as expression patterns of mcy genes mirrored those of PSI and II genes.

## CHAPTER VI

### THE INFLUENCE OF LIGHT ON ELECTRON BEAM INDUCED DAMAGE IN *M.*

### *AERUGINOSA*

#### **Abstract**

The use of electron beam (eBeam) technology for the remediation of microcystins in water treatment has been proven effective at low doses. However, treatment must also be effective for the producing cyanobacteria to truly eliminate public health risks. This study was undertaken to understand the effect of incubation conditions on eBeam induced cell damage to *Microcystis aeruginosa*. *M. aeruginosa* cell cultures were exposed to eBeam doses, incubated in the absence of light, and sampled over time. Cell concentrations gradually declined over the incubation period but declined less significantly than cultures incubated in the light following eBeam exposure. Both intracellular and extracellular microcystin-LR (MC-LR) increased significantly in both 2 and 5 kGy treated dark incubated cultures. Finally, DNA fragmentation patterns of dark incubated eBeam treated cultures were comparable to light incubated cultures. This study suggests that light is the main driver of cell lysis following eBeam exposure.

#### **Introduction**

In order to understand the influence of light on eBeam treatment induced cell damage, we repeated our study from chapter V but incubated *M. aeruginosa* cells without light following eBeam treatment. We hypothesized that, in the absence of light, *M. aeruginosa* cell lysis would be delayed. Therefore, the specific research questions we pursued were a) to determine cell concentration over time following eBeam treatment in

dark incubated cultures, b) to determine intracellular and extracellular MC-LR production over time following eBeam treatment in dark incubated cultures, and c) to investigate DNA fragmentation patterns as a function of eBeam dose and time following eBeam treatment in dark incubated cultures.

## **Materials and Methods**

### *Laboratory Propagation of M. aeruginosa*

*M. aeruginosa* (LB 2385, origin: Little Rideau Lake, Ontario, Canada) was purchased from UTEX Culture Collection of Algae in Austin, TX. The cyanobacteria were cultured in a modified Bold 3N medium (without soil-water extract) under a 12/12 day/night cycle at ~20°C on an orbital shaker at ~100 rpm. Cell titers were determined using chlorophyll absorbance (680 nm) read on a Synergy H1 Hybrid Multi-Mode Microplate Reader (Biotek, Winooski, VT) using Gen5 Microplate Reader and Imager software using an initially prepared standard curve.

### *Electron Beam Treatment*

eBeam irradiation treatments were performed at the National Center for Electron Beam Research at Texas A&M University in College Station, TX. A high energy (10 MeV), 15 kW pulsed S-band linear accelerator was used (dose rate 3 kGy/sec) for treatment and dose validation was completed using industry standard alanine (L- $\alpha$ -alanine) dosimeters and EPR based spectroscopy using the Bruker e-scan reader (Billerica, MA). Cultures were irradiated in 30 ml round-bottom screw cap culture tubes (Corning Inc., Corning, NY) following preliminary dose-mapping studies were to confirm a dose uniformity of one in vials.



### *Quantification of Microcystin-LR*

Microcystin-LR concentrations in culture samples were analyzed analytically at the Integrated Metabolomic Analysis Core (IMAC) at Texas A&M University as described previously.<sup>135</sup> Briefly, supernatant samples were filtered through a 0.2 µm syringe filter and further methanol extracted to measure extracellular MC-LR. Cyanobacterial cell pellet samples were extracted using a methanol:chloroform:water based extraction method to measure intracellular MC-LR. Quantification of MC-LR was completed using untargeted liquid chromatography high resolution accurate mass spectrometry (LC-HRAMS) analysis.

### *DNA Extraction and Fragmentation Analysis*

DNA extraction was completed using the DNeasy UltraClean Microbial Kit (Qiagen, Germantown, MD). DNA samples were quantified using the DropletQuant (PerkinElmer, Waltham, MA) on DropletViewer/cDrop Software version 3.2.0.128 (PerkinElmer). Fragment size was then analyzed using the Agilent Fragment Analyzer 5300 (Agilent, Santa Clara, CA) and data was evaluated using Agilent ProSize Data Analysis Software version 4.0.0.3.

## **Results and Discussion**

The purpose of this study was to investigate the effect of culture conditions (ie. presence of light) on eBeam treatment damage to *M. aeruginosa* cells. Similarly to chapter V, all samples in this study were taken from the same experimental cultures to create matching datasets. Turbid *M. aeruginosa* cultures were exposed to target doses of 0, 2, or 5 kGy in biological triplicate. Actual doses received were 2.19 and 5.37 kGy.

Following irradiation treatment, cells were incubated in the dark until the end of the study timeframe. Samples were collected following treatment at 0, 2, 4, 6, 24, and 96 hours. Cultures were analyzed for cell growth, MC-LR production, and DNA fragmentation. Data sets from chapter V will be referred to as light incubated cultures (LIC) and new data will be referred to as dark incubated cultures (DIC).

#### *M. aeruginosa Cell Growth in Dark Incubation Conditions*

*M. aeruginosa* DIC cell growth was monitored over time after eBeam treatment at 0, 2, or 5 kGy. Figure 32 shows the cell concentrations of DICs over 96 hours following irradiation as compared to LICs. At hour 0 (immediately after irradiation), cell concentration in DIC were approximately  $3 \times 10^6 - 5 \times 10^6$  cells/ml. LICs had 0-hour cell concentrations around  $2 \times 10^6$  cells/ml (Figure 32B). However, as this difference in cell concentration was reflected in unirradiated cultures, this was assumed to be due to biologic variability. Overall, both treated and nontreated DICs exhibited a decline in cell concentration over time. Previous studies have indicated that in prolonged darkness, *M. aeruginosa* cells lost their ability to use stored energy and maintain metabolic integrity after more than 7 days.<sup>190</sup> DIC cell concentration therefore may have declined over time due to lack of energy from inability to photosynthesize. DICs treated at 2 kGy showed a 8.4% decline over 24 hours. LICs treated at 2 kGy showed a 46.5% decline over the same time period. DICs at 5 kGy showed a 37.3% decline over 24 hours. LICs treated cultures treated at 5 kGy showed a 43.7% decline over the same time period. Lastly, nontreated DICs showed a 3.6% decline over 24 hours while untreated LICs showed a 14.8% increase over the same time period.

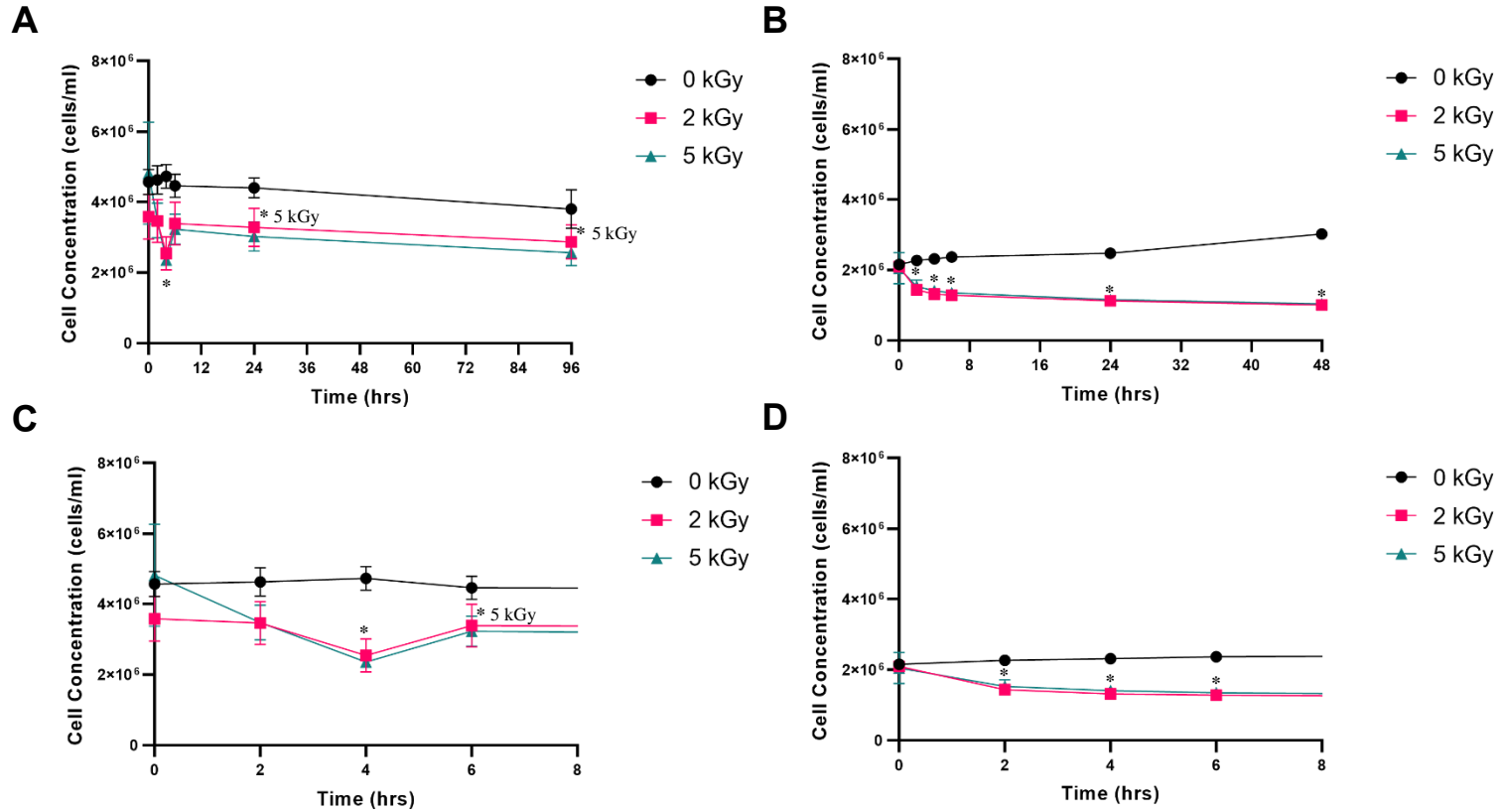


Figure 32. Response of *M. aeruginosa* cells to 0, 2.19, and 5.37 kGy ebeam irradiation doses. A) Cell concentrations in eBeam treated cultures incubated in the dark over 96 hours. B) Cell concentrations in eBeam treated cultures incubated in the light (12:12 day:night) over 48 hours. C) Zoomed in view on dark incubated cultures from 0 – 6 hours. D) Zoomed in view on light incubated cultures from 0 – 6 hours. (Error bars represented as standard deviation; \* =  $p \leq 0.05$  determined via Tukey's multiple comparisons test)

Photodamage to cyanobacteria has been observed when light energy exceeds the capacity of the organisms' photosynthetic capabilities. PSII is the most light-sensitive complex and damage to the susceptible D1 and D2 proteins in the complex are known to decrease the organism's growth and productivity.<sup>175</sup> Following eBeam irradiation, an abundance of free radicals are introduced into the system. In animal cells, these reactive oxygen species (ROS) have been seen to effect membrane integrity through lipid peroxidation, cross-linking and/or breakage of bonds in membrane lipids, and protein degradation.<sup>191</sup> In plants, low doses of gamma irradiation have been seen to cause dilation of thylakoid membranes and loss of stacking structure.<sup>123</sup> Damage to thylakoid membranes following ionizing radiation has also been observed by Agarwal et al. (2008).<sup>121</sup> They confirmed that PSII inactivation was enhanced by light following gamma irradiation, presumably due to a role of light in activation of proteins required for light recovery of PSII.<sup>121</sup> In this study, DICs showed greater cell concentrations over a 24 hour period than LICs. This suggests that, similar to gamma irradiation, light augments the damage to photosynthetic machinery induced by eBeam treatment. Due to the nature of photosynthetic process, and its susceptibility to light damage, continuous repair is occurring.<sup>192</sup> The ability of ROS generated by eBeam treatment to damage these repair mechanisms, suggests that the presence of light following irradiation is detrimental to cell death.

#### *M. aeruginosa Toxin Production in Dark Incubation Cultures (DIC)*

MC-LR concentration was also monitored in DICs to compare the potential synthesis of MC-LR in the absence of light. Similarly to LIC, MC-LR extracted from the

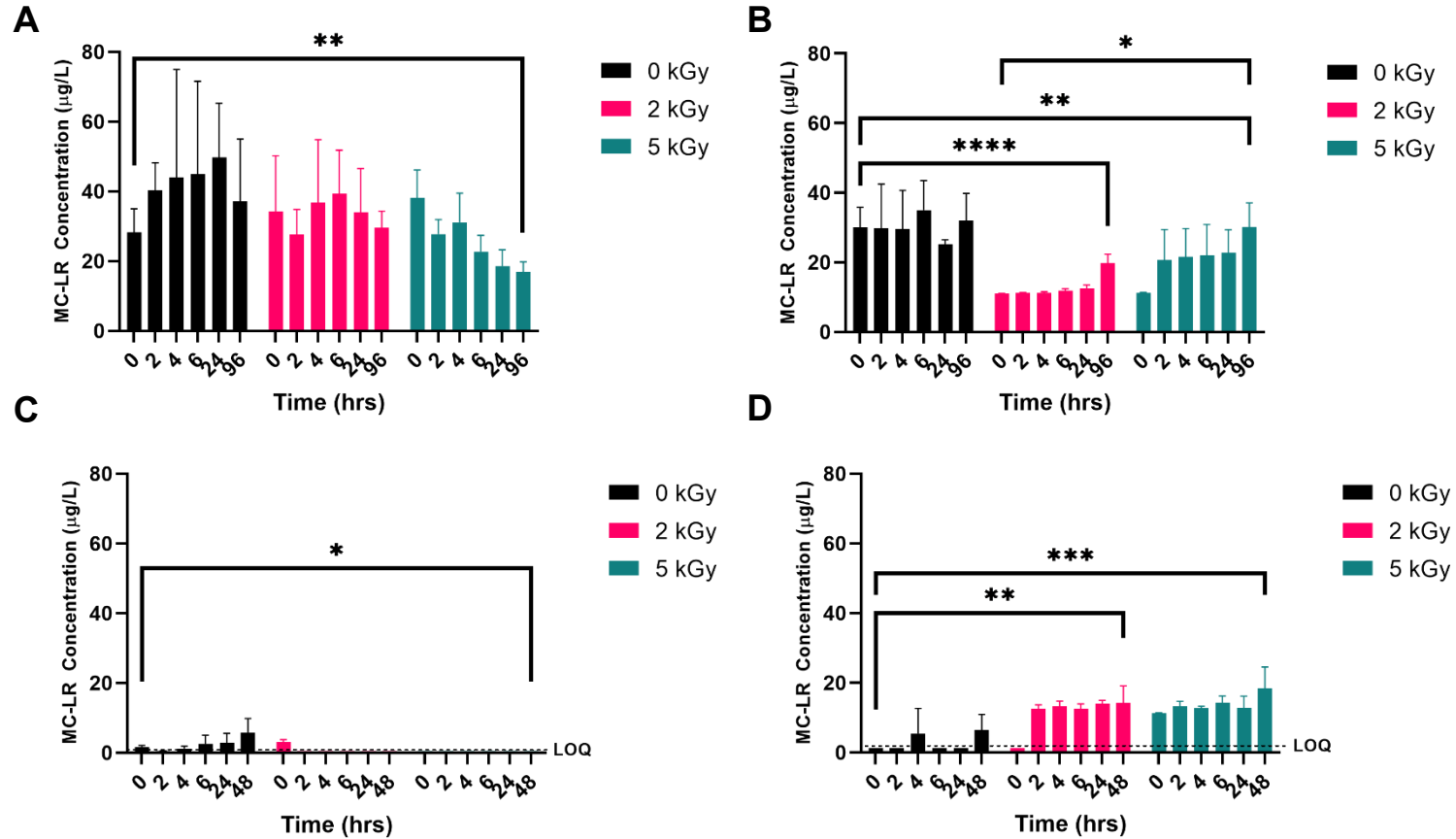


Figure 33. Intracellular and extracellular MC-LR concentrations following eBeam treatment at 0, 2.19, and 5.37 kGy over time. A) Intracellular MC-LR concentration in eBeam treated cultures incubated in the dark over 96 hours. B) Extracellular MC-LR concentration in eBeam treated cultures incubated in the dark over 96 hours. C) Intracellular MC-LR concentration in eBeam treated cultures incubated in the light over 48 hours. D) Extracellular MC-LR concentration in eBeam treated cultures incubated in the light over 48 hours. (Error bars represented as standard deviation; \* =  $p \leq 0.05$ ; \*\* =  $p \leq 0.01$ ; \*\*\* =  $p \leq 0.001$ ; \*\*\*\* =  $p \leq 0.0001$ )

cellular fraction of the cultures was considered intracellular MC-LR, and MC-LR extracted from the supernatant fraction of the cultures was considered extracellular MC-LR (Figure 33). Overall, MC-LR concentrations in DICs were much higher than LICs for both intra- and extra-cellular fractions. It is important to note that starting cell titers in DICs were slightly higher than in LICs. In 2 kGy treated cultures, intracellular MC-LR concentrations remained elevated throughout the sampling time period and were not significantly different from MC-LR concentrations in untreated DICs (Figure 33A). In 5 kGy treated cultures, there was an overall 55.7% decline in MC-LR concentrations over the experimental time period. In untreated DICs, MC-LR concentrations rose by 42.5% within the first 2 hours but then remained relatively constant over the remaining experimental time points. In the extracellular MC-LR fraction, 2 kGy treated DICs MC-LR concentrations gradually rose over 24 hours, but then increased sharply at 96 hours (Figure 33B). In 5 kGy treated DICs, extracellular MC-LR also increased over time, similar to patterns seen in 5 kGy treated LICs (Figure 33B and D). Finally, untreated DICs had extracellular MC-LR concentrations that remained stable over the 96-hour experimental window.

As discussed previously, studies have potentially linked MC-LR production in *M. aeruginosa* to oxidative stress protection. The increase in MC-LR production in DICs may be due to cell survival in the absence of light, extending the potential time window for continued metabolic activity following eBeam treatment. Contrarily, a study by Kaebernick et al. (2000) observed that *mcyB* and *mcyD* transcript levels were increased under high light conditions and under increased red light.<sup>166</sup> However in this study, it

appears that oxidative stress via eBeam treatment, not light, was the main driver for MC-LR production. It is possible that the cell is responding to ROS accumulation from eBeam treatment as if it were ROS accumulation from photosystem damage. The addition of light to irradiated cultures appears to further increase oxidative stress in cells past the ability for cellular repair.

#### *eBeam Induced DNA Fragmentation*

We sought to further understand the effect of light on eBeam treated *M. aeruginosa* cultures by investigating trends in DNA fragmentation. Figure 34 shows the percent of DNA fragments binned by fragment size in 0, 2, and 5 kGy treated DICs and LICs. Similarly to LICs, 2 and 5 kGy eBeam treated DICs showed a significantly greater percentage of shorter fragments (50 – 10,000 bp length) than nontreated cultures (Figure 34A). Alternatively, the 2 kGy and 5 kGy DICs showed significantly lower percentages of mid-size fragments (10,000 – 20,000 bp length) as compared to untreated DICs (Figure 34B). Both treated and untreated DICs showed very few (<10%) 20,000 – 30,000 bp length fragments and this was also lower than LICs (Figures 34C and 34F).

DNA fragmentation in DICs was very similar to fragmentation seen in LICs. This suggests that the primary source of this fragmentation is indeed from eBeam treatment, and not from incubation conditions. Further, the similarity in fragment size suggests that production of MC-LR is not linked to DNA fragmentation, as DICs and LICs showed vastly different amounts of MC-LR in cultures. As discussed previously, studies on other bacterial species show that following eBeam treatment, cells remain structurally intact.<sup>91,94,170</sup> This data corroborates our previous conclusion that cell lysis of

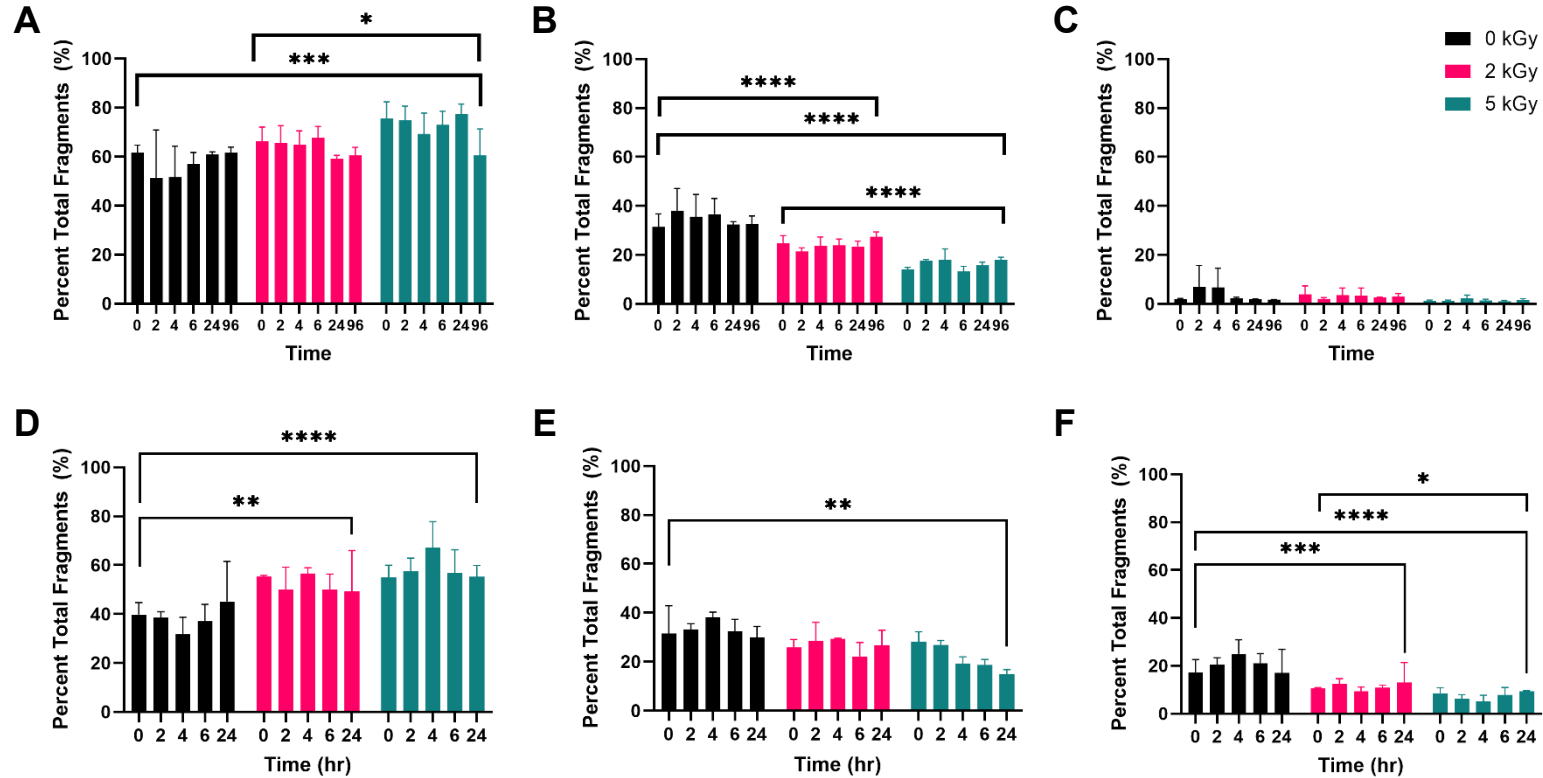


Figure 34. DNA fragmentation as a percent of total DNA fragments in eBeam treated *M. aeruginosa* cultures over time. A) 50 – 10,000 bp length fragments in dark incubated cultures over 96 hours; B) 10,000 – 20,000 bp length fragments in dark incubated cultures over 96 hours; C) 10,000 – 30,000 bp length fragments in dark incubated cultures over 96 hours; D) 50 – 10,000 bp length fragments in light incubated cultures over 48 hours; E) 10,000 – 20,000 bp length fragments in light incubated cultures over 48 hours; F) 10,000 – 30,000 bp length fragments in light incubated cultures over 48 hours. (Error bars represented as standard deviation; \* =  $p \leq 0.05$ ; \*\* =  $p \leq 0.01$ ; \*\*\* =  $p \leq 0.001$ ; \*\*\*\* =  $p \leq 0.0001$ )



*M. aeruginosa* cells is not linked to differences in DNA damage and fragmentation, but instead to the photosynthetic nature of cyanobacteria.

## **Conclusion**

This study aimed at investigating the influence of light on *M. aeruginosa* cell survival following eBeam treatment. Our previous work has demonstrated that *M. aeruginosa* cells lyse following incubation in lighted conditions after eBeam treatment. Therefore, the study in chapter V was repeated in dark incubation conditions and compared to data collected in light incubation conditions.

Cell concentration in DICs declined gradually over the study time period in all cultures, presumably due to a lack of stored energy from prolonged absence of light. Overall, cell concentrations declined less over the study duration than in LICs. MC-LR concentrations in both intracellular and extracellular fractions in DICs were significantly higher than concentrations in LICs. This could be due to a longer time window before cell death where cells remain metabolically active. Finally, DNA fragmentation patterns were similar between DICs and LICs. This suggests that DNA damage does not influence the ability of *M. aeruginosa* cells to synthesize MC-LR. Overall, this study confirms that cell lysis in *M. aeruginosa* cultures following eBeam treatment is due to light damage following irradiation, and not eBeam treatment itself.

## CHAPTER VII

### APPLICABILITY OF ELECTRON BEAM TECHNOLOGY FOR THE REMEDICATION OF MICROCYSTIN-LR IN SURFACE WATERS FROM MULTIPLE GEOGRAPHIC LOCATIONS

#### **Abstract**

A study was performed to investigate the effects of surface water quality parameters on the degradation of microcystin-LR (MC-LR) using high energy electron beam (eBeam) technology. Surface water samples were collected across different geographic locations in the U.S. Water quality parameters including pH, alkalinity, TDS, and dissolved oxygen were measured in all samples. Degradation of MC-LR in all samples, regardless of parameter concentrations, were above 99%. The effect of natural organic matter (NOM) on MC-LR degradation was also investigated in the presence of fulvic acid. Similarly, degradation efficiency of MC-LR exceeded 99% for all concentrations of fulvic acid at 5 kGy. This study suggests that surface water quality has negligible effect on the degradation of MC-LR via eBeam treatment. The results indicate eBeam technology is a promising technology for the treatment of water contaminated with microcystins.

#### **Introduction**

The goal of this study was to employ eBeam treatment on collected water samples to understand how water quality effects MC-LR degradation. The underlying hypothesis was that parameters that scavenge oxidative species (such as low pH and high alkalinity) would decrease degradation efficiency of MC-LR. Therefore, the objectives

of the present study were i) to identify the influence of pH, alkalinity, total dissolved solids (TDS), and dissolved oxygen in surface water samples on the eBeam degradation of MC-LR; and ii) to determine the effect of fulvic acid (FA) on eBeam degradation of MC-LR.

## **Materials and Methods**

### *Sampling*

Samples were solicited from 22 locations throughout the U.S. as representative samples for the various geographic regions in the lower 48 states and Hawaii (Figure 35). Surface water sources that supply drinking water in each location were determined using the USEPA's Drinking Water Mapping Application to Protect Source Waters (DWMAPS).<sup>193</sup> Volunteers were provided with three 60 ml low-density polyethylene bottles (Thermo Fisher Scientific, Waltham, MA) and a water sampling protocol. All samples were taken in triplicate. Samples were then mailed back to College Station, TX where they were stored for further analysis.

### *Water Chemistry*

The pH, alkalinity, total dissolved solids (TDS), and dissolved oxygen were measured in samples to understand the diversity of the water chemistries from the different locations. pH was measured with a Manual 430 pH Meter (Corning, Corning, NY) and calibrated with reference standards pH  $4.00 \pm 0.01$  and  $10.00 \pm 0.01$  (VWR, Radnor, PA). A HI775-Alkalinity handheld colorimeter (Hanna Instruments, Woonsocket, RI) was used to measure alkalinity levels. The instrument range was 0 to 500 mg/L of  $\text{CaCO}_3$ . TDS was measured using a Traceable Conductivity/TDS Pocket

Tester with Calibration Meter (Cole-Parmer, Chicago, IL). The TDS factor was set to 0.66, the temperature normalization value was set to 25°C, and the temperature compensation coefficient was set to 2.0% as recommended for freshwater for this instrument. The instrument range was 0 to 1999 mg/L. A Model 830 Dissolved Oxygen Meter (Orion, Beverly, MA) was calibrated and used to measure the dissolved oxygen within the water samples. The probe was inserted into the samples and gently stirred until the measurements were stable.

#### *Electron Beam Treatment*

Electron beam irradiation dosing was performed at Texas A&M University's National Center for Electron Beam Research in College Station, TX. A high energy (10 MeV), 15 kW pulsed S-band linear accelerator was used (dose rate 3 kGy/sec). L- $\alpha$ -alanine dosimeters and EPR based spectroscopy using the Bruker e-scan reader (Billerica, MA) were used to confirm dose received. Initial dosing experiments were conducted to determine dose used for spiked surface water samples. This was completed using 3 mg/L MC-LR spiked in deionized water. The target doses were 1, 2, and 5 kGy, and doses received were 1.27, 2.04, and 5.05 kGy. A 5 kGy dose resulted in a 98% reduction from non-treated samples and was therefore used as the dose for remaining experiments.

The experimental samples were exposed to a target dose of 5 kGy in 2 ml glass screw-thread vials (VWR International, Radnor, PA). Preliminary dose-mapping studies were performed on vials used for irradiation to confirm dose uniformity ratio.

#### *Water Samples Treatment and Quantification*

For surface water samples, 1 ml aliquots were spiked with 3 mg/L microcystin-LR (purity  $\geq$  95%, Cayman Chemical, Ann Arbor, MI). Samples were irradiated at a target dose of 5 kGy and the actual dose received was  $5.11 \pm 0.079$  kGy.

Quantification of MC-LR after irradiation was determined biologically using the EPA preferred ADDA-specific ELISA kit (Eurofins Abraxis inc., Warminster, PA).<sup>116</sup> The ELISA kit standard curve ranged from 0.15 - 5.0  $\mu\text{g/L}$ . Plates were read on a Synergy H1 Hybrid Multi-Mode Microplate Reader (Biotek, Winooski, VT) using Gen5 Microplate Reader and Imager software.

#### *Effect of Fulvic Acid*

The effect of natural organic matter (NOM) was additionally investigated using FA (98.3% purity, AdipoGen Life Sciences, San Diego, CA). Samples were prepared to contain 0, 50, or 100  $\mu\text{g/L}$  fulvic acid and 2 mg/L MC-LR. Samples were irradiated at a target dose of 5 kGy and the actual dose received was  $5.11 \pm 0.079$  kGy. Similarly, MC-LR in samples was quantified using an ADDA-specific ELISA kit (Eurofins Abraxis inc., Warminster, PA).

#### *Data Analysis*

The data was statistically analyzed and visualized using commercially available GraphPad Prism software, version 9.1.2 (GraphPad Software, San Diego, CA). Shapiro-Wilks tests and qq-plots were used to verify normality of data. According to these results, a two-way ANOVA was used followed by the Šídák's multiple comparisons test. The tests were performed with a significance of 95% ( $p < 0.05$ ).

### **Results and Discussion**

### *Chemistry of Surface Water Samples*

Surface water quality in the United States varies both temporally and spatially depending upon water volume, sediment composition, biodiversity, and other stressors and pollution.<sup>194,195</sup> In this study, samples were solicited from 22 locations across the lower 48 states and Hawaii to represent geographic differences in surface water composition (Figure 35; <https://bit.ly/2UeZhAO>). Samples were then analyzed for pH, alkalinity, total dissolved solids (TDS), and dissolved oxygen (Appendix B).

Generally, the pH range in surface water systems is 6.5 to 8.5 as corroborated by the water samples obtained in this study.<sup>196,197</sup> pH remained relatively consistent among sample locations with Lake Keowee, SC having the lowest pH ( $6.24 \pm 0.026$ ) and the Southern California Water Supply having the highest pH ( $8.12 \pm 0.02$ ) (Figure 36A). pH can affect a variety of chemical and biologic processes in water by altering the solubility, transport, and bioavailability of many chemicals and pollutants. Low pH has been associated with nearby mining operations, industrial effluents, and agricultural runoff while high pH has been associated with alkaline geology and soils, oil and gas brines, and limestone gravel roads in the waterbody vicinity.<sup>197</sup>

Alkalinity is related to the acid-neutralizing capacity of a liquid due to the presence of chemical species such as bicarbonate, carbonates, and hydroxides.<sup>198</sup> Alkalinity measurements in sample locations had much more variability ranging from 11.67 – 183.33 mg/L of CaCO<sub>3</sub> in the Merrimack River, NH and the Mississippi River, IA, respectively (Figure 36B). Alkalinity is most often determined from the rocks and sediments surrounding the body of water. Alkalinity normally ranges from 20-200 mg/L



Figure 35. Sampling locations of water samples used in this study. An interactive version of this map can be accessed here: <https://bit.ly/2UeZhAO>

of CaCO<sub>3</sub> but has the potential to exceed 400 mg/L of CaCO<sub>3</sub> in areas with high amounts of urban runoff or limestone application.<sup>198</sup>

Total dissolved solids (TDS) represent the sum of all organic and inorganic substances dissolved in water. Measurable sample TDS values ranged from 21.33 – 840.67 in samples from Lake Keowee, SC and the Southern California Water Supply, respectively (Figure 36C). However, one sample location, Salt River, AZ was above our limit of detection (LOD). TDS is not often considered a health hazard, but instead the USEPA includes TDS as a voluntary guideline for water quality.<sup>199</sup> TDS is often indicative of ionic strength within a water body and amounts of TDS influence mineral content in water.<sup>200</sup> High TDS content is more likely in ground water than surface water, but high TDS content may cause toxicity to aquatic organisms due to mineral shifts as well as corrosion of plumbing fixtures. Concentrations greater than 500 mg/L are not recommended for drinking water.<sup>201</sup>

Finally, dissolved oxygen is a measure of the oxygen gas incorporated in the water. Dissolved oxygen in samples ranged from 63.33% in the Mississippi River, IA samples, to 91% in the Rio Grande Irrigation Canal, TX samples (Figure 36D). Oxygen normally enters the water through direct atmospheric absorption or through the production of oxygen via aquatic plants.<sup>202</sup> Low dissolved oxygen is far more likely than excessive dissolved oxygen and can result from algal blooms, high temperature, and ammonia content. Healthy dissolved oxygen levels typically range from 80-120% (6.5 – 8 mg/L) and values of less than 2 mg/L indicate hypoxic zones.<sup>203</sup>

Overall, pH, alkalinity, TDS, and dissolved oxygen values measured in samples



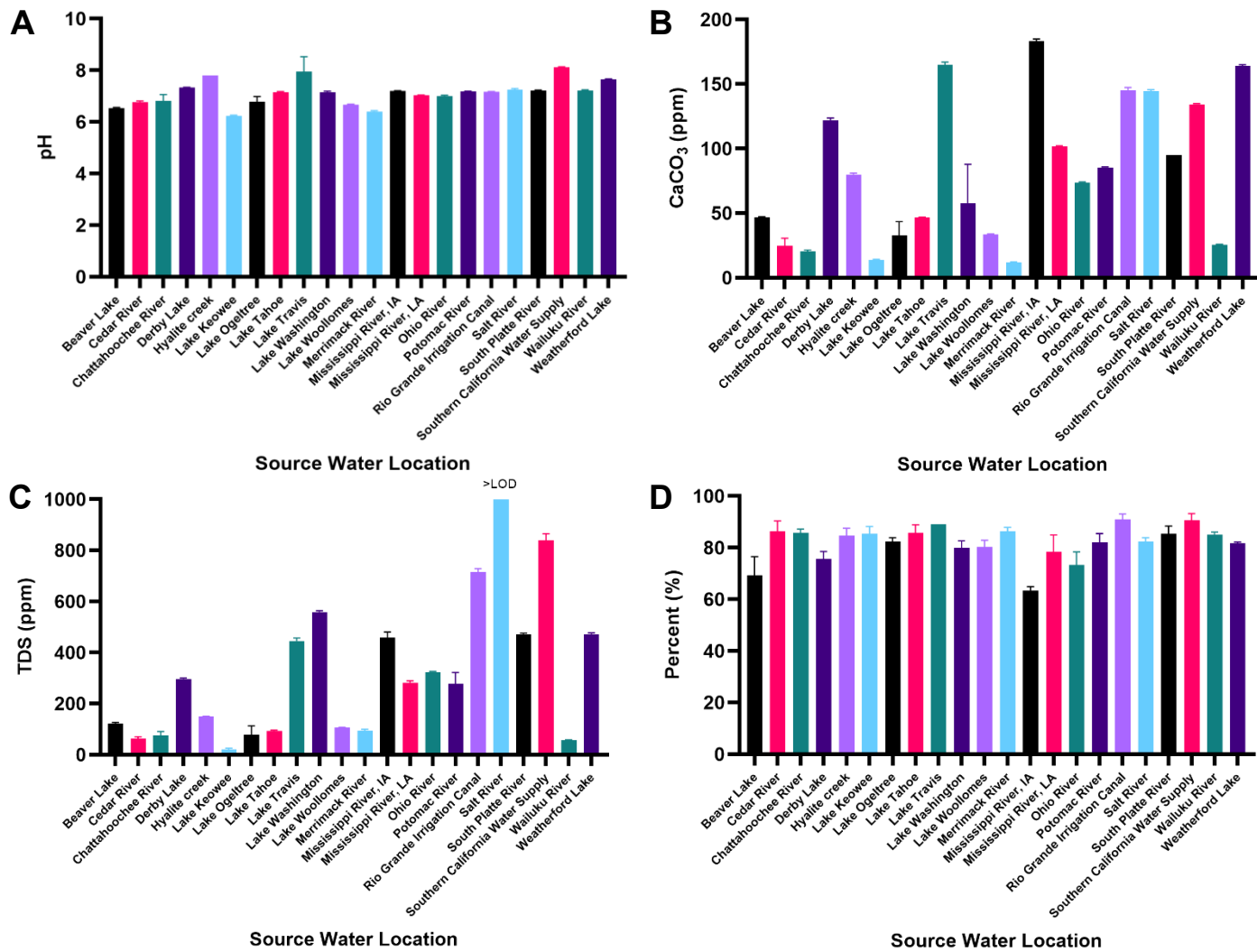


Figure 36. Water quality parameters measured in surface water samples. A) pH; B) Alkalinity; C) TDS; D) Dissolved oxygen. (Error bars represent standard deviation.)

were within expected ranges for each parameter, respectively. High alkalinity was observed in more urban locations such as Lake Travis, TX, Weatherford Lake, TX, the Mississippi River, and Salt River, AZ. However less urban locations that still had high alkalinity measurements included Hyalite Creek, MT and Derby Lake, VT. This may be indicative of sediment composition lending to high alkalinity or in the case of Derby Lake, VT, the presence of dairy farming nearby (Figure 36B). Similar locations also contained high amounts of TDS. The Southern California Water Supply and Salt River, AZ samples contained the greatest amount of TDS at  $840.68 \pm 24.7$  and  $>LOD$ , respectively. This may be due to runoff and leaching from natural deposits in both locations as most of Southern California's water supply is imported from the Colorado River.<sup>204,205</sup>

#### *Effect of Water Quality on MC-LR Degradation*

MC-LR in all 22 source water samples were significantly reduced with removal efficiencies ranging from 99.81-99.98% (Figure 37). Locations with the highest remaining MC-LR following eBeam treatment were the Chattahoochee River, GA ( $6.63 \pm 3.98$   $\mu\text{g/L}$  from  $3423.05 \pm 1036.12$   $\mu\text{g/L}$ ), Lake Washington, FL ( $7.28 \pm 4.78$   $\mu\text{g/L}$  from  $3747.16 \pm 321.97$   $\mu\text{g/L}$ ), and the Mississippi River, IA ( $6.31 \pm 4.57$   $\mu\text{g/L}$  from  $3454.74 \pm 921.93$   $\mu\text{g/L}$ ). Despite this, the three locations did not show similarities in their alkalinity, TDS, or dissolved oxygen content (Table 13).

Locations with the greatest MC-LR degradation following eBeam treatment were Lake Keowee, SC ( $0.73 \pm 0.23$   $\mu\text{g/L}$  from  $5335.54 \pm 1774.63$   $\mu\text{g/L}$ ), Lake Woollomes, CA ( $1.45 \pm 0.48$   $\mu\text{g/L}$  from  $4036.70 \pm 226.63$   $\mu\text{g/L}$ ), and Salt River, AZ ( $0.75 \pm 0.13$

Table 13. Water samples with the highest remaining MC-LR following  $5.11 \pm 0.079$  kGy eBeam treatment.

Source Water Location	pH	Alkalinity (mg/L of CaCO <sub>3</sub> )	TDS (mg/L)	Dissolved Oxygen (%)	MC-LR Remaining (%)
Chattahoochee River, GA	$6.81 \pm 0.25$	$20.33 \pm 1.15$	$75.33 \pm 15.04$	$85.67 \pm 1.53$	0.19
Lake Washington, FL	$7.15 \pm 0.04$	$57.66 \pm 30.24$	$558.67 \pm 4.73$	$80 \pm 2.65$	0.19
Mississippi River, IA	$7.20 \pm 0.02$	$183.33 \pm 1.53$	$459 \pm 21.70$	$63.33 \pm 1.53$	0.18

Table 14. Water samples with the lowest remaining MC-LR following  $5.11 \pm 0.079$  kGy eBeam treatment.

Source Water Location	pH	Alkalinity (mg/L of CaCO <sub>3</sub> )	TDS (mg/L)	Dissolved Oxygen (%)	MC-LR Remaining (%)
Lake Keowee, SC	$6.24 \pm 0.03$	$13.67 \pm 0.58$	$21.33 \pm 4.04$	$85.33 \pm 2.89$	0.01
Lake Woollomes, CA	$6.67 \pm 0.02$	$33.33 \pm 0.58$	$105.67 \pm 1.53$	$80.33 \pm 2.52$	0.02
Salt River, AZ	$7.25 \pm 0.04$	$144.67 \pm 1.15$	>LOQ?	$82.33 \pm 1.53$	0.02

$\mu\text{g/L}$  from  $4185.93 \pm 1031.87 \mu\text{g/L}$ ). Similarly, no trends were observed between any measured parameters and MC-LR breakdown (Table 14).

pH, alkalinity, TDS, and dissolved oxygen were chosen as measured parameters due to their noted ability in literature to effect MC-LR breakdown in various oxidative treatment strategies.<sup>206–208</sup> All water quality parameters, especially alkalinity and TDS, ranged widely in collected surface water samples. Regardless of each sample's water chemistry, degradation efficiency in all samples exceeded 99%, and there were no trends observed between water parameters and degradation. For example, the Salt River, AZ samples and the Mississippi River, IA samples both contained high measured alkalinity ( $144.67 \pm 1.15 \text{ mg/L}$  of CaCO<sub>3</sub> and  $183.33 \pm 1.53 \text{ mg/L}$  of CaCO<sub>3</sub>, respectively). Despite

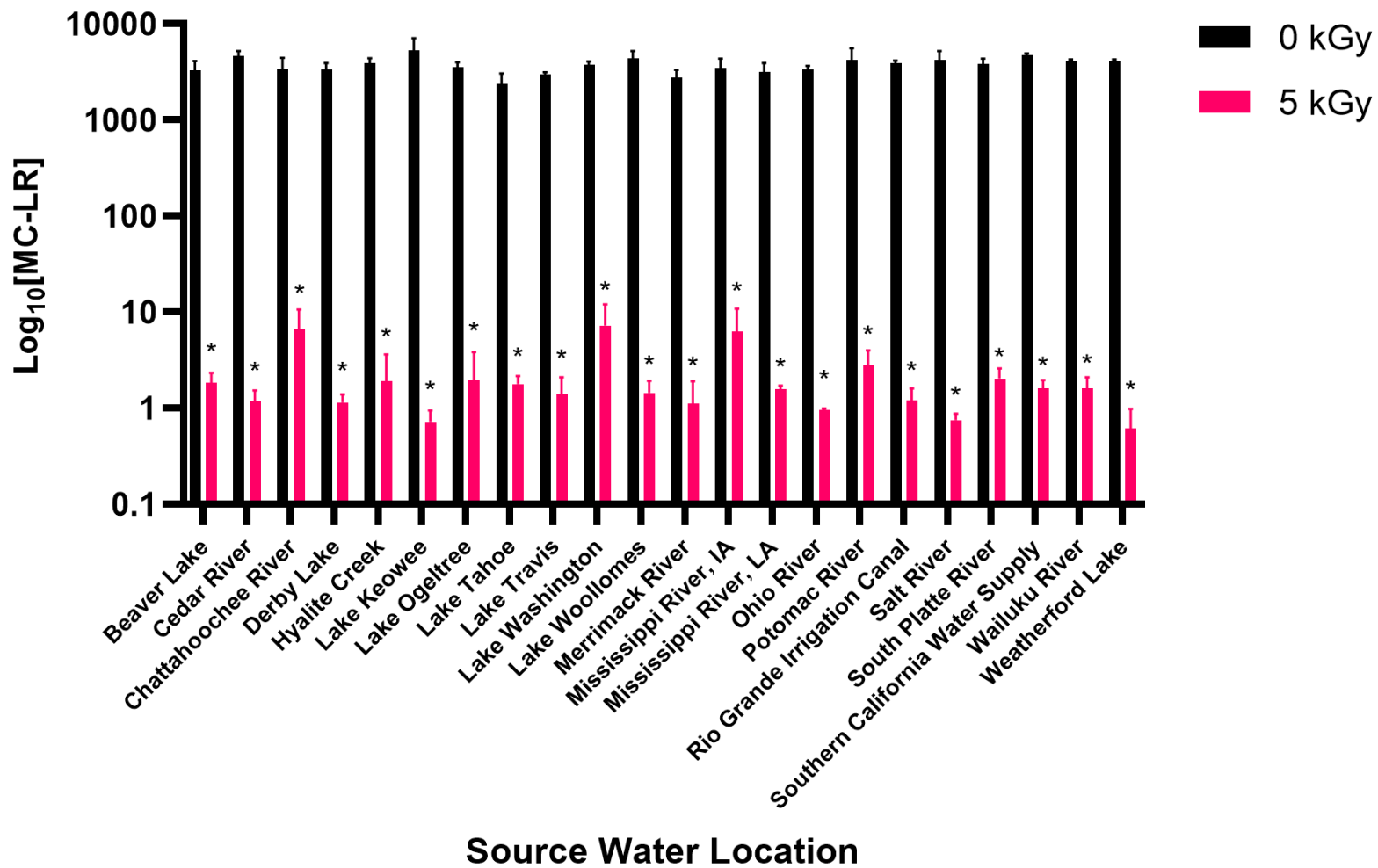


Figure 37. MC-LR degradation in surface water samples following eBeam treatment at  $5.11 \pm 0.079$  kGy. ( $p \leq 0.0001$ ; error bars represent standard deviation).

this similarity, the Salt River, AZ samples showed 99.9% degradation efficiency with 5 kGy treated samples containing  $0.75 \pm 0.13 \mu\text{g/L}$  MC-LR, and the Mississippi River, IA samples showed 99.8% degradation efficiency with 5 kGy treated samples containing  $6.31 \pm 4.57 \mu\text{g/L}$  MC-LR. Nevertheless, these differences of MC-LR degradation efficiency are overall negligible. These results suggest that eBeam treatment of MC-LR in surface water is not water quality dependent and further underscores the utility of eBeam technology over other chemical treatments.

#### *Fulvic Acid Effects on MC-LR Degradation*

NOM has been shown to have negative impacts on MC-LR degradation for a variety of AOPs.<sup>24,206,207,209</sup> As with the parameters previously discussed, NOM can influence the concentration of radicals and their contributions to MC-LR degradation. NOM consists mainly of fulvic acid and other humic substances and may act as a scavenger for hydroxyl radicals depending on solution pH.<sup>206</sup> In this experiment, fulvic acid (FA) was utilized to study the effects of NOM on eBeam degradation of MC-LR (Figure 38). Samples containing both 50  $\mu\text{g/L}$  and 100  $\mu\text{g/L}$  FA showed an overall decrease in MC-LR degradation at 5 kGy. However, degradation of spiked MC-LR was still significant at all concentrations of FA employed with degradation efficiencies of 99.99%, 99.96%, and 99.92% for 0  $\mu\text{g/L}$ , 50  $\mu\text{g/L}$ , and 100  $\mu\text{g/L}$ , respectively.

NOM is comprised of an array of moieties with various charges including carboxylic and phenolic functional groups. Therefore, solution pH can influence the overall charges of NOM. Increasing pH of solution results in an overall negative charge

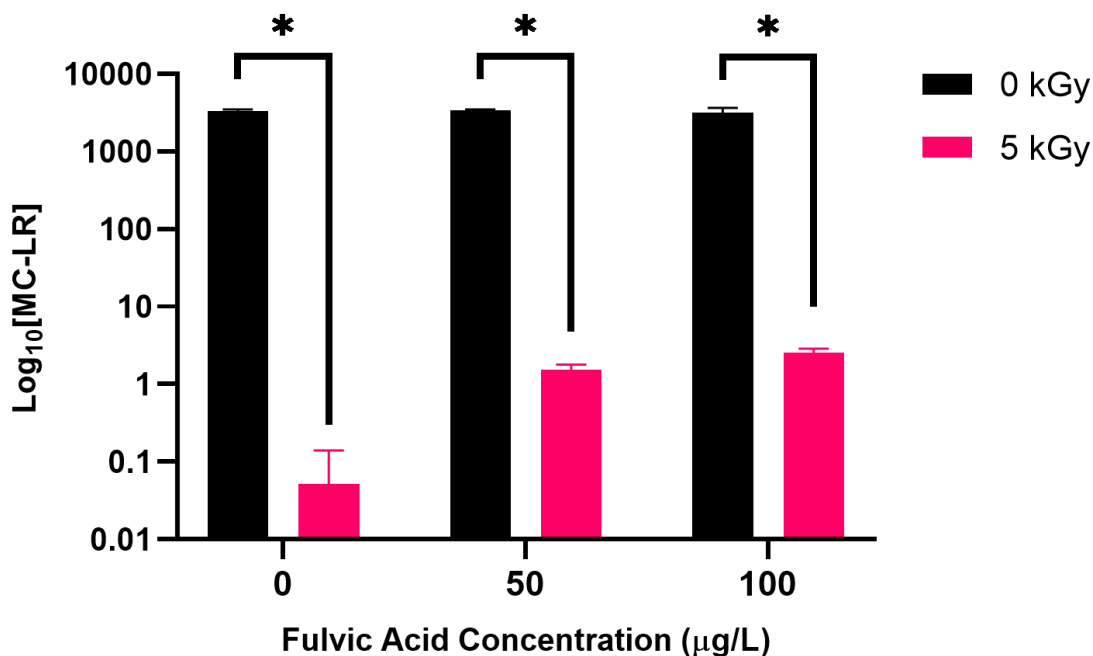


Figure 38. MC-LR degradation in deionized water supplemented with 0, 50, or 100 µg/L FA following eBeam treatment at  $5.11 \pm 0.079$  kGy. ( $p \leq 0.0001$ ; error bars represent standard deviation).

on phenolic type groups in both FA and humic acids (HA) while at lower pH this negative charge is associated with carboxylic groups.<sup>210</sup> Further studies should be completed to determine differences in potential NOM radical scavenging as a function of pH to understand the full effects of NOM concentration of MC-LR degradation by eBeam technology.

### Conclusion

We investigated several water parameters that may influence eBeam degradation of MC-LR using surface water samples gathered around the U.S. All samples were analyzed for pH, alkalinity, TDS, and dissolved oxygen. Although some samples showed greater rates of degradation than others, average degradation efficiency at 5 kGy across

water samples was above 99%. No trends were observed in any measured parameters as influencers of MC-LR degradation. We also investigated the influence of FA on MC-LR breakdown. MC-LR degradation efficiency was decreased in samples containing FA and was concentration dependent. However, degradation at all tested concentrations was still significant ( $p \leq 0.0001$ ). These results can help provide an understanding of potential interactions of water quality parameters with degradation of MC-LR using eBeam. Further research is needed to understand the influence of each of these parameters separately determine optimal treatment parameters for eBeam treatment of MC-LR in surface waters.

## CHAPTER VIII

### CONCLUSION

#### **Summary**

In order to continue supplying clean drinking water to a growing global population, there is a need for reliable treatment technologies to remove pollutants from our water. Harmful cyanobacterial blooms (cyanoHABs) are overgrowths of cyanobacteria in surface water that produce a variety of neuro- and hepato-toxic cyanotoxins. *Microcystis aeruginosa* is the most commonly found cyanobacterial species in freshwater blooms and is responsible for producing the cyanotoxin class known as microcystins (MCs).<sup>8</sup> Over the past few decades, MCs and other cyanotoxins have been responsible for a number of human, livestock, and pet poisonings due to contaminated drinking and recreational water sources. The costs of these blooms spread across markets with economic losses occurring in human health, tourism, fisheries, and water treatment.<sup>211-214</sup>

The overarching goal of the three aims of this project were to investigate the ability of high energy electron beam (eBeam) technology to treat the cyanotoxin, microcystin-LR (MC-LR), and the producing cyanobacteria, *M. aeruginosa*, in drinking water. In these studies: MC-LR degradation and residual toxicity were investigated following eBeam treatment; *M. aeruginosa* cell growth and function were inspected following eBeam treatment; and the effects of different surface water parameters on MC-LR degradation were explored in field samples.



1. Environmentally relevant concentrations of MC-LR were fully degraded in water at low doses of eBeam treatment (400 Gy). This degradation is mediated primarily by oxidative species produced via the radiolysis of water.
2. eBeam treated MC-LR was unable to bind in specific bioassays nor able to cause toxicity *in vitro* to HEPG2 cells. Degradation products of MC-LR following eBeam treatment may lack the bioactive ADDA (3-amino-9-methoxy-2,6,8-trimethyl-10-phenyldeca-4,6-dienoic acid) moiety responsible for toxicity of the molecule.
3. *M. aeruginosa* cells were killed at doses  $\geq 2$  kGy. The cells were non-culturable up to 14 days following eBeam treatment. The cells lysed following eBeam treatment, but did so after a time delay. This time delay appears to be approximately 2 hours in lighted incubation conditions.
4. Prior to cell lysis, *M. aeruginosa* cells appear to retain metabolic activity as determined through gene expression analyses. eBeam treatment dose influences differential gene expression more than the amount of time following irradiation. Genes associated with photosystem I and II and microcystin synthesis were overall downregulated in eBeam treated cultures.
5. Cell lysis following eBeam treatment results from damage to photosynthetic machinery in *M. aeruginosa* and light reduces the time delay between treatment and cell lysis.

6. Even at elevated MC-LR concentrations, water quality parameters had little effect on eBeam induced MC-LR degradation in surface water samples and degradation efficiencies were as high as 99.9%.

### **Novelty of Research**

These studies represent the most comprehensive look to date into the effects of eBeam treatment on both MC-LR degradation and *M. aeruginosa* cell function. These studies are the first to investigate MC-LR degradation products and their resulting toxicity following eBeam treatment. Furthermore, these studies are also the first to consider the further production of MC-LR by *M. aeruginosa* following eBeam treatment. The results of these studies prove that eBeam technology is an effective tool for the remediation of waters contaminated with *M. aeruginosa* and MC-LR, although further parameter optimization and treatment placement is still needed. Ultimately, these studies allow for an increased understanding of the susceptibility of cyanobacteria to ionizing radiation, as well as demonstrate the utility of eBeam irradiation technology for use in water treatment of emerging pollutants.

## CHAPTER IX

### FUTURE RESEARCH

#### **Future Directions for *M. aeruginosa***

*Microcystis aeruginosa* cells, unlike previously studied bacteria, lyse following eBeam treatment. While lysis is beneficial from a water treatment standpoint, it opens questions as to the cause of this lysis. When examined in particular incubation conditions (light vs. dark), *M. aeruginosa* cells responded differently, with cell death being delayed in the absence of light. This project demonstrates that after eBeam treatment, but prior to cell lysis, cells are able to enter a metabolically active yet non-culturable (MAyNC) state. In this state, cells may continue synthesis of MC-LR. Due to constraints of this project, gene expression of cultures incubated in dark conditions following eBeam treatment were not investigated. However, given that *M. aeruginosa* cells maintain cell integrity longer in the absence of light, there is an increased time window for metabolic activity following treatment.

Therefore, the avenues for future research of eBeam irradiated *Microcystis aeruginosa* are as follows:

1. There is a need to further understand the role of light in cell damage following irradiation treatment. Do cells remain metabolically active prior to cell lysis in the absence of light? Are cells able to repair eBeam induced damage in the absence of light?
2. There is a need to investigate other cyanotoxin producing cyanobacteria and their response to eBeam treatment. Do other photosynthetic bacteria undergo cell lysis

following eBeam treatment? Is eBeam treatment effective for a range of bloom forming species?

### **Future Directions for MC-LR**

MC-LR degradation was observed at low doses of eBeam treatment. Unlike studies completed with other forms of ionizing radiation, larger mass degradation products were not observed in our studies. A larger amount of degradation products were observed in t-butanol amended samples, suggesting that eBeam induced MC-LR degradation is primarily oxidative. However, the degradation of the parent MC-LR toxin was observed in all amended samples suggesting oxidative species may also play a role in eBeam degradation. It was observed that toxicity was eliminated in irradiated MC-LR. Still, understanding the degradation mechanism may aid in predicting similar chemicals' degradation following eBeam treatment.

Therefore, the avenues for future research of eBeam irradiated MC-LR are as follows:

1. There is a need to further investigate the degradation pathway of MC-LR exposed to eBeam irradiation. Could MC-LR be mineralized at high doses of eBeam irradiation? Are certain chemical bonds or functional groups on MC-LR more susceptible to eBeam irradiation?
2. Further research is necessary to understand the interactions of MC-LR with other pollutants of interests in water treatment. Could other emerging contaminants of concern inhibit MC-LR degradation? Could eBeam treated

MC-LR form any disinfection byproducts with other contaminants in the water treatment process?

### **Future Directions for Implementation**

Current water treatment strategies employ a mix of conventional treatment technologies and chemical additives. These strategies follow a sequence of events for efficient removal of a variety of water contaminants. eBeam presents a promising addition to these strategies, with benefits depending on location/placement within the water treatment scheme. Due to the observation of MC-LR presence in treated *M. aeruginosa* cultures, there is a need to understand the most beneficial location for eBeam technology within the existing treatment infrastructure.

Therefore, the avenues for future research of eBeam technology implementation are as follows:

1. There is a need for further research to investigate the ideal placement of eBeam technology within existing water treatment schemes. Should eBeam treatment occur first to induce cell rupture for downstream degradation of MC-LR? Should eBeam treatment occur following cellular removal for the degradation of the MC-LR toxin? Should a double pass system be developed for both cell lysis and MC-LR degradation by eBeam irradiation? If cells are light sensitive, should eBeam treatment be coupled with light in the treatment process to assure cell death? Finally, could the coupling of eBeam technology with other treatment strategies like ozone increase the effectiveness of cell and toxin removal?

2. Further research is necessary to investigate the ability of eBeam technology to treat water treatment plant residuals, such as sediments and sludges, contaminated with *M. aeruginosa* and MC-LR. Could eBeam have secondary applications in water treatment for the treatment of hazardous waste products? Is eBeam technology able to degrade MC-LR and induce cell lysis in low moisture content solids?

## REFERENCES

1. Philip, A., Sims, E., Houston, J. & Konieczny, R. *Troubled Water*. <http://troubledwater.news21.com/> (2017).
2. Office of Water, Office of Ground Water and Drinking Water & Drinking Water Protection Division. *Drinking Water Infrastructure Needs Survey and Assessment: Sixth Report to Congress*. [https://www.epa.gov/sites/production/files/2018-10/documents/corrected\\_sixth\\_drinking\\_water\\_infrastructure\\_needs\\_survey\\_and\\_assessment.pdf](https://www.epa.gov/sites/production/files/2018-10/documents/corrected_sixth_drinking_water_infrastructure_needs_survey_and_assessment.pdf) (2018).
3. Chorus, I. & Bartram, J. *Toxic cyanobacteria in water: A guide to their public health consequences, monitoring, and management*. *Limnology and Oceanography* vol. 45 (CRC Press, Inc, 1999).
4. Paerl, H. W. & Otten, T. G. Harmful Cyanobacterial Blooms: Causes, Consequences, and Controls. *Microbial Ecology* **65**, 995–1010 (2013).
5. American Water Works Association. *Cyanotoxins in US Drinking Water: Occurrence, Case Studies and State Approaches to Regulation*. [www.awwa.org](http://www.awwa.org) (2016).
6. Environmental Protection Agency. *Impacts of Climate Change on the Occurrence of Harmful Algal Blooms*. (2013).
7. Munoz, M. *et al.* Degradation of widespread cyanotoxins with high impact in drinking water (microcystins, cylindrospermopsin, anatoxin-a and saxitoxin) by CWPO. *Water Research* **163**, 114853 (2019).
8. Buratti, F. M. *et al.* Cyanotoxins: producing organisms, occurrence, toxicity, mechanism of action and human health toxicological risk evaluation. *Archives of Toxicology* **91**, 1049–1130 (2017).
9. Chow, C. W. K., Drikas, M., House, J., Burch, M. D. & Velzeboer, R. M. A. The impact of conventional water treatment processes on cells of the cyanobacterium *Microcystis aeruginosa*. *Water Research* **33**, 3253–3262 (1999).
10. Newcombe, G. & Nicholson, B. Water Treatment Options for Dissolved Cyanotoxins. *Journal of Water Supply: Research and Technology* **53**, 227–239 (2004).
11. Maghsoudi, E. *et al.* Biodegradation of multiple microcystins and cylindrospermopsin in clarifier sludge and a drinking water source: Effects of

- particulate attached bacteria and phycocyanin. *Ecotoxicology and Environmental Safety* **120**, 409–417 (2015).
12. Xu, H. *et al.* Behaviors of *Microcystis aeruginosa* cells during floc storage in drinking water treatment process. *Scientific Reports* **6**, 1–13 (2016).
  13. US Environmental Protection Agency. State HABs Monitoring Programs and Resources. <https://www.epa.gov/cyano-habs/state-habs-monitoring-programs-and-resources>.
  14. National Wildlife Federation. *2014 Harmful Algal Bloom State Survey Summary of Results and Recommendations*. (2014).
  15. Steffen, M. M. *et al.* Ecophysiological Examination of the Lake Erie *Microcystis* Bloom in 2014: Linkages between Biology and the Water Supply Shutdown of Toledo, OH. (2017) doi:10.1021/acs.est.7b00856.
  16. Clark, J. M. *et al.* Satellite monitoring of cyanobacterial harmful algal bloom frequency in recreational waters and drinking water sources. *Ecological Indicators* **80**, 84–95 (2017).
  17. Barros, M. U. G. *et al.* Environmental factors associated with toxic cyanobacterial blooms across 20 drinking water reservoirs in a semi-arid region of Brazil. *Harmful Algae* **86**, 128–137 (2019).
  18. Carmichael, W. W. *et al.* Human Fatalities from Cyanobacteria: Chemical and Biological Evidence for Cyanotoxins. *Environmental Health Perspectives* **109**, 663–668 (2001).
  19. Jochimsen, E. M. *et al.* Liver Failure and Death after Exposure to Microcystins at a Hemodialysis Center in Brazil. *New England Journal of Medicine* **338**, 873–878 (1998).
  20. Sharma, V. K. *et al.* Destruction of microcystins by conventional and advanced oxidation processes: A review. *Separation and Purification Technology* **91**, 3–17 (2012).
  21. Chang, J. *et al.* Ozonation degradation of microcystin-LR in aqueous solution: Intermediates, byproducts and pathways. *Water Research* **63**, 52–61 (2014).
  22. Park, J.-A. *et al.* Oxidation of microcystin-LR by the Fenton process: Kinetics, degradation intermediates, water quality and toxicity assessment. *Chemical Engineering Journal* **309**, 339–348 (2017).



23. Zong, W., Sun, F. & Sun, X. Oxidation by-products formation of microcystin-LR exposed to UV/H<sub>2</sub>O<sub>2</sub>: Toward the generative mechanism and biological toxicity. *Water Research* **47**, 3211–3219 (2013).
24. Rositano, J., Newcombe, G., Nicholson, B. & Sztajn bok, P. Ozonation of nom and algal toxins in four treated waters. *Water Research* **35**, 23–32 (2001).
25. Teixeira, M. R. & Rosa, M. J. Comparing dissolved air flotation and conventional sedimentation to remove cyanobacterial cells of *Microcystis aeruginosa*: Part II. The effect of water background organics. *Separation and Purification Technology* **53**, 126–134 (2007).
26. United States Environmental Protection Agency. *Cyanobacteria and Cyanotoxins: Information for Drinking Water Systems*. (2014).
27. United States Environmental Protection Agency. Drinking Water Contaminant Candidate List 4-Final. *Federal Register* **81**, 81099–81114 (2016).
28. Preece, E. P., Hardy, F. J., Moore, B. C. & Bryan, M. A review of microcystin detections in Estuarine and Marine waters: Environmental implications and human health risk. *Harmful Algae* **61**, 31–45 (2017).
29. *Handbook on Cyanobacteria: Biochemistry, Biotechnology, and Applications*. (Nova Science Publishers, Inc., 2009).
30. Francis, G. Poisonous Australian Lake. *Nature* **18**, 11–12 (1878).
31. Mahmood, N. A., Carmichael, W. & Pfahler, D. Anticholinesterase poisonings in dogs from a cyanobacterial (blue-green alga) bloom dominated by *Anabaena flos-aquae*. *American Journal of Veterinary Research* **49**, 500–503 (1988).
32. Fitzgerald, S. D. & Poppenga, R. H. Toxicosis due to microcystin hepatotoxins in three Holstein heifers. *J. Vet. Diagn. Invest.* **5**, 651–653 (1993).
33. Gupta, S. Cyanobacterial toxins: Microcystin-LR in Drinking-water. in *Guidelines for drinking-water quality* (ed. World Health Organization) 95–110 (World Health Organization, 1998).
34. Matsunaga, H. *et al.* Possible Cause of Unnatural Mass Death of Wild Birds in a Pond in Nishinomiya, Japan: Sudden Appearance of Toxic Cyanobacteria. *Natural Toxins* **7**, 81–84 (1999).
35. Krienitz, L. *et al.* Contribution of hot spring cyanobacteria to the mysterious deaths of Lesser Flamingos at Lake Bogoria, Kenya. *FEMS Microbiology Ecology* **43**, 141–148 (2003).

36. Nasri, H., El Herry, S. & Bouaïcha, N. First reported case of turtle deaths during a toxic *Microcystis* spp. bloom in Lake Oubeira, Algeria. *Ecotoxicology and Environmental Safety* **71**, 535–544 (2008).
37. van der Merwe, D. *et al.* Investigation of a *Microcystis aeruginosa* cyanobacterial freshwater harmful algal bloom associated with acute microcystin toxicosis in a dog. *Journal of Veterinary Diagnostic Investigation* **24**, 679–687 (2012).
38. Backer, L. C., Landsberg, J. H., Miller, M., Keel, K. & Taylor, T. K. Canine cyanotoxin poisonings in the United States (1920s-2012): review of suspected and confirmed cases from three data sources. *Toxins* **5**, 1597–628 (2013).
39. Yu, S., Zhao, N. & Zi, X. The relationship between cyanotoxin (microcystin, MC) in pond-ditch water and primary liver cancer in China. *Zhonghua zhong liu za zhi [Chinese journal of oncology]* **23**, 96–9 (2001).
40. Trevino-Garrison, I. *et al.* Human illnesses and animal deaths associated with freshwater harmful algal blooms-Kansas. *Toxins* **7**, 353–66 (2015).
41. Tanabe, Y., Hodoki, Y., Sano, T., Tada, K. & Watanabe, M. M. Adaptation of the freshwater bloom-forming cyanobacterium *Microcystis aeruginosa* to brackish water is driven by recent horizontal transfer of sucrose genes. *Frontiers in Microbiology* **9**, 1150 (2018).
42. Vasconcelos, V. M., Sivonen, K., Evans, W. R., Carmichael, W. W. & Namikoshi, M. Hepatotoxic microcystin diversity in cyanobacterial blooms collected in portuguese freshwaters. *Water Research* **30**, 2377–2384 (1996).
43. Tsuji, K. *et al.* *Stability of Microcystins from Cyanobacteria: Effect of Light on Decomposition and Isomerization*. *Environmental Science and Technology* vol. 28 (1994).
44. Song, W., De La Cruz, A. A., Rein, K. & O’Shea, K. E. Ultrasonically induced degradation of microcystin-LR and -RR: identification of products, effect of pH, formation and destruction of peroxides. *Environmental science & technology* **40**, 3941–6 (2006).
45. Eriksson, J. E., Grönberg, L., Nygård, S., Slotte, J. P. & Meriluoto, J. A. O. Hepatocellular uptake of 3H-dihydromicrocystin-LR, a cyclic peptide toxin. *Biochimica et Biophysica Acta (BBA) - Biomembranes* **1025**, 60–66 (1990).
46. Fischer, W. J. *et al.* Organic anion transporting polypeptides expressed in liver and brain mediate uptake of microcystin. *Toxicology and Applied Pharmacology* **203**, 257–263 (2005).

47. Valério, E., Chaves, S. & Tenreiro, R. Diversity and Impact of Prokaryotic Toxins on Aquatic Environments: A Review. *Toxins* **2**, 2359–2410 (2010).
48. Lu, H. *et al.* Characterization of Organic Anion Transporting Polypeptide 1b2-null Mice: Essential Role in Hepatic Uptake/Toxicity of Phalloidin and Microcystin-LR. *Toxicological Sciences* **103**, 35–45 (2008).
49. Craig, M. *et al.* Molecular mechanisms underlying the interaction of motuporin and microcystins with type-1 and type-2A protein phosphatases. *Biochemistry and Cell Biology* **74**, 569–578 (1996).
50. Campos, A. & Vasconcelos, V. Molecular mechanisms of microcystin toxicity in animal cells. *International journal of molecular sciences* **11**, 268–87 (2010).
51. Douglas, P., Moorhead, G. B. G., Ye, R. & Lees-Miller, S. P. Protein Phosphatases Regulate DNA-dependent Protein Kinase Activity. *The Journal of Biological Chemistry* **276**, 18992–18998 (2001).
52. Chen, L. *et al.* The Interactive Effects of Cytoskeleton Disruption and Mitochondria Dysfunction Lead to Reproductive Toxicity Induced by Microcystin-LR. *PLoS ONE* **8**, e53949 (2013).
53. Kondo, F. *et al.* Formation, Characterization, and Toxicity of the Glutathione and Cysteine Conjugates of Toxic Heptapeptide Microcystins. *Chem. Res. Toxicol.* vol. 5 (1992).
54. Fumio Kondo *et al.* Detection and Identification of Metabolites of Microcystins Formed in Vivo in Mouse and Rat Livers. *Chem. Res. Toxicol.* **9**, 1355–1359 (1996).
55. International Agency for Research on Cancer. *IARC Monographs on the Evaluation of Cyanobacterial Peptide Toxins.* (2010).
56. United States Environmental Protection Agency. Health Effects from Cyanotoxins. <https://www.epa.gov/cyanohabs/health-effects-cyanotoxins>.
57. Environmental Protection Agency. *Health Effects Support Document for the Cyanobacterial Toxin Microcystins.* (2015).
58. United States Environmental Protection Agency. *Toxicological Reviews of Cyanobacterial Toxins: Microcystins LR, RR, YR, and LA.* (2006) doi:EPA/600/R-06/139.

59. Environmental Protection Agency. EPA Drinking Water Health Advisories for Cyanotoxins. <https://www.epa.gov/cyanohabs/epa-drinking-water-health-advisories-cyanotoxins> (2015).
60. Ibelings, B. W., Backer, L. C., Kardinaal, W. E. A. & Chorus, I. Current approaches to cyanotoxin risk assessment and risk management around the globe. *Harmful Algae* **40**, 63–74 (2014).
61. United States Environmental Protection Agency. *Drinking Water Health Advisory for the Cyanobacterial Microcystin Toxins*. <https://www.epa.gov/sites/production/files/2017-06/documents/microcystins-report-2015.pdf> (2015).
62. United States Environmental Protection Agency. Guidelines and Recommendations. [https://19january2017snapshot.epa.gov/nutrient-policy-data/guidelines-and-recommendations\\_.html](https://19january2017snapshot.epa.gov/nutrient-policy-data/guidelines-and-recommendations_.html) (2018).
63. Bláha, L., Babica, P., Maršálek, B. & Luděk Bláha, A. Toxins produced in cyanobacterial water blooms-toxicity and risks. *Interdisc Toxicol* **2**, 36–41 (2009).
64. Wiegand, C. & Pflugmacher, S. Ecotoxicological effects of selected cyanobacterial secondary metabolites a short review. *Toxicology and Applied Pharmacology* **203**, 201–218 (2005).
65. Ferrão-Filho, A. da S. & Kozłowsky-Suzuki, B. Cyanotoxins: Bioaccumulation and Effects on Aquatic Animals. *Marine Drugs* **9**, 2729–2772 (2011).
66. Mankiewicz, J., Tarczynska, M., Tarczyn´ska, T., Walter, Z. & Zalewski, M. Natural Toxins from Cyanobacteria. *Acta Biologica Cracoviensia* **45**, (2003).
67. Pearson, L. *et al.* On the Chemistry, Toxicology and Genetics of the Cyanobacterial Toxins, Microcystin, Nodularin, Saxitoxin and Cylindrospermopsin. *Marine Drugs* **8**, 1650–1680 (2010).
68. *The Cyanobacteria: molecular biology, genomics, and evolution*. (Caister Academic Press, 2008).
69. Carmichael, W. W., Mahmood, N. A. & Hyde, E. G. Natural Toxins from Cyanobacteria (Blue-Green Algae). in *Marine Toxins* (eds. Hall, S. & Strichartz, G.) 87–106 (ACS Publications, 1990). doi:10.1021/bk-1990-0418.ch006.
70. Jiang, X., Lee, S., Mok, C. & Lee, J. Sustainable methods for decontamination of microcystin in water using cold plasma and UV with reusable TiO<sub>2</sub> nanoparticle coating. *International Journal of Environmental Research and Public Health* **14**, (2017).

71. Fan, J., Hobson, P., Ho, L., Daly, R. & Brookes, J. The effects of various control and water treatment processes on the membrane integrity and toxin fate of cyanobacteria. *Journal of Hazardous Materials* **264**, 313–322 (2014).
72. Nickelsen, M. G., Cooper, W. J., Lin, K., Kurucz, C. N. & Waite, T. D. High Energy Electron Beam Generation of Oxidants for the Treatment of Benzene and Toluene in the Presence of Radical Scavengers. *Pergamon Wat. Res* **28**, 1227–1237 (1994).
73. Yu, J., Hu, J., Tanaka, S. & Fujii, S. Perfluorooctane sulfonate (PFOS) and perfluorooctanoic acid (PFOA) in sewage treatment plants. *Water Research* **43**, 2399–2408 (2009).
74. Praveen, C., Jesudhasan, P. R., Reimers, R. S. & Pillai, S. D. Electron beam inactivation of selected microbial pathogens and indicator organisms in aerobically and anaerobically digested sewage sludge. *Bioresource Technology* **144**, 652–657 (2013).
75. He, S., Wang, J., Ye, L., Zhang, Y. & Yu, J. Removal of diclofenac from surface water by electron beam irradiation combined with a biological aerated filter. *Radiation Physics and Chemistry* **105**, 104–108 (2014).
76. Wang, J. & Chu, L. Irradiation treatment of pharmaceutical and personal care products (PPCPs) in water and wastewater: An overview. *Radiation Physics and Chemistry* vol. 125 56–64 (2016).
77. Pillai, S. D. & Shayanfar, S. Electron Beam Technology and Other Irradiation Technology Applications in the Food Industry. in *pplications of Radiation Chemistry in the Fields of Industry, Biotechnology and Environment* 249–268 (2017). doi:10.1007/978-3-319-54145-7\_9.
78. Chmielewski, A. G., Kang, C. M., Kang, C. S. & Vujic, J. L. *Radiation Technology - Introduction to Industrial and Environmental Applications*. (Seoul National University Press, 2006).
79. Miller, R. B. *Electronic Irradiation of Foods: An Introduction to Food Irradiation*. (Springer US, 2005). doi:10.1007/0-387-28386-2\_1.
80. IBA. *Review of Radiation Sterilization Technologies for Medical Devices*.
81. Attix, F. H. *Introduction to Radiological Physics and Radiation Dosimetry*. (John Wiley & Sons, 2008).
82. Hieke, A.-S. C. Investigating the Inactivation, Physiological Characteristics, and Transcriptomic Responses of Bacteria Exposed to Ionizing Radiation. (2015).

83. Mavragani, I. v., Nikitaki, Z., Kalospyros, S. A. & Georgakilas, A. G. Ionizing radiation and complex DNA damage: From prediction to detection challenges and biological significance. *Cancers* **11**, 1789 (2019).
84. Desouky, O., Ding, N. & Zhou, G. Targeted and non-targeted effects of ionizing radiation. *Journal of Radiation Research and Applied Sciences* **8**, 247–254 (2015).
85. Wallace, S. S. Base excision repair: a critical player in many games. *DNA repair* **19**, 14–26 (2014).
86. Daly, M. J. A new perspective on radiation resistance based on *Deinococcus radiodurans*. *Nature Reviews Microbiology* **7**, 237–245 (2009).
87. Reisz, J. A., Bansal, N., Qian, J., Zhao, W. & Furdai, C. M. Effects of Ionizing Radiation on Biological Molecules-Mechanisms of Damage and Emerging Methods of Detection. *Antioxidants and Redox Signaling* **21**, (2014).
88. Chan, H. L. *et al.* Proteomic analysis of UVC irradiation-induced damage of plasma proteins: Serum amyloid P component as a major target of photolysis. *FEBS Letters* **580**, 3229–3236 (2006).
89. Jesudhasan, P. R. *et al.* Electron-Beam Inactivated Vaccine Against Salmonella Enteritidis Colonization in Molting Hens. *Avian Diseases* **59**, 165–170 (2015).
90. Hieke, A.-S. C. & Pillai, S. D. Escherichia coli Cells Exposed to Lethal Doses of Electron Beam Irradiation Retain Their Ability to Propagate Bacteriophages and Are Metabolically Active. *Frontiers in Microbiology* **9**, 2138 (2018).
91. Bhatia, S. S. & Pillai, S. D. A Comparative Analysis of the Metabolomic Response of Electron Beam Inactivated E. coli O26:H11 and Salmonella Typhimurium ATCC 13311. *Frontiers in Microbiology* **10**, 694 (2019).
92. Bhatia, S. S., Wall, K. R., Kerth, C. R. & Pillai, S. D. Benchmarking the minimum Electron Beam (eBeam) dose required for the sterilization of space foods. *Radiation Physics and Chemistry* **143**, 72–78 (2018).
93. Secanella-Fandos, S., Noguera-Ortega, E., Olivares, F., Luquin, M. & Julián, E. Killed but metabolically active mycobacterium bovis bacillus Calmette-Guérin retains the antitumor ability of live bacillus Calmette-Guérin. *Journal of Urology* **191**, 1422–1428 (2014).
94. Praveen, C. *et al.* Assessment of microbiological correlates and immunostimulatory potential of electron beam inactivated metabolically active

- yet non culturable (MAyNC) Salmonella Typhimurium. *PLOS ONE* **16**, e0243417 (2021).
95. *Environmental Applications of Ionizing Radiation*. (John Wiley & Sons, 1998).
  96. An, J. S. & Carmichael, W. W. Use of a colorimetric protein phosphatase inhibition assay and enzyme linked immunosorbent assay for the study of microcystins and nodularins. *Toxicon* **32**, 1495–1507 (1994).
  97. Carmichael, W. W. The Toxins of Cyanobacteria. *Scientific American* **270**, 78–84 (1994).
  98. Morton, S. D. & Derse, P. H. Use of Gamma Radiation to Control Algae. *Environmental Science and Technology* **2**, 1041–1043 (1968).
  99. Kraus, M. P. Resistance of blue-green algae to <sup>60</sup>Co gamma radiation. *Radiation Botany* **9**, 481–489 (1969).
  100. Khan, J. A., Shah, N. S. & Khan, H. M. Decomposition of atrazine by ionizing radiation: Kinetics, degradation pathways and influence of radical scavengers. *Separation and Purification Technology* **156**, 140–147 (2015).
  101. Ma, S. H. *et al.* EB degradation of perfluorooctanoic acid and perfluorooctane sulfonate in aqueous solution. *Nuclear Science and Techniques* **28**, 137 (2017).
  102. Zhang, J. B., Zheng, Z., Yang, G. J. & Zhao, Y. F. Degradation of microcystin by gamma irradiation. *Nuclear Instruments and Methods in Physics Research Section A: Accelerators, Spectrometers, Detectors and Associated Equipment* **580**, 687–689 (2007).
  103. Henry, K. M. & Donahue, N. M. Effect of the OH Radical Scavenger Hydrogen Peroxide on Secondary Organic Aerosol Formation from  $\alpha$ -Pinene Ozonolysis. *Aerosol Science and Technology* **45**, 696–700 (2011).
  104. Song, W. *et al.* Radiolysis studies on the destruction of microcystin-LR in aqueous solution by hydroxyl radicals. *Environmental science & technology* **43**, 1487–92 (2009).
  105. Zheng, B. *et al.* The removal of *Microcystis aeruginosa* in water by gamma-ray irradiation. *Separation and Purification Technology* **85**, 165–170 (2012).
  106. Kang, H. Feasibility Test to Control Algal Bloom Using Electron Beam Irradiation. in *Status of industrial scale radiation treatment of wastewater and its future* 87–90 (International Atomic Energy Agency, 2004).

107. Liu, S., Zhao, Y., Jiang, W., Wu, M. & Ma, F. Inactivation of *Microcystis aeruginosa* by Electron Beam Irradiation. *Water, Air, & Soil Pollution* **225**, 2093 (2014).
108. Liu, S. *et al.* Control of *Microcystis aeruginosa* growth and associated microcystin cyanotoxin remediation by electron beam irradiation (EBI). *RSC Advances* **5**, 31292–31297 (2015).
109. Liu, S., Tan, Y., Ma, F., Fu, H. & Zhang, Y. Effects of electron beam irradiation on proteins and exopolysaccharide production and changes in *Microcystis aeruginosa* Effects of electron beam irradiation on proteins and exopolysaccharide production and changes in *Microcystis aeruginosa*. *Radiation Biology* **96**, (2020).
110. Lubenau, J. O. & Strom, D. J. Safety and Security of Radiation Sources in the Aftermath of 11 September 2001. *Health Physics* **83**, 155–164 (2002).
111. National Science and Technology Council, Committee on Homeland and National Security, Subcommittee on Nuclear Defense Research and Development & Interagency Working Group on Alternatives to High-Activity Radioactive Sources. *Transitioning From High-Activity Radioactive Sources to Non-Radioisotopic (Alternative) Technologies - A Best Practices Guide for Federal Agencies*. (2016).
112. Chou, J. W., Skornicki, M. & Cohen, J. T. Unintended consequences of the potential phase-out of gamma irradiation. *F1000 Research* **7**, (2018).
113. Chaychian, M., Al-Sheikhly, M., Silverman, J. & McLaughlin, W. L. The mechanisms of removal of heavy metals from water by ionizing radiation. *Radiation Physics and Chemistry* **53**, 145–150 (1998).
114. He, S., Wang, J., Ye, L., Zhang, Y. & Yu, J. Removal of diclofenac from surface water by electron beam irradiation combined with a biological aerated filter. *Radiation Physics and Chemistry* **105**, 104–108 (2014).
115. Department of Energy. *Workshop on Energy and Environmental Applications of Accelerators*. (2015) doi:10.2172/1358082.
116. Zaffiro, A., Rosenblum, L. & Wendelken, S. C. *Method 546: Determination of Total Microcystins and Nodularins in Drinking Water and Ambient Water by Adda Enzyme-Linked Immunosorbent Assay*. <https://www.epa.gov/sites/production/files/2016-09/documents/method-546-determination-total-microcystins-nodularins-drinking-water-ambient-water-adda-enzyme-linked-immunosorbent-assay.pdf> (2016).



117. Zhou, W. *et al.* Cinnamaldehyde Induces PCD-Like Death of *Microcystis aeruginosa* via Reactive Oxygen Species Article in *Water Air and Soil Pollution · Cinnamaldehyde Induces PCD-Like Death of Microcystis aeruginosa via Reactive Oxygen Species*. (2011) doi:10.1007/s11270-010-0571-1.
118. Lung, H.-M. *et al.* Microbial decontamination of food by electron beam irradiation. *Trends in Food Science & Technology* **44**, 66–78 (2015).
119. Pillai, S. D. & Shayanfar, S. Electron beam processing of fresh produce – A critical review. *Radiation Physics and Chemistry* **143**, 85–88 (2018).
120. Silindir, M. & Özer, A. Y. Sterilization Methods and the Comparison of E-Beam Sterilization with Gamma Radiation Sterilization. *J. Pharm. Sci* **34**, 43–53 (2009).
121. Agarwal, R., Rane, S. S. & Sainis, J. K. Effects of  $^{60}\text{Co}$   $\gamma$  radiation on thylakoid membrane functions in *Anacystis nidulans*. *Journal of Photochemistry and Photobiology B: Biology* **91**, 9–19 (2008).
122. Kovács, E. & Keresztes, A. Effect of gamma and UV-B/C radiation on plant cells. *Micron* **33**, 199–210 (2002).
123. Strydom, G. J., van Staden, J. & Smith, M. T. The effect of gamma radiation on the ultrastructure of the peel of banana fruits. *Environmental and Experimental Botany* **31**, 43–49 (1991).
124. Tahergorabi, R., Matak, K. E. & Jaczynski, J. Application of electron beam to inactivate *Salmonella* in food: Recent developments. *Food Research International* **45**, 685–694 (2012).
125. Osborne, J. C., Miller, J. H. & Kempner, E. S. Molecular mass and volume in radiation target theory. *Biophysical Journal* **78**, 1698–1702 (2000).
126. Humpage, A. R., Magalhaes, V. F. & Froscio, S. M. Comparison of analytical tools and biological assays for detection of paralytic shellfish poisoning toxins. *Analytical and Bioanalytical Chemistry* **397**, 1655–1671 (2010).
127. Steinmann, J., Huelsewede, J., Buer, J. & Rath, P.-M. Comparison and evaluation of a novel bioassay and high-performance liquid chromatography for the clinical measurement of serum voriconazole concentrations. *Mycoses* **54**, e421–e428 (2011).
128. Santana, M. V. E., Zhang, Q. & Mihelcic, J. R. Influence of water quality on the embodied energy of drinking water treatment. *Environmental Science and Technology* **48**, 3084–3091 (2014).

129. Rocha, J. N. *et al.* PNAG-specific equine IgG 1 mediates significantly greater opsonization and killing of *Prescottella equi* (formerly *Rhodococcus equi*) than does IgG 4/7. *Vaccine* **37**, 1142–1150 (2019).
130. Pearson, L. A., Hisbergues, M., Börner, T., Dittmann, E. & Neilan, B. A. Inactivation of an ABC transporter gene, *mcyH*, results in loss of microcystin production in the cyanobacterium *Microcystis aeruginosa* PCC 7806. *Applied and Environmental Microbiology* **70**, 6370–6378 (2004).
131. Rohrlack, T. & Hyenstrand, P. Fate of intracellular microcystins in the cyanobacterium *Microcystis aeruginosa* (Chroococcales, Cyanophyceae). *Phycologia* **46**, 277–283 (2007).
132. Fawell, J. K., James, C. P. & James, H. A. *Toxins from blue-green algae: toxicological assessment of microcystin-LR and a method for its determination in water*. *Foundation for Water Research* (1994).
133. Zhou, L., Yu, H. & Chen, K. Relationship between microcystin in drinking water and colorectal cancer. *Biomedical and Environmental Sciences* **15**, 166–171 (2002).
134. Wang, L., Batchelor, B., Pillai, S. D. & Botlaguduru, V. S. v. Electron beam treatment for potable water reuse: Removal of bromate and perfluorooctanoic acid. *Chemical Engineering Journal* **302**, 58–68 (2016).
135. Folcik, A. M., Klemashevich, C. & Pillai, S. D. Response of *Microcystis aeruginosa* and Microcystin-LR to electron beam irradiation doses. *Radiation Physics and Chemistry* **186**, 109534 (2021).
136. Ma, S. H. *et al.* EB degradation of perfluorooctanoic acid and perfluorooctane sulfonate in aqueous solution. *Nuclear Science and Techniques* **28**, 137 (2017).
137. Cong, J., Wen, G., Huang, T., Deng, L. & Ma, J. Study on enhanced ozonation degradation of para-chlorobenzoic acid by peroxymonosulfate in aqueous solution. *Chemical Engineering Journal* **264**, 399–403 (2015).
138. von Piechowski, M., Thelen, M.-A., Hoigne, J. & Buhler, R. E. tert-Butanol as an OH-Scavenger in the Pulse Radiolysis of Oxygenated Aqueous Systems. *Berichte der Bunsengesellschaft für physikalische Chemie* **96**, 1448–1454 (1992).
139. Trojanowicz, M. *et al.* Application of ionizing radiation in decomposition of perfluorooctanoate (PFOA) in waters. *Chemical Engineering Journal* **357**, 698–714 (2019).

140. Trojanowicz, M. *et al.* Application of ionizing radiation in decomposition of perfluorooctane sulfonate (PFOS) in aqueous solutions. *Chemical Engineering Journal* **379**, 122303 (2020).
141. Buxton, G. v, Greenstock, C. L., Phillips Helman, W., Ross, A. B. & Helman, W. P. Critical Review of Rate Constants for Reactions of Hydrated Electrons, Hydrogen Atoms and Hydroxyl Radicals ( $\cdot\text{OH}/\cdot\text{O}$ ) in Aqueous Solution. *Aqueous Solution Journal of Physical and Chemical Reference Data* **17**, 23103 (1988).
142. Chang, J. *et al.* Ozonation degradation of microcystin-LR in aqueous solution: Intermediates, byproducts and pathways. *Water Research* **63**, 52–61 (2014).
143. Trogen, G.-B. *et al.* Conformational Studies of Microcystin-LR Using NMR Spectroscopy and Molecular Dynamics Calculations. *Biochemistry* **35**, 3197–3205 (1996).
144. Ranković, B. *et al.* Utilization of gamma and e-beam irradiation in the treatment of waste sludge from a drinking water treatment plant. *Radiation Physics and Chemistry* **177**, 109174 (2020).
145. Zhu, F. *et al.* Electron beam irradiation of typical sulfonamide antibiotics in the aquatic environment: Kinetics, removal mechanisms, degradation products and toxicity assessment. *Chemosphere* **274**, 129713 (2021).
146. Ting, T. M. & Jamaludin, N. Decolorization and decomposition of organic pollutants for reactive and disperse dyes using electron beam technology: Effect of the concentrations of pollutants and irradiation dose. *Chemosphere* **73**, 76–80 (2008).
147. Ponomarev, A. v & Ershov, B. G. The Green Method in Water Management: Electron Beam Treatment. *Environmental Science and Technology* **54**, 5331–5344 (2020).
148. Patel, H. *et al.* nf-core/rnaseq: nf-core/rnaseq v3.0 - Silver Shark. (2020).
149. Dobin, A. *et al.* STAR: ultrafast universal RNA-seq aligner. *Bioinformatics* **29**, 15–21 (2013).
150. Danecek, P. *et al.* Twelve years of SAMtools and BCFtools. *GigaScience* **10**, 1–4 (2021).
151. Wang, L., Wang, S. & Li, W. RSeQC: quality control of RNA-seq experiments. *Bioinformatics* **28**, 2184–2185 (2012).

152. García-Alcalde, F. *et al.* Qualimap: evaluating next-generation sequencing alignment data. *Bioinformatics* **28**, 2678–2679 (2012).
153. Picard Toolkit. (2019).
154. Daley, T. & Smith, A. D. Predicting the molecular complexity of sequencing libraries. *Nature Methods* *2013 10:4* **10**, 325–327 (2013).
155. Sayols, S., Scherzinger, D. & Klein, H. dupRadar: a Bioconductor package for the assessment of PCR artifacts in RNA-Seq data. *BMC Bioinformatics* **17**, 1–5 (2016).
156. Liao, Y., Smyth, G. K. & Shi, W. featureCounts: an efficient general purpose program for assigning sequence reads to genomic features. *Bioinformatics* **30**, 923–930 (2014).
157. Love, M. I., Huber, W. & Anders, S. Moderated estimation of fold change and dispersion for RNA-seq data with DESeq2. *Genome Biology* **15**, 1–21 (2014).
158. Ewels, P., Magnusson, M., Lundin, S. & Käller, M. MultiQC: summarize analysis results for multiple tools and samples in a single report. *Bioinformatics* **32**, 3047–3048 (2016).
159. Yuan, S., Cohen, D. B., Ravel, J., Abdo, Z. & Forney, L. J. Evaluation of Methods for the Extraction and Purification of DNA from the Human Microbiome. *PLOS ONE* **7**, e33865 (2012).
160. Chu, C., Li, X. & Wu, Y. GAPPadder: a sensitive approach for closing gaps on draft genomes with short sequence reads. *BMC Genomics* **20**, 1–10 (2019).
161. Qian, H. *et al.* The Effects of Hydrogen Peroxide on the Circadian Rhythms of *Microcystis aeruginosa*. *PLoS ONE* **7**, (2012).
162. Min, H., Guo, H. & Xiong, J. Rhythmic gene expression in a purple photosynthetic bacterium, *Rhodobacter sphaeroides*. *FEBS Letters* **579**, 808–812 (2005).
163. Colón-López, M. S. & Sherman, L. A. Transcriptional and Translational Regulation of Photosystem I and II Genes in Light-Dark- and Continuous-Light-Grown Cultures of the Unicellular Cyanobacterium *Cyanothece* sp. Strain ATCC 51142. *Journal of Bacteriology* **180**, 519 (1998).
164. Praveen, C. *et al.* Assessment of microbiological correlates and immunostimulatory potential of electron beam inactivated metabolically active

- yet non culturable (MAyNC) *Salmonella* Typhimurium.  
doi:10.1371/journal.pone.0243417.
165. Omid, A., Esterhuizen-Londt, M. & Pflugmacher, S. Still challenging: the ecological function of the cyanobacterial toxin microcystin-What we know so far. *Toxin Reviews* **37**, 87–105 (2017).
  166. Kaebernick, M., Neilan, B. A., Börner, T. & Dittmann, E. Light and the Transcriptional Response of the Microcystin Biosynthesis Gene Cluster. *Applied and Environmental Microbiology* **66**, 3387 (2000).
  167. Zilliges, Y. *et al.* The Cyanobacterial Hepatotoxin Microcystin Binds to Proteins and Increases the Fitness of *Microcystis* under Oxidative Stress Conditions. *PLOS ONE* **6**, e17615 (2011).
  168. Hutchinson, F. The Molecular Basis for Radiation Effects on Cells. *Cancer Research* **26**, 2045–2052 (1966).
  169. Daly, M. J. A new perspective on radiation resistance based on *Deinococcus radiodurans*. *Nature Reviews Microbiology* **7**, 237–245 (2009).
  170. Hieke, A.-S. C. & Pillai, S. D. *Escherichia coli* Cells Exposed to Lethal Doses of Electron Beam Irradiation Retain Their Ability to Propagate Bacteriophages and Are Metabolically Active. *Frontiers in Microbiology* **9**, 2138 (2018).
  171. Bhatia, S. S. Investigations into Metabolically Active yet Non-Culturable (MAyNC) *Clostridium perfringens* to Control Necrotic Enteritis in Broiler Chickens. (2021).
  172. Tang, C., Zhang, Z., Tian, S. & Cai, P. Transcriptomic responses of *Microcystis aeruginosa* under electromagnetic radiation exposure. *Scientific Reports* / **11**, 2123 (123AD).
  173. Pascual, M. B., Mata-Cabana, A., Florencio, F. J., Lindahl, M. & Cejudo, F. J. A comparative analysis of the NADPH thioredoxin reductase C-2-Cys peroxiredoxin system from plants and cyanobacteria. *Plant physiology* **155**, 1806–1816 (2011).
  174. Stanne, T. M., Pojidaeva, E., Andersson, F. I. & Clarke, A. K. Distinctive types of ATP-dependent Clp proteases in cyanobacteria. *The Journal of biological chemistry* **282**, 14394–14402 (2007).
  175. *Cyanobacteria: From Basic Science to Applications*. (Academic Press, 2019).

176. Komenda, J. Role of two forms of the D1 protein in the recovery from photoinhibition of photosystem II in the cyanobacterium *Synechococcus* PCC 7942. *Biochimica et Biophysica Acta (BBA) - Bioenergetics* **1457**, 243–252 (2000).
177. Golden, S. S. Light-Responsive Gene Expression in Cyanobacteria. *Journal of Bacteriology* **177**, 1651–1654 (1995).
178. Nowaczyk, M. M. *et al.* Psb27, a Cyanobacterial Lipoprotein, Is Involved in the Repair Cycle of Photosystem II. *The Plant Cell* **18**, 3121 (2006).
179. Xiao, Y. *et al.* Structural insights into cyanobacterial photosystem II intermediates associated with Psb28 and Tsl0063. *Nature Plants* 1–11 (2021) doi:10.1038/s41477-021-00961-7.
180. Dobakova, M., Sobotka, R., Tichy, M. & Komenda, J. Psb28 protein is involved in the biogenesis of the photosystem II inner antenna CP47 (PsbB) in the cyanobacterium *Synechocystis* sp. PCC 6803. *Plant physiology* **149**, 1076–1086 (2009).
181. Sakata, S., Mizusawa, N., Kubota-Kawai, H., Sakurai, I. & Wada, H. Psb28 is involved in recovery of photosystem II at high temperature in *Synechocystis* sp. PCC 6803. *Biochimica et Biophysica Acta* **1827**, 50–59 (2013).
182. Sasi, S., Venkatesh, J., Daneshi, R. F. & Gururani, M. A. Photosystem II Extrinsic Proteins and Their Putative Role in Abiotic Stress Tolerance in Higher Plants. *Plants* **7**, (2018).
183. Rhee, J.-S., Dahms, H.-U., Choi, B.-S., Lee, J.-S. & Choi, I.-Y. Identification and analysis of whole microcystin synthetase genes from two Korean strains of the cyanobacterium *Microcystis aeruginosa*. *Genes & Genomics* **34**, 435–439 (2012).
184. Tillett, D. *et al.* Structural organization of microcystin biosynthesis in *Microcystis aeruginosa* PCC7806: an integrated peptide–polyketide synthetase system. *Chemistry & Biology* **7**, 753–764 (2000).
185. Kaebnick, M., Dittmann, E., Börner, T. & Neilan, B. A. Multiple Alternate Transcripts Direct the Biosynthesis of Microcystin, a Cyanobacterial Nonribosomal Peptide. *Applied and Environmental Microbiology* **68**, 449–455 (2002).
186. Straub, C., Quillardet, P., Vergalli, J., Marsac, N. T. de & Humbert, J.-F. A Day in the Life of *Microcystis aeruginosa* Strain PCC 7806 as Revealed by a Transcriptomic Analysis. *PLOS ONE* **6**, e16208 (2011).

187. Renaud, S. L., Pick, F. R. & Fortin, N. Effect of Light Intensity on the Relative Dominance of Toxigenic and Nontoxigenic Strains of *Microcystis aeruginosa*. *Applied and Environmental Microbiology* **77**, 7016 (2011).
188. Pineda-Mendoza, R. M., Zuniga, G. & Martinez-Jeronimo, F. Microcystin production in *Microcystis aeruginosa*: effect of type of strain, environmental factors, nutrient concentrations, and N:P ratio on mcyA gene expression. *Aquatic Ecology* **50**, 103–119 (2016).
189. Sielaff, H. *et al.* The mcyF gene of the microcystin biosynthetic gene cluster from *Microcystis aeruginosa* encodes an aspartate racemase. *Biochemical Journal* **373**, 909 (2003).
190. Furusato, E., Asaeda, T. & Manatunge, J. Tolerance for prolonged darkness of three phytoplankton species, *Microcystis aeruginosa* (Cyanophyceae), *Scenedesmus quadricauda* (Chlorophyceae), and *Melosira ambigua* (Bacillariophyceae). *Hydrobiologia* **527**, 153–162 (2004).
191. Leyko, W. & Bartosz, G. Membrane Effects of Ionizing Radiation and Hyperthermia. *International Journal of Radiation Biology and Related Studies in Physics* **49**, 770 (1985).
192. Liu, J., Lu, Y., Hua, W. & Last, R. L. A New Light on Photosystem II Maintenance in Oxygenic Photosynthesis. *Frontiers in Plant Science* **10**, 975 (2019).
193. United States Environmental Protection Agency. Drinking Water Mapping Application to Protect Source Waters (DWMAPS). <https://www.epa.gov/sourcewaterprotection/drinking-water-mapping-application-protect-source-waters-dwmaps>.
194. Poudel, D. D., Lee, T., Srinivasan, R., Abbaspour, K. & Jeong, C. Y. Assessment of seasonal and spatial variation of surface water quality, identification of factors associated with water quality variability, and the modeling of critical nonpoint source pollution areas in an agricultural watershed. *Journal of Soil and Water Conservation* **68**, (2013).
195. Cooley, S. W., Ryan, J. C. & Smith, L. C. Human alteration of global surface water storage variability. *Nature* **591**, 78–81 (2021).
196. Oram, B. The pH of Water. *Water Research Center* <https://water-research.net/index.php/ph>.
197. United States Environmental Protection Agency Office of Research and Development. Causal Analysis/Diagnosis Decision Information System

- (CADDIS): pH. <https://www.epa.gov/caddis-vol2/caddis-volume-2-sources-stressors-responses-ph> (2017).
198. United States Geological Survey. Alkalinity and Water. [https://www.usgs.gov/special-topic/water-science-school/science/alkalinity-and-water?qt-science\\_center\\_objects=0#qt-science\\_center\\_objects](https://www.usgs.gov/special-topic/water-science-school/science/alkalinity-and-water?qt-science_center_objects=0#qt-science_center_objects).
  199. United States Environmental Protection Agency. Secondary Drinking Water Standards: Guidance for Nuisance Chemicals. <https://www.epa.gov/sdwa/secondary-drinking-water-standards-guidance-nuisance-chemicals>.
  200. Development, U. S. E. P. A. O. of R. and. Causal Analysis/Diagnosis Decision Information System (CADDIS): Ionic Strength. <https://www.epa.gov/caddis-vol2/ionic-strength> (2017).
  201. United States Geological Survey. Chloride, Salinity, and Dissolved Solids. [https://www.usgs.gov/mission-areas/water-resources/science/chloride-salinity-and-dissolved-solids?qt-science\\_center\\_objects=0#qt-science\\_center\\_objects](https://www.usgs.gov/mission-areas/water-resources/science/chloride-salinity-and-dissolved-solids?qt-science_center_objects=0#qt-science_center_objects).
  202. Development, U. S. E. P. A. O. of R. and. Causal Analysis/Diagnosis Decision Information System (CADDIS): Dissolved Oxygen. (2017).
  203. United States Geological Survey. Dissolved Oxygen and Water. [https://www.usgs.gov/special-topic/water-science-school/science/dissolved-oxygen-and-water?qt-science\\_center\\_objects=0#qt-science\\_center\\_objects](https://www.usgs.gov/special-topic/water-science-school/science/dissolved-oxygen-and-water?qt-science_center_objects=0#qt-science_center_objects).
  204. The Metropolitan Water District of Southern California. *2021 Annual Drinking Water Quality Report*. [http://www.mwdh2o.com/pdf\\_about\\_your\\_water/2.3.1\\_annual\\_water\\_quality\\_report.pdf](http://www.mwdh2o.com/pdf_about_your_water/2.3.1_annual_water_quality_report.pdf) (2021).
  205. Arizona Department of Environmental Quality. *Ambient Groundwater Quality of the Salt River Basin: A 2001-2015 Baseline Study*. (2016).
  206. He, X. *et al.* Efficient removal of microcystin-LR by UV-C/H<sub>2</sub>O<sub>2</sub> in synthetic and natural water samples. *Water Research* **46**, 1501–1510 (2012).
  207. Pelaez, M., de la Cruz, A. A., O’Shea, K., Falaras, P. & Dionysiou, D. D. Effects of water parameters on the degradation of microcystin-LR under visible light-activated TiO<sub>2</sub> photocatalyst. *Water Research* **45**, 3787–3796 (2011).
  208. Trojanowicz, M., Bojanowska-Czajka, A., Bartosiewicz, I. & Kulisa, K. Advanced Oxidation/Reduction Processes treatment for aqueous



- perfluorooctanoate (PFOA) and perfluorooctanesulfonate (PFOS) – A review of recent advances. *Chemical Engineering Journal* **336**, 170–199 (2018).
209. Sun, Q. *et al.* Effects of fulvic acid size on microcystin-LR photodegradation and detoxification in the chlorine/UV process. *Water Research* **193**, 116893 (2021).
210. Kinniburgh, D. G., van Riemsdijk, W. H., Koopal, L. K. & Benedetti, M. F. Ion Binding to Humic Substances: Measurements, Models, and Mechanisms. in *Adsorption of Metals by Geomedia* (ed. Jenne, E. A.) 483–520 (Elsevier, 1998). doi:10.1016/b978-012384245-9/50024-4.
211. Smith, R. B., Bass, B., Sawyer, D., Depew, D. & Watson, S. B. Estimating the economic costs of algal blooms in the Canadian Lake Erie Basin. *Harmful algae* **87**, (2019).
212. Kouakou, C. R. C. & Poder, T. G. Economic impact of harmful algal blooms on human health: a systematic review. *Journal of water and health* **17**, 499–516 (2019).
213. National Oceanic and Atmospheric Administration. Hitting us where it hurts: The untold story of harmful algal blooms. *Science and Data*  
<https://www.fisheries.noaa.gov/west-coast/science-data/hitting-us-where-it-hurts-untold-story-harmful-algal-blooms> (2021).
214. Space-o. The algae bloom challenge to drinking water. [https://www.space-o.eu/the-algae-bloom-challenge-to-drinking-water/#\\_edn2](https://www.space-o.eu/the-algae-bloom-challenge-to-drinking-water/#_edn2) (2018).

## APPENDIX A

### CRITICAL REVIEW SEARCH TERMS

Table 15. Defined search terms used for critical literature review and the number of papers identified with each database.

<b>Search terms used</b>	<b>Databases</b>	<b>Found</b>
electron + beam + microcystin	Google Scholar	13
electron + beam + microcystis	Science Direct	1
electron + beam + irradiation + microcystin	Pubmed	0
electron + beam + irradiation + microcystis		
ebeam + irradiation + microcystin		
ebeam + irradiation + microcystis		
ebeam + microcystin		
ebeam + microcystis		
electron + beam + cyanobacteria		
ebeam + cyanobacteria		
electron + beam + irradiation + cyanobacteria		
ebeam + irradiation + cyanobacteria		
gamma + microcystin		
gamma + microcystis		
gamma + irradiation + microcystin		
gamma + irradiation + microcystis		
gamma + cyanobacteria		
gamma + irradiation + cyanobacteria		
$\gamma$ + irradiation + microcystin		
$\gamma$ + irradiation + microcystis		
$\gamma$ + irradiation + cyanobacteria		
x ray + irradiation + microcystin		
x ray + irradiation + microcystis		
x ray + microcystin		
x ray + microcystis		
x ray + irradiation + cyanobacteria		
ionizing + radiation + microcystin		
ionizing + radiation + microcystis		

APPENDIX B

WATER QUALITY PARAMETER DATA

Table 16. MC-LR concentrations ( $\mu\text{g/L}$ ) and degradation efficiency in  $5.11 \pm 0.079$  kGy eBeam treated source water samples and untreated samples. (Error expressed as standard deviation.)

Source Water Location	MC-LR ( $\mu\text{g/L}$ )		MC-LR Degradation (%)
	Untreated (0 kGy)	Treated (5 kGy)	
Beaver Lake, AR	$3304.73 \pm 817.53$	$1.84 \pm 0.49$	99.94
Cedar River, WA	$4674.48 \pm 558.75$	$1.19 \pm 0.35$	99.97
Chattahoochee river, GA	$3423.05 \pm 1036.12$	$6.63 \pm 3.98$	99.81
Derby Lake, VT	$3352.42 \pm 581.83$	$1.15 \pm 0.24$	99.97
Hyalite creek, MT	$3814.20 \pm 546.61$	$2.05 \pm 0.55$	99.95
Lake Keowee, SC	$5335.54 \pm 1774.63$	$0.73 \pm 0.23$	99.99
Lake Ogeltree, AL	$3522.13 \pm 479.59$	$1.96 \pm 1.88$	99.94
Lake Tahoe, CA	$2380.13 \pm 690.77$	$1.79 \pm 0.37$	99.92
Lake Travis, TX	$2981.41 \pm 170.60$	$1.41 \pm 0.69$	99.95
Lake Washington, FL	$3747.16 \pm 321.97$	$7.28 \pm 4.78$	99.81
Lake Woollomes, CA	$4036.70 \pm 226.63$	$0.62 \pm 0.37$	99.98
Merrimack River, NH	$2772.05 \pm 548.76$	$1.12 \pm 0.78$	99.96
Mississippi River, IA	$3454.74 \pm 921.93$	$6.31 \pm 4.57$	99.82
Mississippi River, LA	$3140.80 \pm 770.44$	$1.58 \pm 0.14$	99.95
Ohio River, OH	$3331.27 \pm 331.83$	$0.96 \pm 0.04$	99.97
Potomac River, DC	$4238.81 \pm 1340.22$	$2.80 \pm 1.20$	99.93
Rio Grande River, TX	$3901.88 \pm 262.53$	$1.21 \pm 0.41$	99.97
Salt River, AZ	$4185.93 \pm 1031.87$	$0.75 \pm 0.13$	99.98
South Platte River, CO	$4410.96 \pm 829.61$	$1.45 \pm 0.48$	99.97
Southern California Water Supply, CA	$4077.95 \pm 217.30$	$1.61 \pm 0.50$	99.96
Wailuku River, HI	$3874.70 \pm 517.07$	$1.91 \pm 1.71$	99.95
Weatherford Lake, TX	$4692.93 \pm 232.93$	$1.60 \pm 0.37$	99.97

Table 17. Measured water quality parameters in source water samples. (Error expressed as standard deviation).

Source Water Location	pH	Alkalinity (mg/L of CaCO <sub>3</sub> )	TDS (mg/L)	Dissolved Oxygen (%)
Beaver Lake, AR	6.54 ± 0.02	46.67 ± 0.58	121.33 ± 4.51	69.33 ± 7.23
Cedar River, WA	6.76 ± 0.06	24.67 ± 5.86	62.00 ± 8.54	86.33 ± 4.04
Chattahoochee River, GA	6.81 ± 0.25	20.33 ± 1.15	75.33 ± 15.04	85.67 ± 1.53
Derby Lake, VT	7.33 ± 0.02	122.00 ± 1.73	297.00 ± 3.61	75.67 ± 2.89
Hyalite creek, MT	7.80 ± 0.00	80.00 ± 1.00	148.67 ± 2.08	84.67 ± 2.89
Lake Keowee, SC	6.24 ± 0.03	13.67 ± 0.58	21.33 ± 4.04	85.33 ± 2.89
Lake Ogeltree, AL	6.78 ± 0.21	32.67 ± 10.69	77.00 ± 35.54	82.33 ± 1.53
Lake Tahoe, CA	7.15 ± 0.04	46.33 ± 0.58	91.67 ± 4.73	85.67 ± 3.21
Lake Travis, TX	7.94 ± 0.59	165.00 ± 2.00	445.33 ± 11.68	89.00 ± 0.00
Lake Washington, FL	7.15 ± 0.04	57.67 ± 30.24	558.67 ± 4.73	80.00 ± 2.65
Lake Woollomes, CA	6.67 ± 0.02	33.33 ± 0.58	105.67 ± 1.53	80.33 ± 2.52
Merrimack River, NH	6.41 ± 0.03	11.67 ± 0.58	94.67 ± 4.62	86.33 ± 1.53
Mississippi River, IA	7.20 ± 0.02	183.33 ± 1.53	459.00 ± 21.70	63.33 ± 1.53
Mississippi River, LA	7.04 ± 0.01	101.67 ± 0.58	282.00 ± 7.81	78.33 ± 6.66
Ohio River, OH	6.99 ± 0.05	73.67 ± 0.58	324.00 ± 2.65	73.33 ± 5.03
Potomac River, DC	7.18 ± 0.02	85.33 ± 0.58	278.33 ± 43.88	82.00 ± 3.46
Rio Grande Irrigation Canal, TX	7.16 ± 0.02	145.33 ± 2.08	714.33 ± 14.19	91.00 ± 2.00
Salt River, AZ	7.25 ± 0.04	144.67 ± 1.15	>LOD	82.33 ± 1.53
South Platte River, CO	7.22 ± 0.02	95.00 ± 0.00	471.67 ± 4.93	85.33 ± 3.06
Southern California Water Supply, CA	8.12 ± 0.02	134.33 ± 0.58	840.67 ± 24.70	90.67 ± 2.52
Wailuku River, HI	7.22 ± 0.03	25.33 ± 0.58	57.00 ± 1.73	85.00 ± 1.00
Weatherford Lake, TX	7.64 ± 0.03	164.00 ± 1.00	472.00 ± 5.00	81.67 ± 0.58